AD NUMBER

AD866978

NEW LIMITATION CHANGE

TO

Approved for public release, distribution unlimited

FROM

Distribution authorized to U.S. Gov't. agencies and their contractors; Administrative/Operational Use; Feb 1970. Other requests shall be referred to Director, Air Force Aero Propulsion Lab., Wright-Patterson AFB, OH 45433.

AUTHORITY

AFAPL ltr, 12 Apr 1972

AFAPL-TR-69-117

HIGH TEMPERATURE HYDROCARBON FUELS RESEARCH IN AN ADVANCED AIRCRAFT FUEL SYSTEM SIMULATOR ON FUEL AFFB-12-68

Harold Goodman
Royce Bradley

NORTH AMERICAN ROCKWELL CORPORATION/LOS ANGELES DIVISION

TECHNICAL REPORT AFAPL-TR-69-117

FEBRUARY 1970

AIR FORCE AERO PROPULSION LABORATORY
AIR FORCE SYSTEMS COMMAND
WRIGHT-PATTERSON AIR FORCE BASE, OHIO

112

NOTICE

When Government drawings, specifications, or other data are used for any purpose other than in connection with a definitely related Government procurement operation, the United States Government thereby incurs no responsibility nor any obligation whatsoever; and the fact that the Government may have formulated, furnished, or in any way supplied the said drawings, specifications, or other data, is not to be regarded by implication or otherwise as in any manner licensing the holder or any other person or corporation, or conveying any rights or permission to manufacture, use, or sell any patented invention that may in any way be related thereto.

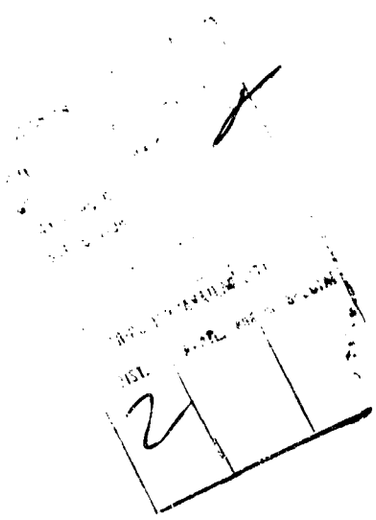

Copies of this report should not be returned unless return is required by security considerations, contractual obligations, or notice on a specific document.

HIGH TEMPERATURE HYDROCARBON FUELS RESEARCH IN AN ADVANCED AIRCRAFT FUEL SYSTEM SIMULATOR ON FUEL AFFB-12-68

Harold Goodman
Royce Bradley

FOREWORD

This report was prepared by the Los Angeles Division of North American Rockwell Corporation under Contract AF33(615)-3228 which bears the Budget Program Sequence No. 6 (63 304801 62405214) and 5 (68 0100 61430014) and Project No. 3048, Task 304805. This contract is monitored by the Air Force Aero Propulsion Laboratory with Lt. Jerry C. Ford as Air Force Project Engineer. The North American Rockwell Program Manager is Mr. Harold Goodman and the Project Engineer is Mr. Royce P. Bradley.

This report covers the fifth fuel series of Phase II which was conducted from 6 December 1968 to 30 July 1969. This report was submitted by the authors on 26 November 1969.

Publication of this report does not constitute Air Force approval of the report's findings or conclusions. It is published only for the exchange and stimulation of ideas.

Arthur V. Churchill

ARTHUR V. CHURCHILL, Chief
Fuels Branch
Fuels, Lubrication, and
Hazards Division

ABSTRACT

Hydrocarbon jet fuels tend to form deposits at elevated temperatures that decrease heat exchanger efficiency and plug screens and filter elements. The Advanced Aircraft Fuel System Simulator provides generalized performance data, with respect to thermal stability, on various advanced fuels that will be used to correlate to small-scale test results and provide information on design criteria for future supersonic aircraft.

In this report, the thermal stability of the fifth fuel (AFFB-12-68) tested in the simulator is quantified in terms of the amount of deposit formed. The quantification of deposit formation is determined under cyclic conditions (mission profiles) and two types of steady-state test conditions (steady-state and steady-state-varied flow).

Deposits were evident in the wing tank after testing at either a maximum skin temperature of 425° or 500° F. The airframe and engine systems were clean except for the manifold and nozzle. There was no evidence of decreased performance of any of the components other than a loss in fuel side heat transfer efficiency of the manifold. The predicted rates of deposit formation under cyclic conditions, based on the radial spectrum of steady-state test fuel temperatures, are in agreement with the rates measured during cyclic conditions.

TABLE OF CONTENTS

LIST OF ILLUSTRATIONS

SECTION I

INTRODUCTION

This program was initiated to furnish an aircraft airframe and engine fuel system simulator and subsequently conduct a fuels research program to investigate advanced hydrocarbon fuel performance with respect to thermal stability under simulated high mach number flight conditions. The simulator is to provide generalized performance data on various advanced fuels that will be used to correlate small-scale thermal stability tests and provide information on design criteria for future supersonic aircraft.

Phase I of this program consisted of the design, installation, and check-out of the Advanced Aircraft Fuel System Simulator. A detailed report on this phase is presented in reference 1. The FAA-SST Fuel System Test Rig, discussed in reference 2, was modified during this phase to increase the fuel system simulation capability to the speed regime of interest. Upon completion of this task, performance tests were conducted, and the simulator was found to fulfill the design profile requirements set forth by the Air Force.

Phase II is a continuing effort which consists of fuel testing in the simulator. Concurrently, the fuels are tested in various small-scale thermal stability devices. The results of the simulator and small-scale devices are then compared. Five fuels have been evaluated, and the number of test cycles performed and the references wherein the tests and analyses results are reported are as follows:

Fuel	Test Series	Manifold Peak Fuel-Out Temp (° F)	Number of Test Cycles	Where Reported
AFFB-8-67	First	600	100	Reference 3
	Second	500	100	
AFFB-9-67	Third	600	123	Reference 4
	Fourth	500	57	
AFFB-10-67	Fifth	600	76	Reference 5
	Sixth	500	66	
AFFB-11-68	Seventh	600	175	Reference 6
AFFB-12-68	Eighth	600	175	This report

SECTION II

FUEL TESTED

The test fuel is designated as AFFB-12-68 and was purchased from Humble Oil and Refining Company. The fuel was analyzed by the supplier 2 August 1968 and the results are shown in table I. On 2 August 1968, the fuel was loaded into 5 tank cars and shipped to Wright-Patterson Air Force Base (WPAFB) from the Baytown, Texas refinery. Approximately 100,000 gallons of the fuel arrived at WPAFB on 14 August 1968 and was loaded into the four lined underground storage tanks used for this program.

As fuel was required, it was delivered to the test site in a 5,000-gallon trailer and loaded into the 25,000-gallon underground storage tank used as the simulator supply tank. The tank is lined with a protective coating conforming to MIL-C-4556B. On 15 October 1968, a total of fifty 55-gallon, epoxy-phenolic-lined drums of fuel AFFB-12-68 were shipped to the Air Force Fuel Bank for future use.

TABLE I. AFFB-12-68 FUEL ANALYSES

Gravity, °API	46.0
Color, saybolt	+30
Distillation, °F (D-86)	
Initial boiling point	370
10 percent	396
20 percent	404
50 percent	422
90 percent	454
Final boiling point	476
Residue, %	1.0
Loss, %	1.0
Aromatics, %	3.0
Flash point, °F (PM)	160
Water tolerance	Pass No. 1
Freezing point, °F	-60
Existent gum, mg/100 ml	0.2
Potential gum, 16 hours, mg/100 ml	0.4
Total sulfur, weight percent	0.0003
Doctor	Pass
Luminometer number	75.6
Corrosion, 2 hours at 212° F	1
Net BTU/pound	18,732
Net BTU/gallon	124,324
Water separometer index, modified	97
Fuel system icing inhibitor, % by volume	0.125
Particulate matter, mg/l	0.4
Lubricity additive, ppm by weight	218 (added bases)
Viscosity at -30° F, cs	13.56
Thermal stability, high-temperature CRC coker	300/500/600
Deposit code	1
Pressure drop	0.2
Thermal precipitation test	Cleaner than standard
Vapor pressure, psia at	
300° F	2.95
500° F	47.0

SECTION III

SIMULATOR TEST CYCLES

SUMMARY OF TEST PROCEDURE AND RESULTS

A total of 175 test cycles were performed on fuel AFFB-12-68, including 142 test cycles conducted with the wing tank at a 500° F maximum tank skin temperature for direct comparison to the 142 test cycles performed on fuels AFFB-10-67 and AFFB-11-68. The remaining 33 test cycles were performed with the tank at a 425° F maximum tank skin temperature for comparison to fuel AFFB-11-68. The operational procedure for the 175 test cycles on the other components was the same as that used in the fifth, sixth and seventh test series.

A summary of significant results of the testing is as follows: At the end of the 142 test cycles, the entire wing tank internal surfaces were discolored and deposits were predominantly on the bottom of the tank. The powdery deposit was as thick as 0.1 inch with some of the crusty deposit as thick as 0.3 inch. Much loose, gritty material was present in the puddle areas. Testing at the 425° F maximum tank skin temperature also revealed the formation of deposits at this lower temperature environment. Upon completion of the 175 test cycles, it was found that no deposits were formed in the airframe or engine lines and components, with the exception of the manifold and nozzle. The manifold data indicate a maximum deposit increase per test cycle of 0.0013 mil, using a deposit thermal conductivity of 0.07 BTU-ft/hr-sq ft-° F. There was no evidence of decreasing performance of the nozzle system.

TEST PROCEDURE AND RESULTS

Unless otherwise stated, the test procedure was the same as reported in reference 5.

WING TANK

Operational Procedure

The average weight of fresh fuel used to fill the tank was 647.5 pounds. A time-temperature history of vapor in the wing tank is shown in figure 1.

A total of 142 test cycles were performed on fuel AFFB-12-68 at the 500° F maximum tank skin temperature environment to permit an equal test cycle comparison with fuels AFFB-10-67 and AFFB-11-68. A second sequence of tests was conducted for an equal test cycle comparison to fuel AFFB-11-68 at a maximum skin temperature of 425° F. The wing tank was

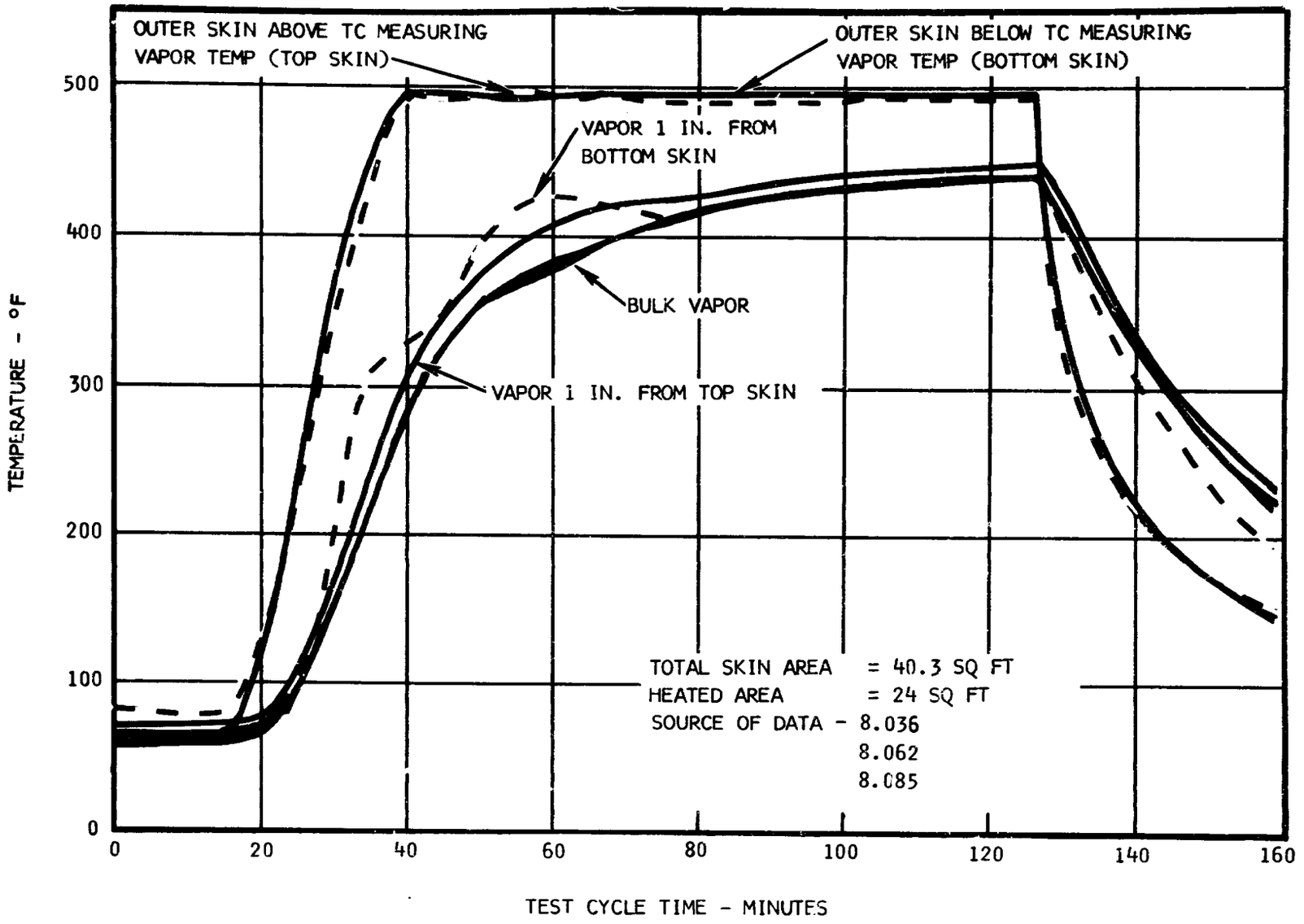

Figure 1. Time-Temperature History of Vapor in Wing Tank (500° F)

cleaned, and the testing was conducted for 33 simulated flights at the reduced temperature environment (figure 2). As in the testing of fuel AFFB-11-68, the two heated probes in the tank were controlled at 425° F and 360° F maximum temperatures, and no vibration was applied to the tank. All other test parameters were identical to those during the 500° F tank testing.

Results

500° F Maximum Skin Temperature

The wing tank was opened after selected test cycles to visually examine the deposits in the wing tank and on the probes and to replace the 2.5-inch probe sections. The following tabulation gives the visual ratings under sunlight of the stainless steel and titanium probes using the CRC Lacquer Rating Scale (reference 7).

Rating After Test Cycle	Total Test Cycles Imposed	Unheated Probe (395° F Max)	425° F Probe	500° F Titanium Probe	(415° F Max)
8.5-inch sections					
8.035	35	6-8	4-6	6-7	4-5
8.070	70	7-8	5-8	4-8	4-6
8.105	105	8	5-8	5-8	5-7
8.142	142	8-9	5-9	3-9	5-8
2.5-inch sections					
8.035	35	6-7	4	6-7	4-5
8.070	35	7	7	3-7	4-5
8.105	35	7-8	6-7	4-7*	7*
8.142	37	8	3-8	3-8	3-8

* The installation of the titanium and stainless steel sections were inadvertently reversed; i.e., the rating shown in the 500° F column is for titanium at 500° F and the rating shown in the titanium column is for stainless steel at a maximum temperature of 415° F. This fortunate occurrence strengthens the validity of previous results (reference 6) that the deposits formed on the unheated stainless steel (approximately 400° F) probes are much darker than the deposits formed on titanium at the same temperature. However, at 500° F there was no visible difference in the color of the deposits.

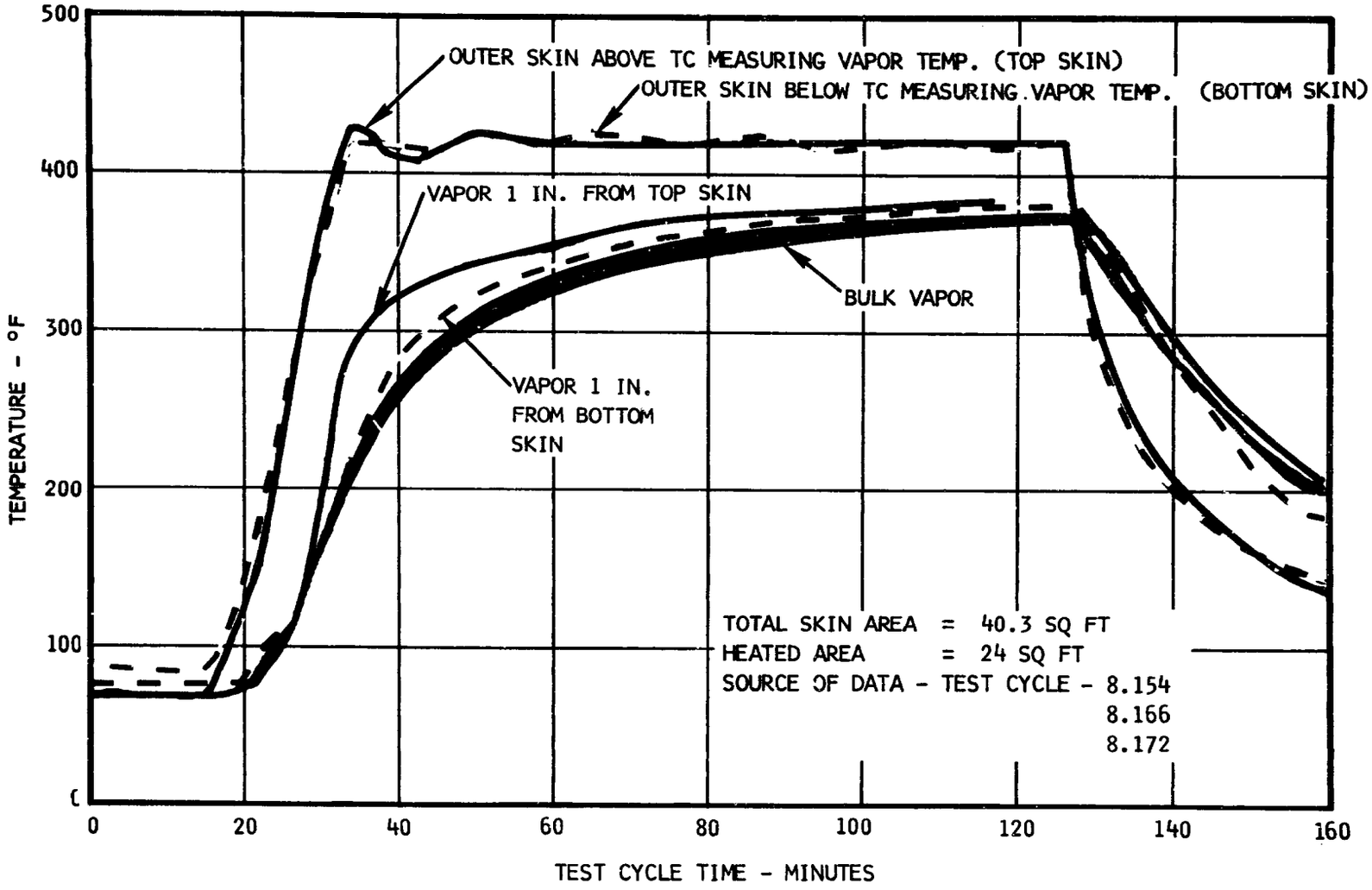

Figure 2. Time-Temperature History of Vapor in Wing Tank (425° F)

The 8.5-inch sections removed after 142 test cycles of operation are shown in figure 3. The amount of deposit formed on the heated stainless steel probes can be seen to be significantly less than that formed on the unheated stainless steel probe. As in previous testing with the other fuels, less deposit was formed on the titanium probe (Ti-6Al-4V) than was formed on the unheated stainless steel probe which was at approximately the same temperature. The order of increasing deposits of the probes is regarded to be as follows:

	500° F	Least
425° F	Titanium (415° F maximum)	
	Unheated (395° F maximum)	Most

The unheated probe had sufficient deposit to completely block any color effect of the tubing material.

The 2.5-inch sections, which were replaced every 35 test cycles, are shown in figure 4. The 500° F, 425° F, and titanium sections are definitely lighter in color than the unheated probe. The 8.5-inch probe sections do not appear to have significantly greater amounts of deposit than the 2.5-inch sections. This is in agreement with data from previous tests indicating that the rate of deposit accumulation on the probes as evident by color is not a linear function of time. The 2.5-inch probes used during the first 35 test cycles did not acquire as much deposit as the 2.5-inch probes used later in the test series. It is regarded that this condition is a result of the overall cleanliness of the wing tank during the initial 35 test cycles.

The entire wing tank was rated five times during the 142 test cycles by making a sketch of the tank showing the location, area, and rating of the deposits. These visual examinations are summarized in the following tabulation.

Rating After Test Cycle	Sides	Vent Area	Tube Trusses	Bottom Dry Areas	Bottom Puddle Areas
8.035	4-5	6-7	3-4	4-5	8-9
8.070	6	7-8	5	4-5	8-9
8.105	7	7-8	5-6	5-6	8-9*
8.142	8	8	5-6	5-6	8-9* (0.1 inch thick)
8.142 (dry)	8	8	5-6	5-6	8-9* (0.1 inch thick)

*Rough deposits

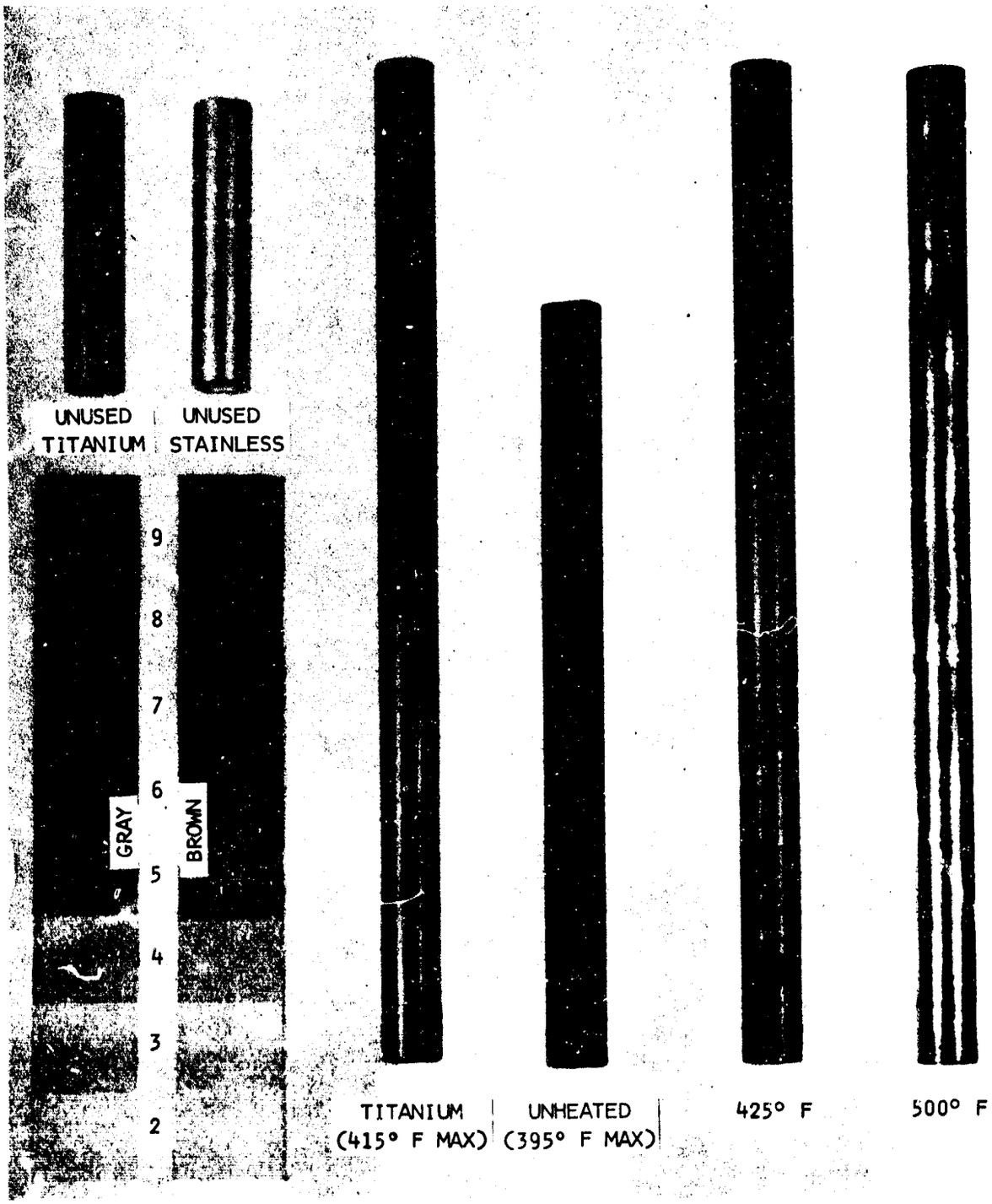

Figure 3. Wing Tank Probes (8.5-Inch Sections)

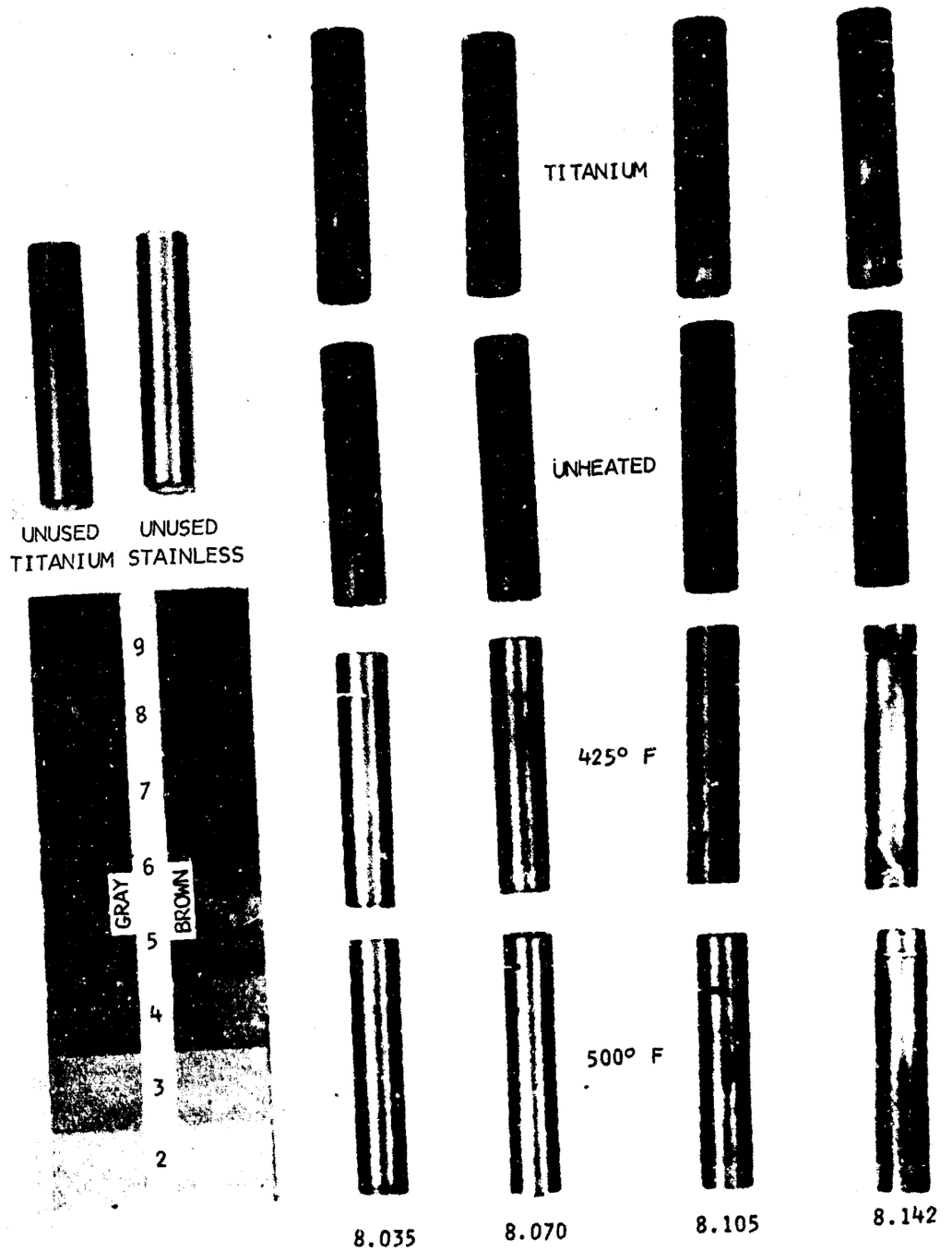

Figure 4. Wing Tank Probes (2.5-Inch Sections)

The 0.1-inch measurement was under the boost pump and was measured after completion of the 142 test cycles. A sketch, made of the wing tank after test cycle 8.142, is shown in figure 5. The ratings shown in figure 5 were obtained after the tank was "dried" by flowing filtered plant air through the tank for approximately 40 hours. It has been found that deposits usually change drastically in appearance when dried. However, the only observed change in the deposits due to drying following test cycle 8.142, was a change from yellowish-gray to gray of the dry areas of the tank bottom.

Comparing colors of the probes, dish, and disk to the wing tank revealed the following.

1. The interior struts at the center of the tank possessed the same appearance as the 425° F and titanium probes.

2. The struts along the sides of the tank appeared similar to the unheated probe.

3. The tank walls compared closely to the unheated probe.

4. The support bar that penetrates through the center of the tank was the same color as the unheated probe.

5. The color of the restrained dish,* disk and 500° F probe were very close to the color of the dry skin portion of the tank bottom.

6. The unrestrained dish compared very closely to the entire tank bottom since it contained black deposit (puddle area) as well as lighter color stain (dry area).

It was observed that a very sharp break in deposit color existed between the bottom dry areas (5-6) and the puddle areas (8-9). The puddle areas of the tank were covered with a rough, tightly adhering, glossy-black deposit with numerous loose deposit particles evident throughout the tank and thickest beneath the boost pump. These areas are shown with the dish, disk, and probes in figure 6. Three of the four photographs show the boost pump area, and the lower left photograph shows the opposite end of the tank.

The accelerating effect of condensation on deposit formation was also observed on the bottom and sides of the tank. The pattern of the deposit beneath the main support bar indicates that fuel vapor was condensing on the bar and dripping onto the tank bottom and also running down the walls. The sidewalls adjacent to the boost pump and thermocouple doors were streaked with a darker heavy deposit indicating that fuel was condensing and running down the walls.

*The unrestrained dish is an extra dish placed in one of the puddle areas of the tank before the test series.

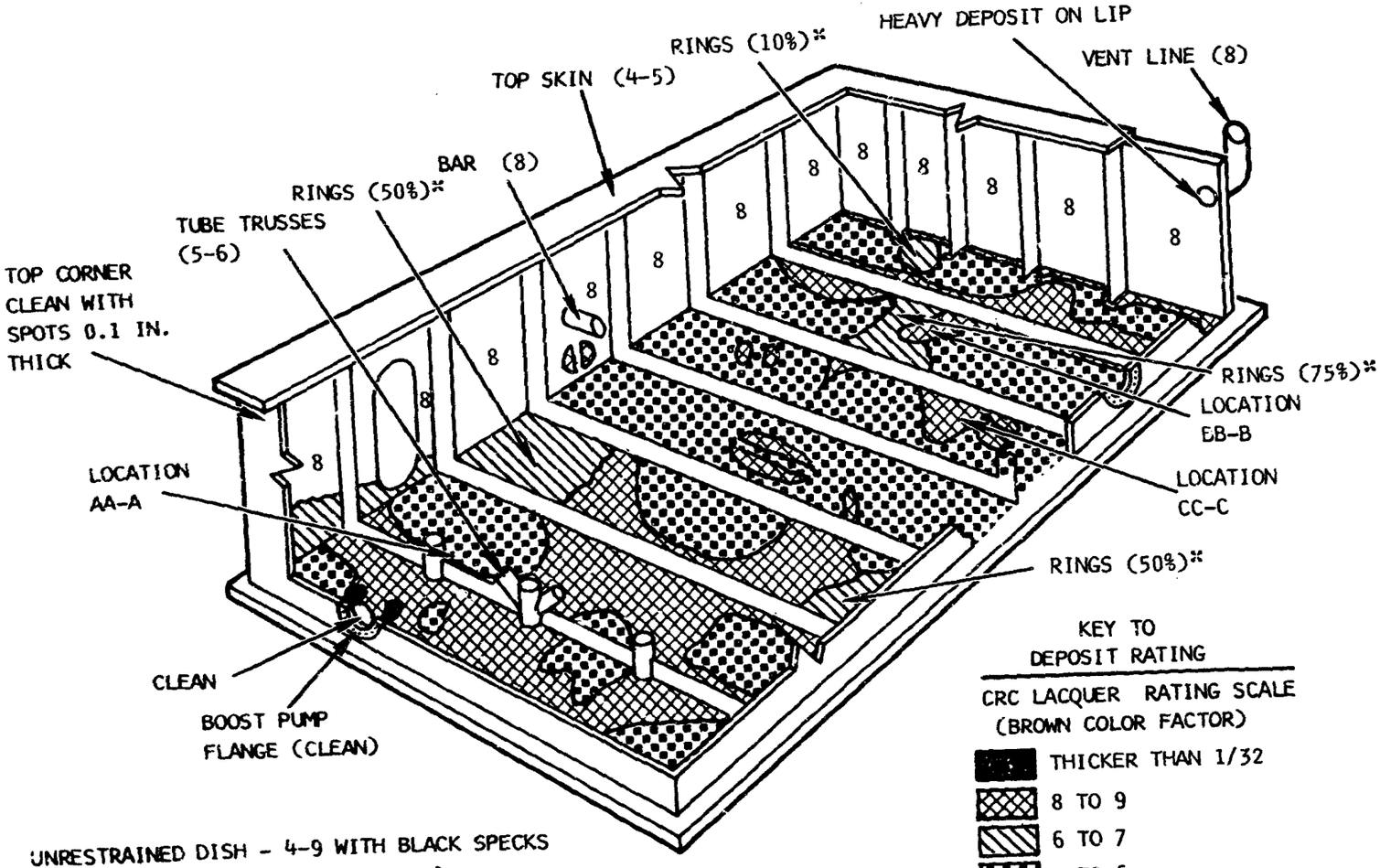

Figure 5. Artist's Conception of 500° F Wing Tank Deposits

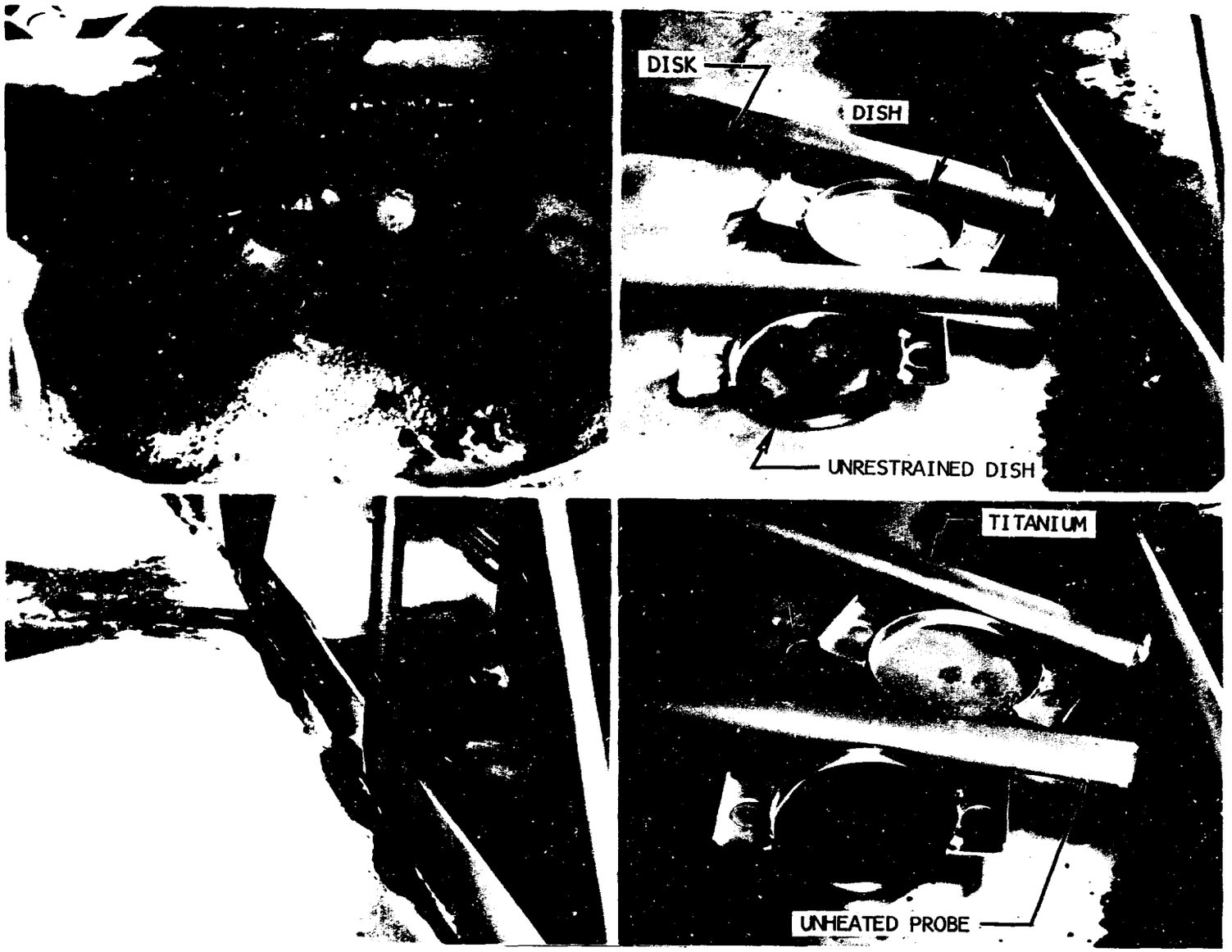

Figure 6. Wing Tank Deposits (500° F)

A large quantity of loose, red, powdery deposit and loose, black, crusty deposit was beneath the cooled boost pump. The powdery deposit reached 0.1 inch thick with some of the crusty deposit as thick as 0.3 inch. The boost pump door (figure 7) was clean except for two areas. A strip of yellow deposit (rating of 4 to 5 on the CRC Lacquer Rating Scale) was evident around the door next to the O-ring groove. There was also a small amount of deposit on the door beneath the thermocouple stub that penetrates the door. This deposit was a light yellow, powdery deposit approximately $\frac{1}{4}$ inch wide by $1\frac{1}{2}$ inch long. The boost pump (figure 7) was clean except for the inboard side of the pump which was covered with a yellow to dark brown deposit (rating of 3 to 9). Thick streaks and spots of deposit indicate that fuel was condensing on the boost pump assembly and running down the sides. The deposit was tightly adhering and was up to 0.05 inches thick.

Prior to cleaning the tank, deposit thickness measurements were obtained with a depth gauge by measuring the deposit height relative to a reference height, removing the deposits, and measuring the distance to the tank bottom. The maximum deposit thickness at the three locations shown in figure 5 are as follows:

Location	Maximum Deposit Thickness - Inches
AA-A	0.0205
BB-B	0.0005
CC-C	0.0006

Four samples of deposits were taken after the 142 test cycles. The samples were analyzed to determine the percent of metals in the inorganic portion of the deposits using emission spectrographic analysis, and the percent ash was also determined. The results obtained are as follows:

Estimated Percent

	Puddle Area	Boost Pump Area		
		Flange	Black - Beneath	Red - Beneath
Sodium	3.0	0.2	6.0	4.0
Silicon	8.0	2.0	2.0	2.0
Calcium	1.0	-	<1.0	<0.7
Aluminum	2.0	0.1	20.0	0.3
Magnesium	2.0	0.08	2.0	4.0
Iron	5.0	0.8	3.0	2.0
Copper	2.0	-	0.3	-
Lead	0.1	-	-	-
Chromium	0.2	-	0.1	0.2
Nickel	0.3	-	0.1	0.2
Titanium	0.07	-	-	0.1
Tin	0.3	-	-	0.07
Manganese	<0.1	-	0.01	<0.07
Ash (residue)	0.7	0.1	0.1	0.7

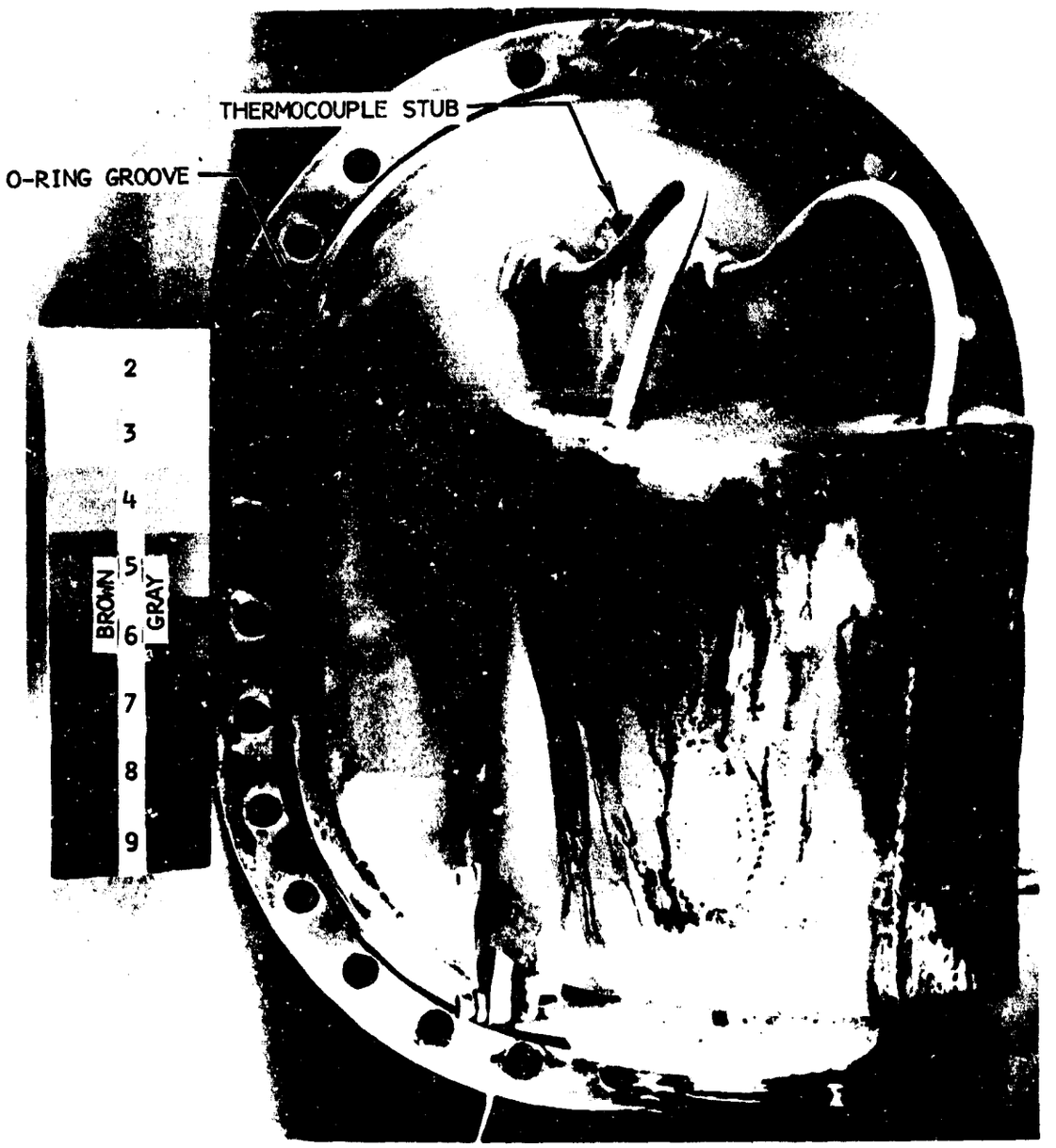

Figure 7. Wing Tank Boost Pump Assembly and Door (500° F)

These results indicate a much lower inorganic deposit content than obtained on the previous fuels tested.

425° F Maximum Skin Temperature

The results of testing fuel AFFB-12-68 in the wing tank for 33 test cycles revealed that deposits are also formed at a maximum skin temperature of 425° F. An artist's sketch of the wing tank deposits is shown in figure 8. The ratings shown in figure 8 were determined after air drying the tank. The entire tank was very slightly stained; however, only the tank puddle areas contained significant amounts of deposit. Photographs of some of these deposits are shown in figure 9. The six black spots shown in the upper left photograph are epoxy from the boost pump and are not considered to have been detrimental to the test results.

The sides of the tank were so slightly stained that detection of the stain required comparison to an unused piece of stainless steel. The deposit in the puddle areas was black and tightly adhered to the tank bottom. The deposits seemed to form nonuniformly and in some cases in concentric circles. There was a sharp break between the puddle and dry areas. The deposit thickness was not sufficient to permit thickness measurements using a depth gage as was done following the 500° F maximum skin temperature testing.

The probes that were contained in the tank for the entire 33 cycles are shown in figure 10. There is no visible difference in the color between the 2.5 and 8.5-inch probes at a given maximum temperature. All of the probes rated less than 2 on the CRC Lacquer Rating Scale-Brown (brown color factor). The order of decreasing discoloration of the probes is 425° F, 360° F, unheated and titanium. The titanium probe was not visibly discolored and the 425° F probe (the most discolored) was only slightly yellowed.

FUSELAGE TANK

The average weight of fresh fuel used to refill the tank was 2,137 pounds. The average weight ratio of residual fuel to fresh fuel was 0.19. A time-temperature history of the fuel and vapor in the fuselage tank is shown in figure 11.

The fuselage tank was inspected after 35, 70, 105, and 175 test cycles. During the inspection following test cycle 35 the only evident discoloration of the tank was a dark streak on the bottom beneath the vent and several white circles on the top. The streak was approximately 3/64 inch wide by 2½ inches long and rated 7 to 8 on the CRC Lacquer Scale-Gray. The white circles appeared to be the result of fuel condensing on the top of the tank, running to the low spots, and forming drops of fuel at the center of each white circle.

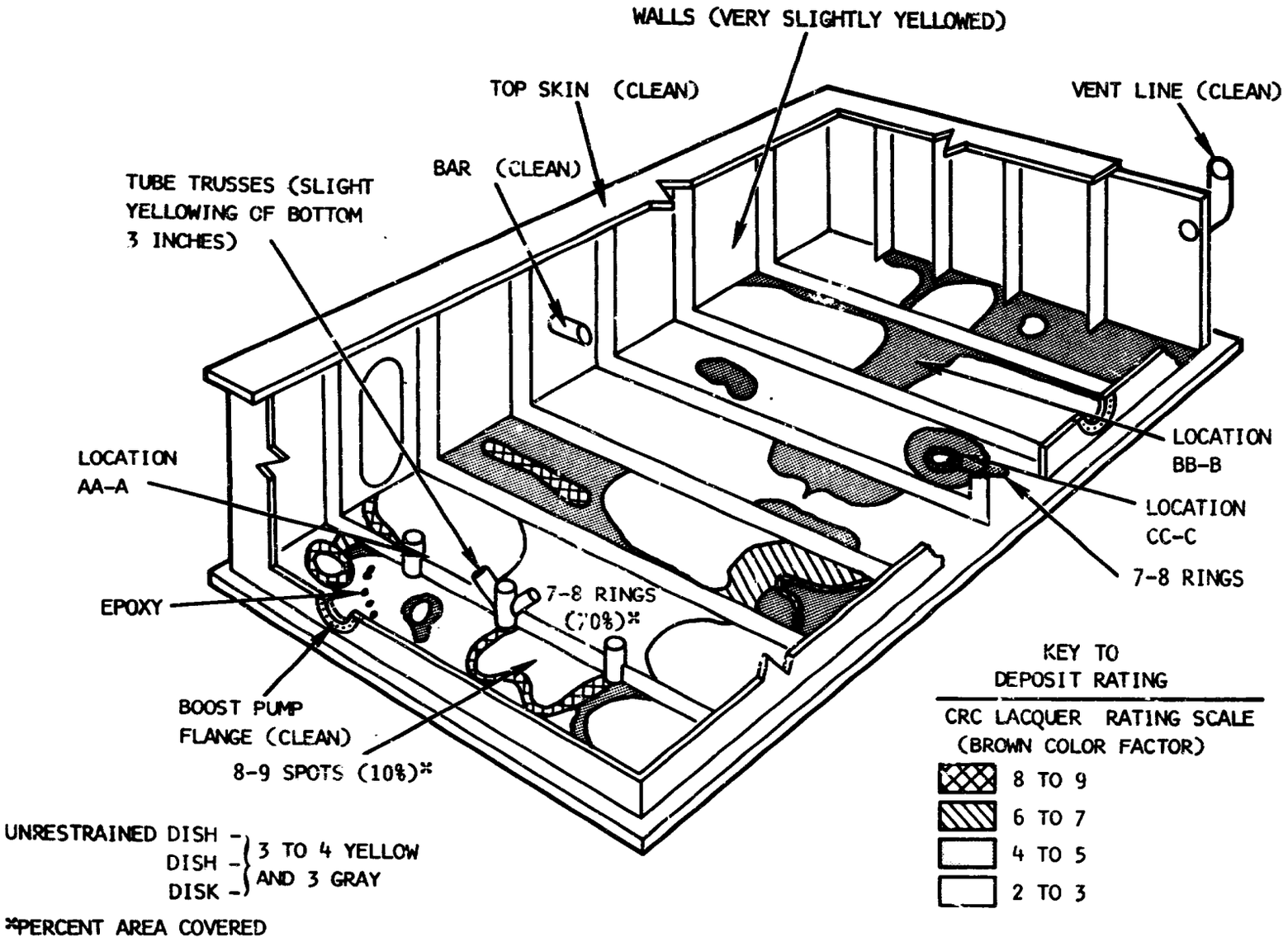

Figure 8. Artist's Conception of 425° F Wing Tank Deposits

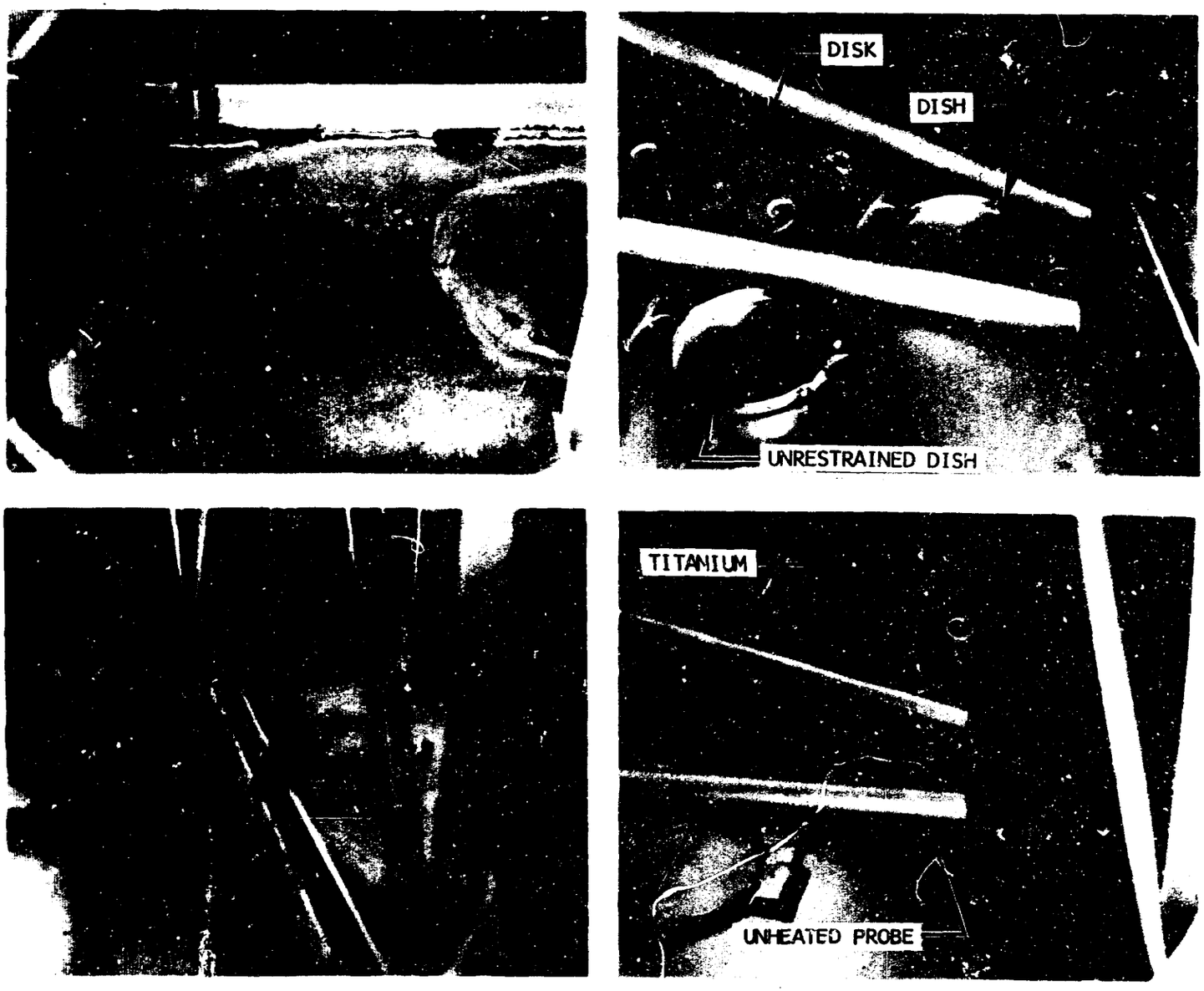

Figure 9. Wing Tank Deposits (425° F)

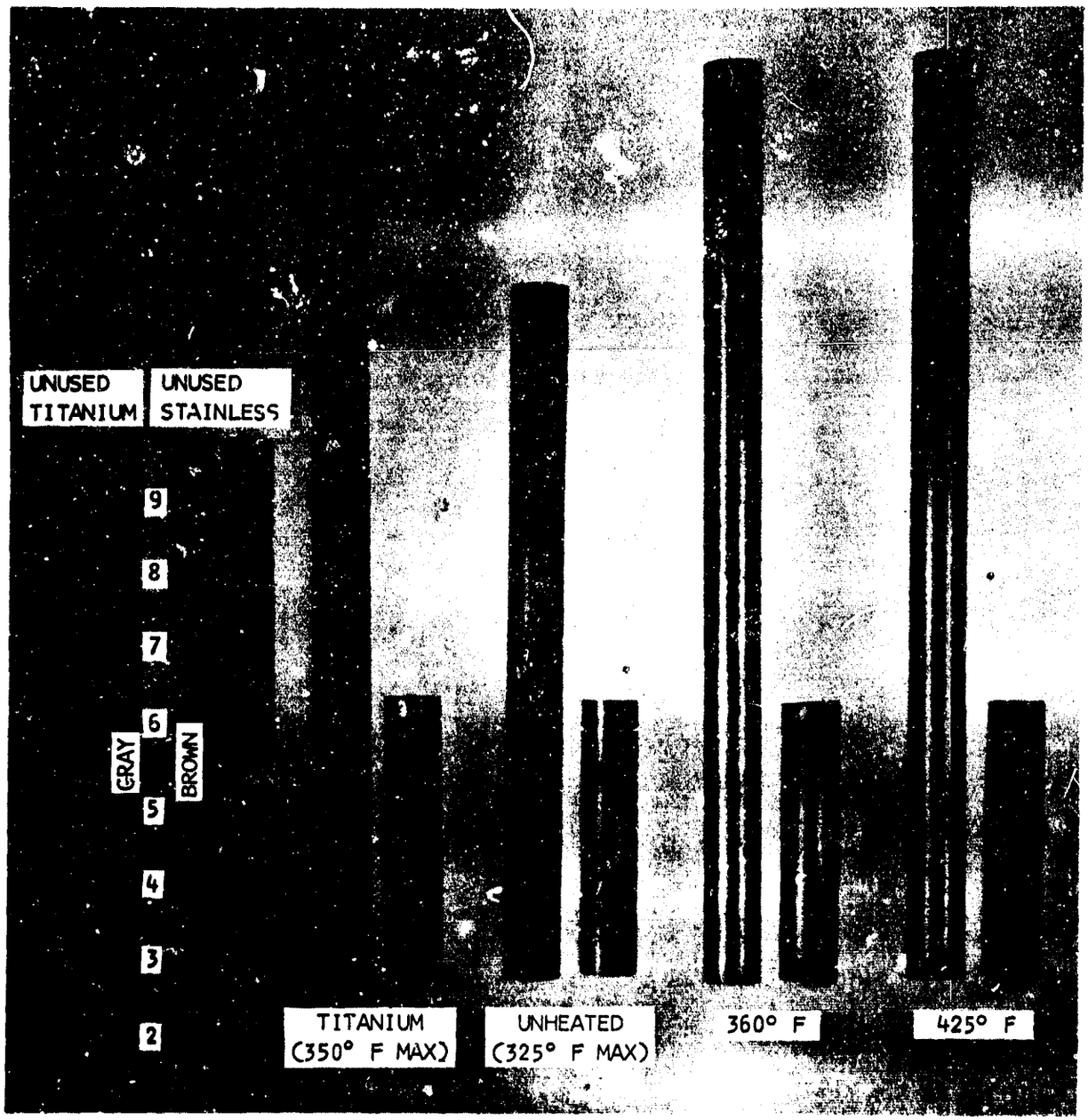

Figure 10. Wing Tank Probes (425° F)

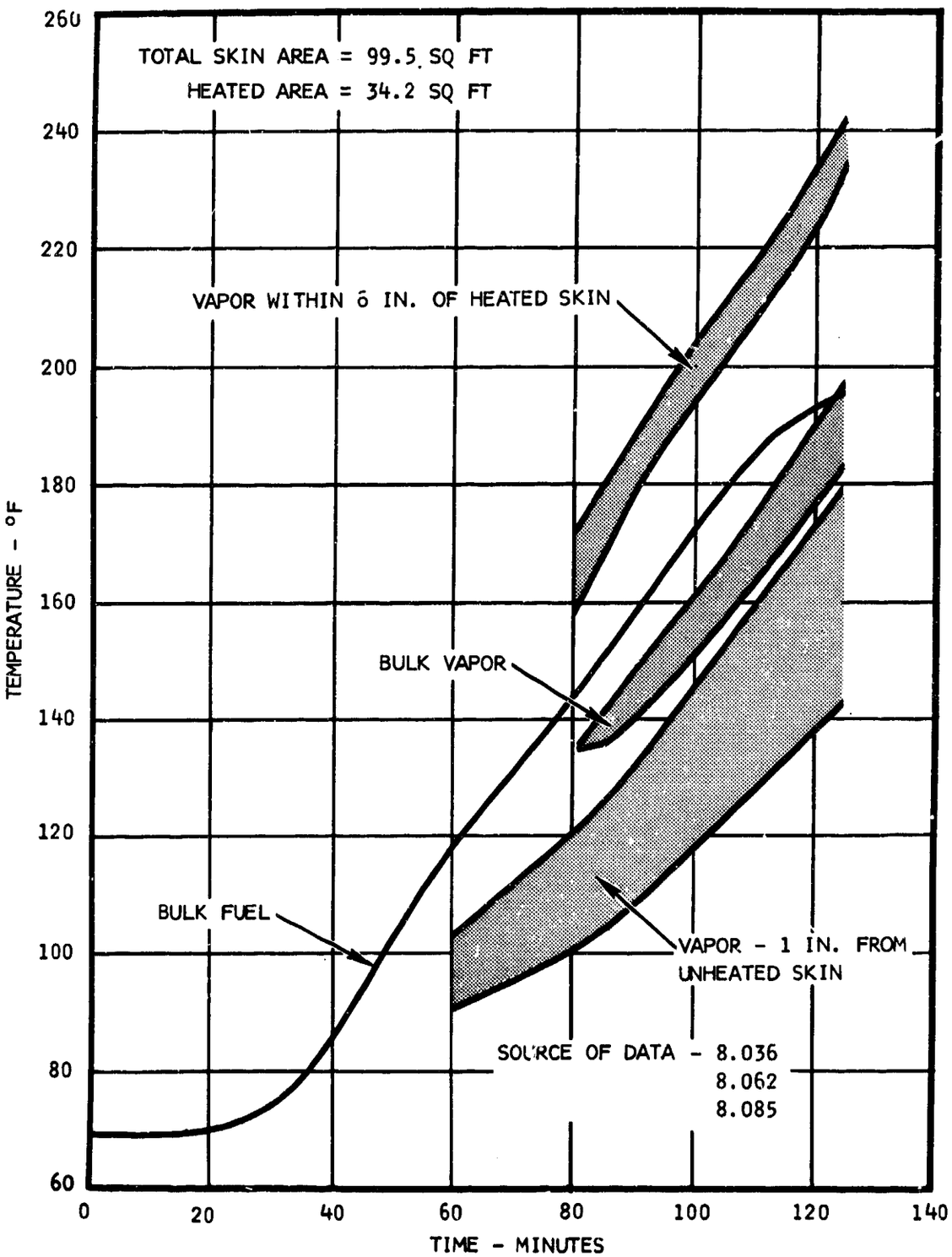

Figure 11. Time-Temperature History of Fuel and Vapor in Fuselage Tank

A spot approximately 1.5 inches in diameter was observed on the tank bottom beneath the vent during the inspection following test cycle 70. The spot rated 5 to 6 on the CRC Laquer Scale-Gray with a 1 inch diameter center rating 3 to 4 on the CRC Laquer Scale-Brown.

At the end of 175 test cycles the circles were slightly yellow (rating of 3 on the CRC Lacquer Scale-Brown). The streak appeared lighter (rating of 6 on the CRC Lacquer Rating Scale-Gray). The apparent lightening is probably due to the yellow spot covering the gray streak. It is considered that the streak was completely formed during the first 35 test cycles. The spot, following completion of 175 test cycles, was approximately 1.5 inches wide and 2.5 inches long, yellow in color and rated 5 on the CRC Lacquer Scale-Brown.

A slight yellowing of the top of the tank next to the support members in the vent area was evident. This discoloration is probably due to condensing of the vapors on the cooler surfaces as the vapors flow toward the vent.

VENT HEATING

The wing tank vent line heating schedule and equipment were the same during the first 142 test cycles as those described in reference 5. After the 142 cycles of testing, the wing tank vent line was found to rate 3 and 7 (CRC Lacquer Scale) at the lower and upper ends, respectively. The wing tank vent line was then cleaned. The vent line was controlled at a maximum temperature of 420° F ± 5° F during the concluding 33 test cycles. The vent line was again examined. No discoloration of the vent line was observed except for a very slight dulling of the surface.

The fuselage tank vent line heating schedule and equipment were the same for the entire 175 test cycles as those described in reference 5. The fuselage tank vent line was clean except for a slight dulling.

FUEL CONDENSATE

Upon completion of each test cycle, the condensate resulting from tank fuel boil off was drained from the vacuum system condenser tank and measured. The average amount of condensate collected was 231 and 180 ml per cycle, during the first 142 and the last 33 test cycles, respectively. A check of the wing tank attitude was made prior to test cycles 8.001 and 8.142. The fuel remaining in the tank was 1,469 and 1,447 ml, respectively.

AIRFRAME FUEL LINES

The lines in the airframe system were found to be free of deposit after 175 test cycles.

AIRFRAME FILTER

Approximately 87,500 gallons of fuel ranging in temperature from 42° to 220° F passed through the 75-micron filter during the cyclic testing. The pressure drop across the filter, measured during the climb portion of each test cycle, is shown in figure 12. The average deviation shown is the mean-square deviation of the sample points from the regression line. It is considered that the pressure drop of the airframe filter did not measurably change during the 175 test cycles.

The airframe filter was removed at the conclusion of the 175 test cycles. A considerable amount of debris was found in the folds of the filter element, however, the filter element was not discolored. The increase in weight of the element was 1.0 gram.

AIRFRAME HEAT EXCHANGER

The overall heat transfer coefficient and pressure drop of the airframe heat exchanger were determined for each test cycle and are shown in figures 13 and 14, respectively. The heat transfer coefficients are corrected to an average fuel temperature of 210° F in the heat exchanger. Analysis of the data, employing the least squares technique, indicates that neither the pressure drop nor the overall heat transfer coefficient changed measurably. The changes indicated are considered to result from the sensitivity of the simulator instrumentation. Inspection of the heat exchanger upon completion of the 175 test cycles revealed no change in color of the fuel or oil side.

ENGINE PUMP SUBSYSTEM

The engine pump fittings were inspected following the steady-state testing and at the end of the eighth test series. Neither inspection revealed any deposit formation in the fittings or subsystem lines.

The pump was disassembled and inspected by the manufacturer and the project engineer upon completion of the aforementioned testing. The pump was found to be in satisfactory condition with no parts damage or excessive wear. The pump contained a slight amount of brown deposit that could only be detected by wiping and examining the wiper.

ENGINE FUEL LINES

After 175 test cycles, the engine system fuel lines were disassembled and inspected. All lines were found to be free of deposit.

ENGINE FILTER

Approximately 87,500 gallons of fuel passed through the engine filter

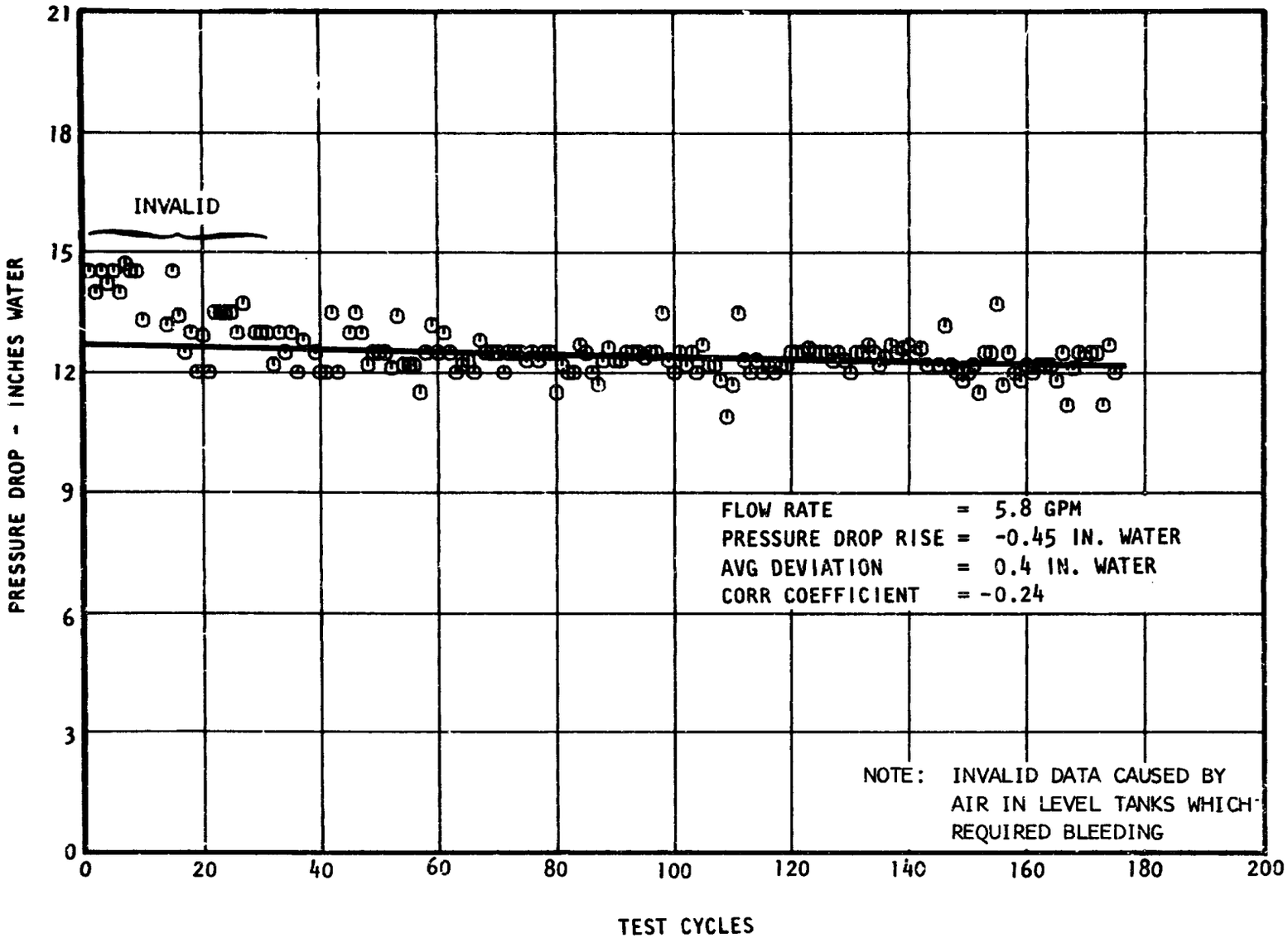

Figure 12. Pressure Drop Across Airframe Filter

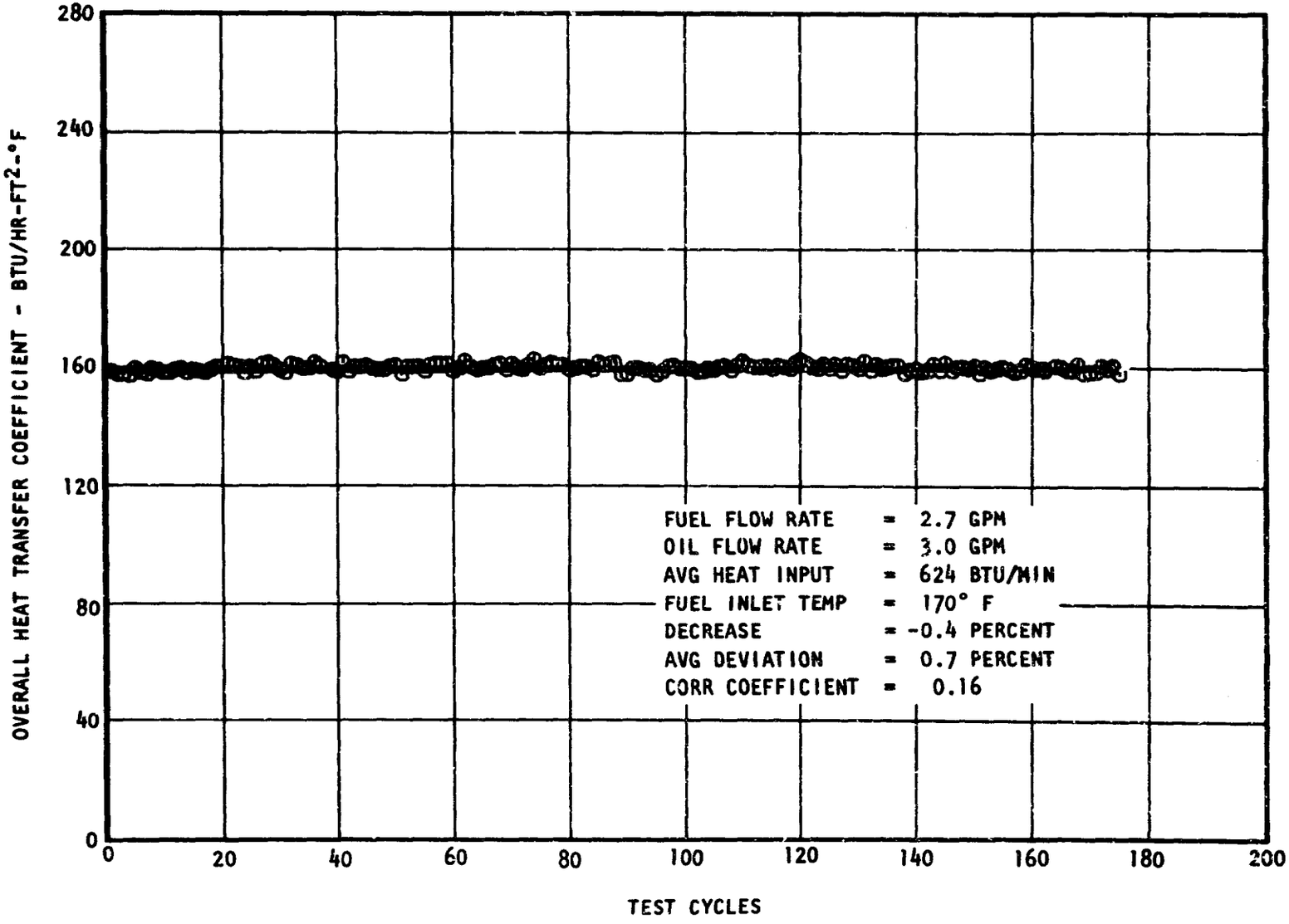

Figure 13. Overall Heat Transfer Coefficient of Airframe Heat Exchanger

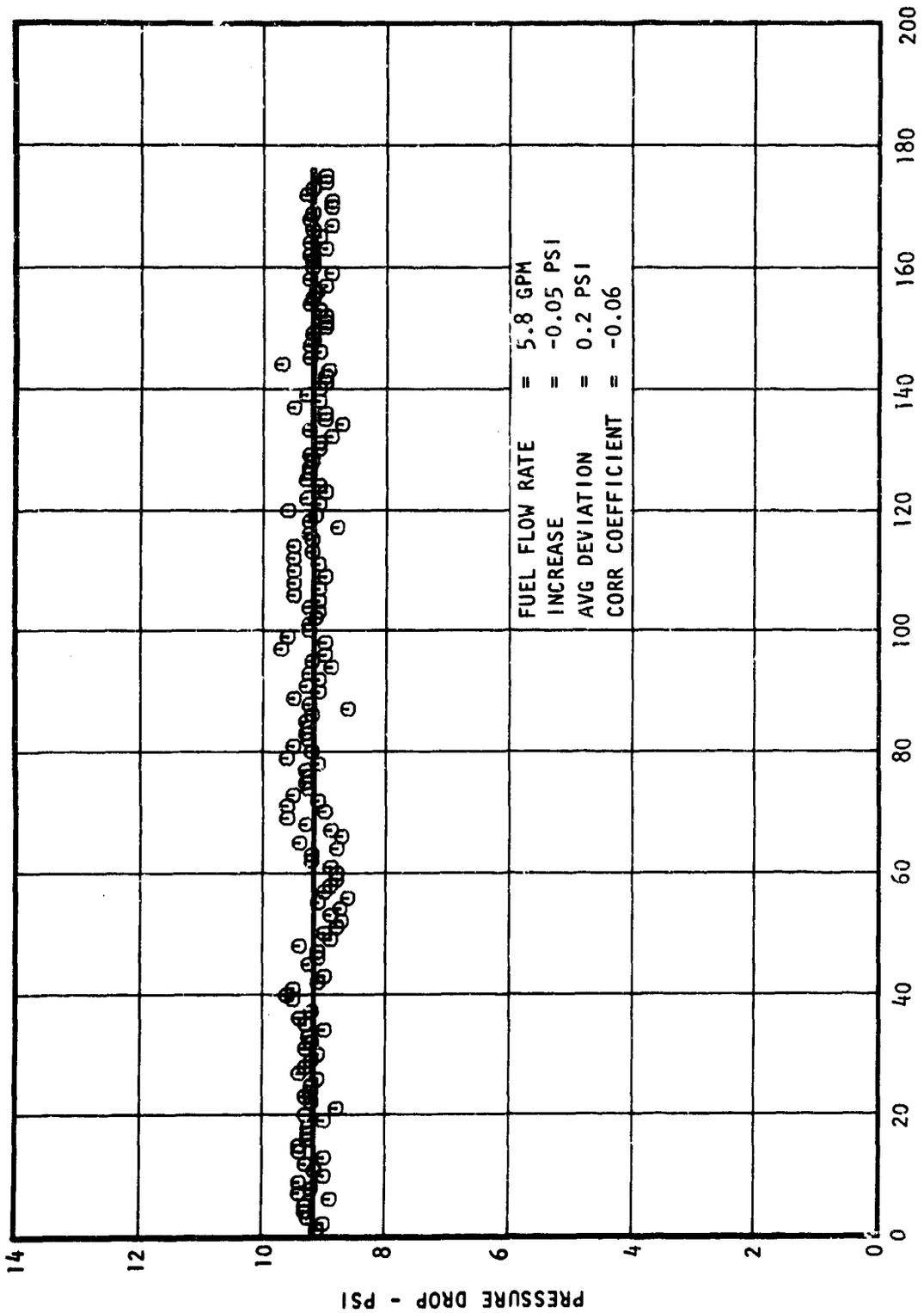

Figure 14. Pressure Drop Across Airframe Heat Exchanger

assembly during the 175 test cycles. Replacement of the filter element was required three times during testing. The replacement intervals can be seen in figure 15 which indicates filter pressure drop, measured during descent conditions, as a function of test cycles. A new filter element was installed prior to test cycle 48 to provide a comparison to the results obtained from previous fuels using a new element. The new filter element had to be cleaned after 73 cycles. A new filter element is used for the comparison since it is difficult to determine the degree of effectiveness of the cleaning process.

ENGINE HEAT EXCHANGER

The engine heat exchanger overall heat transfer coefficients obtained during the 175 test cycles are shown in figure 16. All values are corrected to an average fuel temperature in the heat exchanger of 210° F and an oil flow rate of 3.0 gpm. Figure 16 indicates a small decrease in heat transfer efficiency of the engine heat exchanger (0.9 percent).

The heat exchanger was bisected and the shell removed. The oil side of the tubes were partially covered (30 percent) with a black, very [illegible] wiped substance similar to a graphite suspended lubricant. One of the tubes was cut open and it was found that the fuel side of the tube was in unused condition at the inlet and discolored down the length of the tube. The colors are blue, yellow and orange as if due to heat stain. However, the tube wiped clean with a rag and therefore the discoloration must be deposit. A second tube was cut open and it was found that the discoloration extended to the inlet of the tube. It is considered that both the oil and fuel side deposit contributed to the small change in heat transfer efficiency that was measured.

The pressure drop of the engine heat exchanger was measured and is shown in figure 17. A least squares, straight-line curve fit of the data indicates that the pressure drop across the heat exchanger decreased 0.5 percent. This pressure drop decrease is assumed to have resulted from instrumentation sensitivity.

MANIFOLD

Based on the apparently equal thermal stabilities of fuels AFFB-11-68 and AFFB-12-68 in the manifold as evidenced by the steady-state tests, it was decided to conduct the manifold cyclic testing of fuel AFFB-12-68 under the same conditions as fuel AFFB-11-68. Therefore, a total of 175 test cycles were conducted at the 600° F maximum fuel-out temperature mission profile. The following applies to the eighth test series manifold:

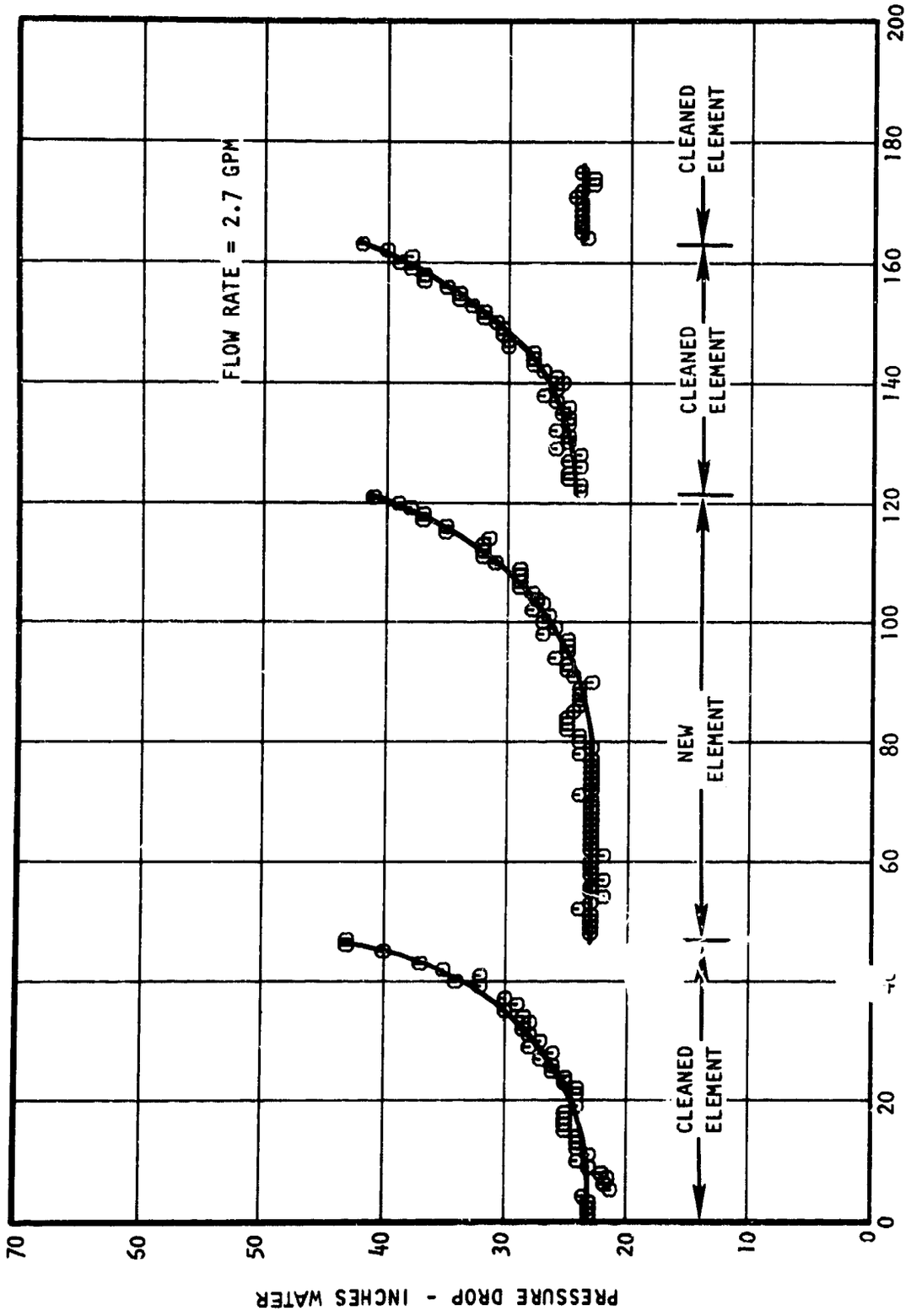

Figure 15. Pressure Drop Across Engine Filter

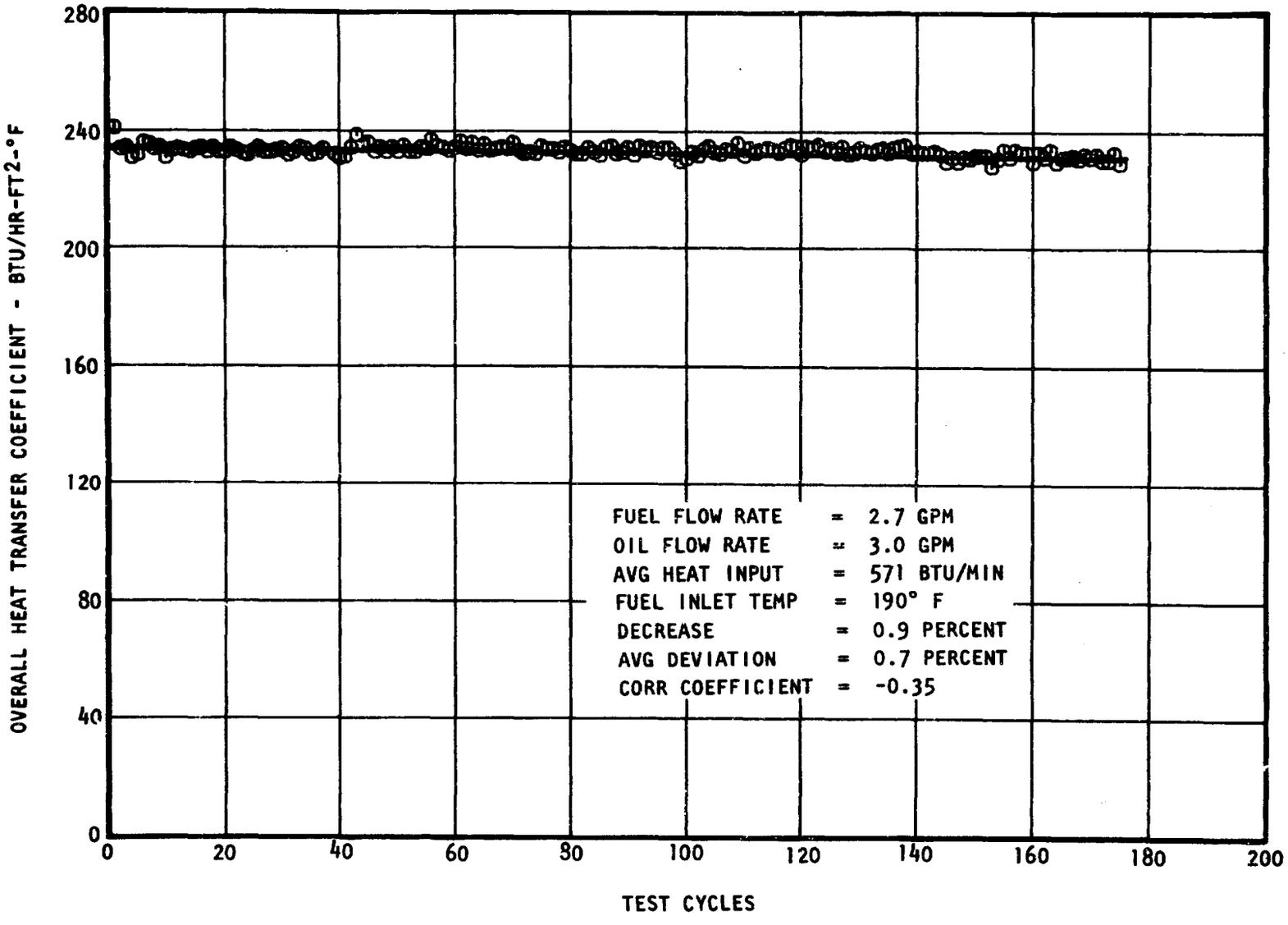

Figure 16. Overall Heat Transfer Coefficient of Engine Heat Exchanger

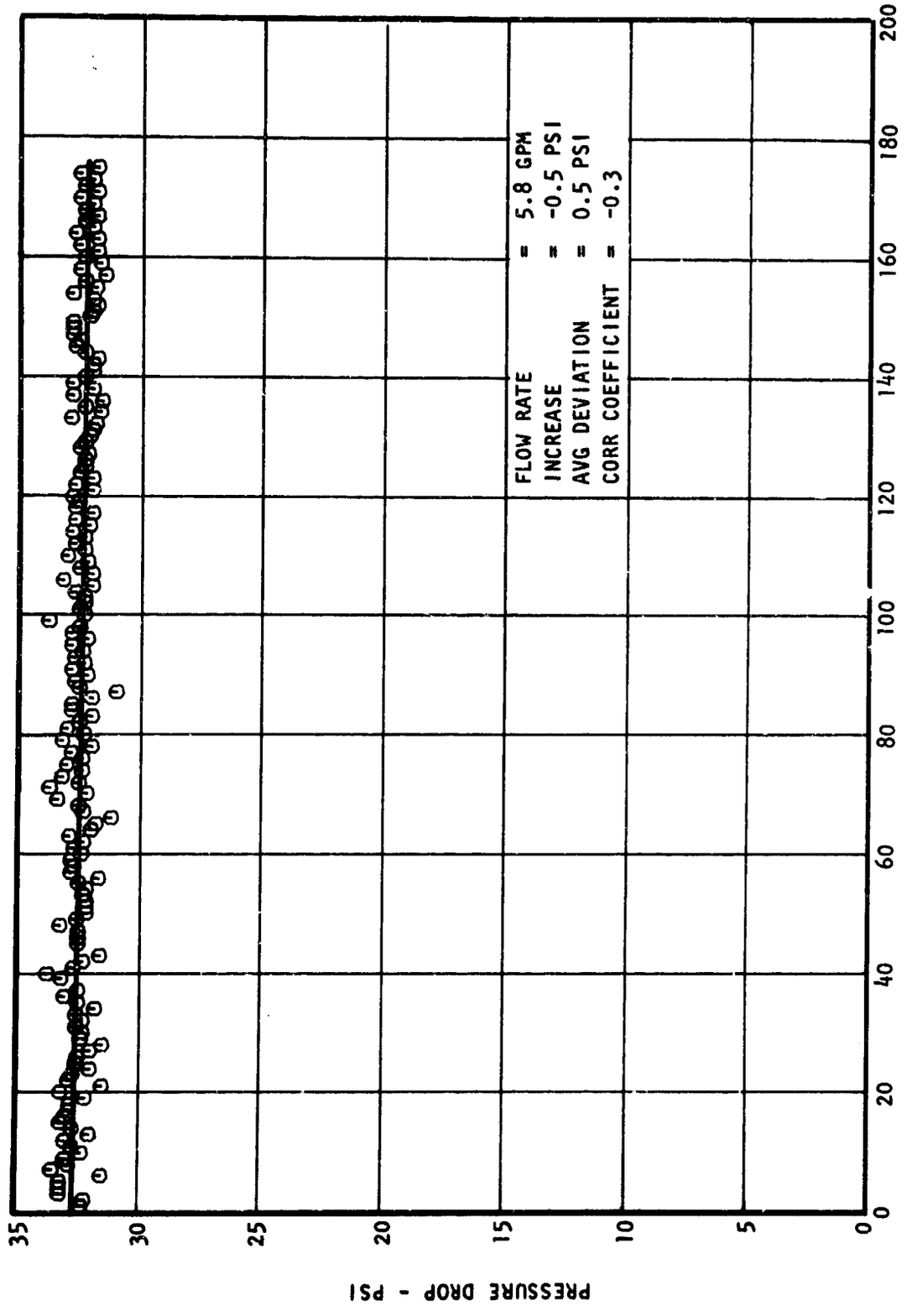

Figure 17. Pressure Drop Across Engine Heat Exchanger

Heated length	114.9 inches
Heat input*	879 BTU/min
Fuel temperature increase*	84.7° (+1.8, -3.7°) F
Max. fuel-out temperature	600° F

*Fuel-in temperature = 290° F, cruise conditions

Results

The manifold performance data are composed of the following five categories:

1. Deposit thermal resistance calculated from test cycle data
2. Micrometer measurements of deposit thickness
3. Microphotographs of deposit
4. Visual color ratings
5. Pressure drops recorded during testing

Deposit Thermal Resistance

The values of deposit thermal resistance (x_d/k_d) calculated for each of the 10 outer tube wall thermocouples are shown in appendix I. Also shown in appendix I are the peak metal temperatures at the beginning of the test series, the total change in x_d/k_d, the rate of change of x_d/k_d per unit test cycle (deposition rate), and the correlation coefficient of the data points. A single first order curve fit was used for each thermocouple location to obtain the deposition rates for TC-1 through TC-4. For TC-5 through TC-10, two first order curve fits using the least squares technique were used for each thermocouple location to obtain the deposition rates since it was indicated that the rate was higher for the latter portion of the test cycles. The intersection of the two straight lines was chosen such that the standard error of estimate of the data points from the lines was a minimum. It was determined that this intersection was at 108 or 109 test cycles. The maximum rate of deposition attained with fuel AFFB-12-68 under cyclic conditions was lower than that attained with fuel AFFB-11-68. However, the sharp change in deposition rate (definite breakpoint) evident with fuel AFFB-11-68 did not occur with fuel AFFB-12-68.

The total changes in x_d/k_d from appendix I and a deposit thermal conductivity (k_d) of 0.07 BTU/hr-ft-°F were used to calculate the deposit thickness at each thermocouple location. The results are shown in figure 18.

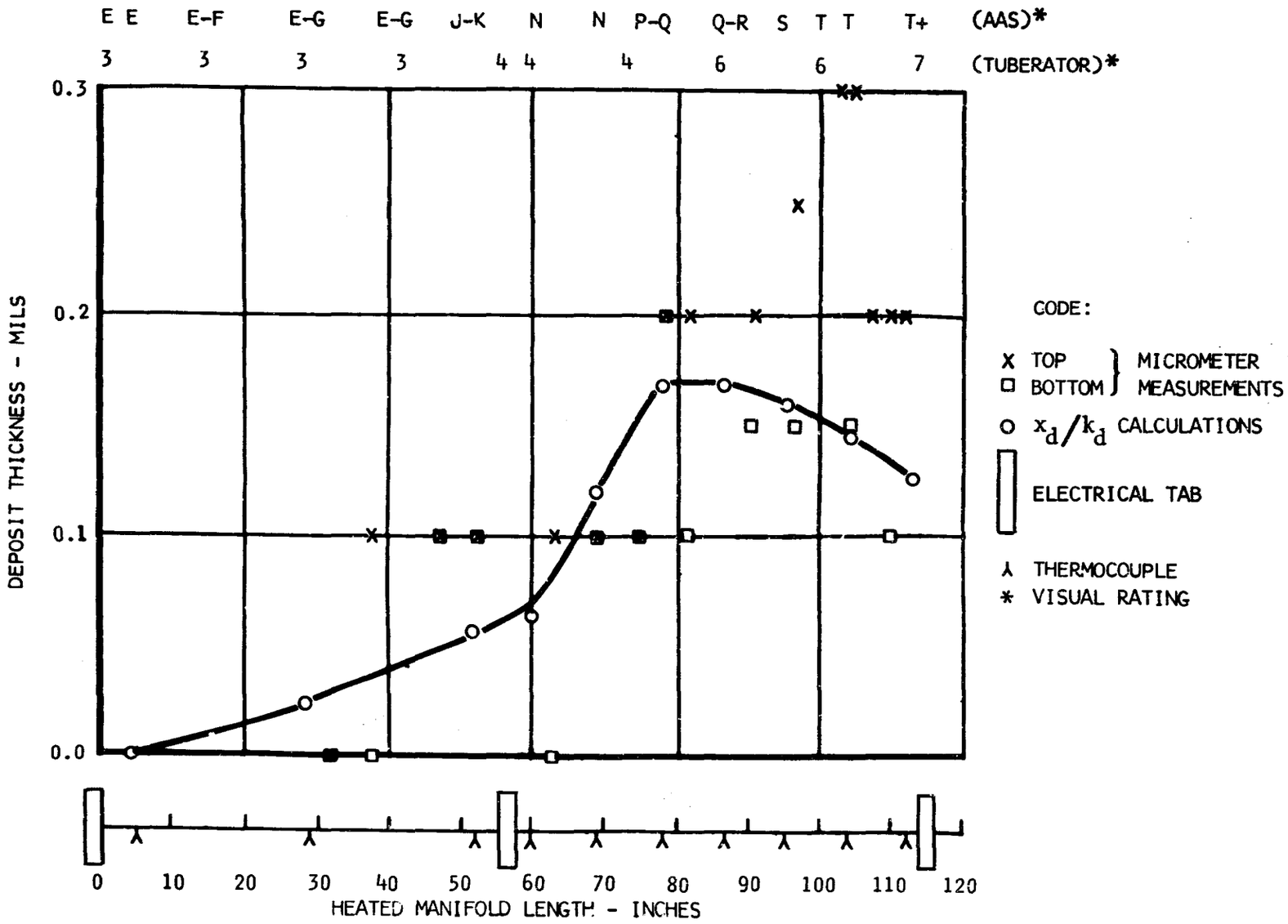

Figure 18. Manifold Deposit Thickness - Eighth Test Series

Micrometer Measurement of Deposit Thickness

Measurements of deposit thickness were obtained for both the top and bottom halves of the manifold using an indicating micrometer. The procedure followed is described in reference 4. The results of these measurements are shown in figure 18. As stated in reference 4, these measurements are considered to be accurate to 0.1 or 0.2 mil; therefore, the resulting scatter of micrometer data points is not unexpected. The data seem to indicate that the deposit is thicker on the top half of the manifold which is in agreement with the results obtained on the seventh test series steady-state manifold (reference 6).

Microphotographs of Deposit

The technique used in obtaining microphotographs of manifold specimens is described on page 47 of reference 5. Based on the calculated deposit thicknesses along the length of the manifold, shown in figure 18, it was decided to obtain microphotos of specimens located 80.0 and 112.2 inches from the inlet electrical tab. Top views of the deposits at 80.0 and 112.2 inches are shown in figure 19.

The microphotographs indicate that the deposit at 80.0 inches is more uniform (lower peak to peak distance and less variation in thickness) than at 112.2 inches. Edge views of the deposits at 80.0 and 112.2 inches (figure 20) indicate that the minimum deposit thicknesses at both locations are close to 0.0 mils. The maximum deposit thickness at 112.2 inches is greater than at 80.0 inches; 0.72 mils versus 0.36 mils.

The thickness determined from x_d/k_d and micrometer measurements are in agreement that the deposits are thicker at 80.0 inches that at 112.2 inches, however, the microphotographs show the maximum deposit thickness to be greater at 112.2 inches. It is considered that the largest contributor to this apparent inconsistency is the difference in deposit thickness uniformity. The less uniform deposit at 112.2 inches, as evidenced by the microphotographs, causes the calculated effective deposit thickness from x_d/k_d measurements to be lower as the result of greater turbulence at the deposit surface. In addition, the total amount of deposit at 112.2 inches may be less than at 80.0 inches. The latter would explain why the micrometer measurements are also lower at 112.2 inches since crushing of the deposit occurs when these measurements are made.

Some disagreement in the measured deposit thickness is to be expected. Microphotographs of the deposit indicate that the deposit forms in a manner that produces an irregular surface. It has been determined (reference 5) that this irregular surface significantly affects measurements below 0.3 mil.

MAGNIFICATION 221X
45-DEGREE ANGLE

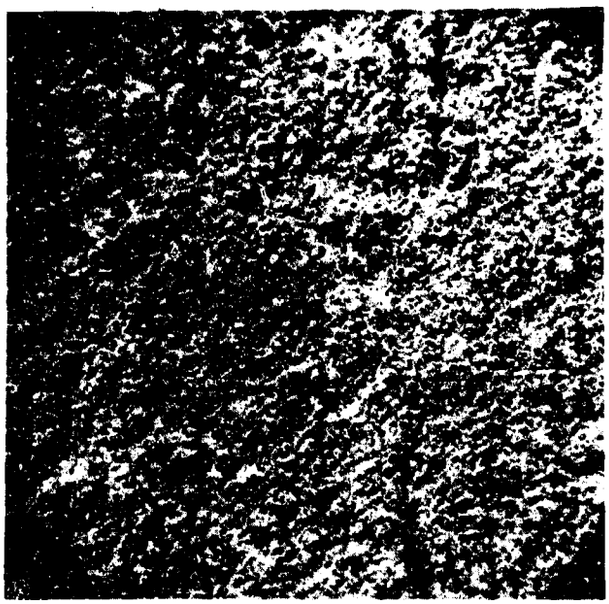

80.0 INCHES
FROM INLET TAB

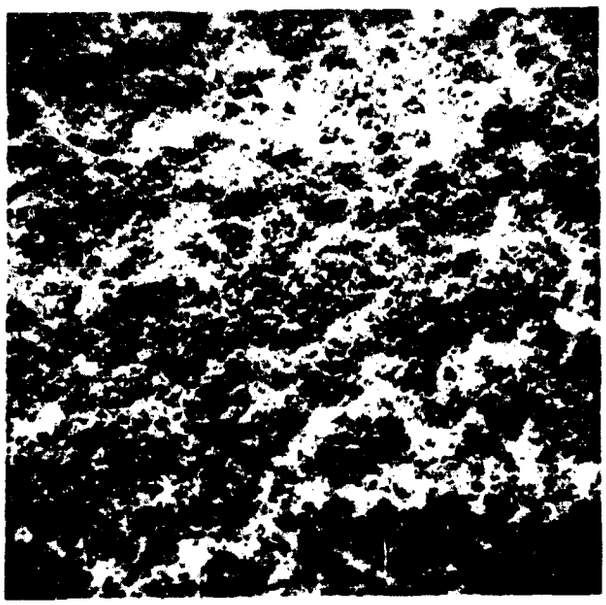

112.2 INCHES
FROM INLET TAB

Figure 19. Top View of Eighth Test Series Manifold

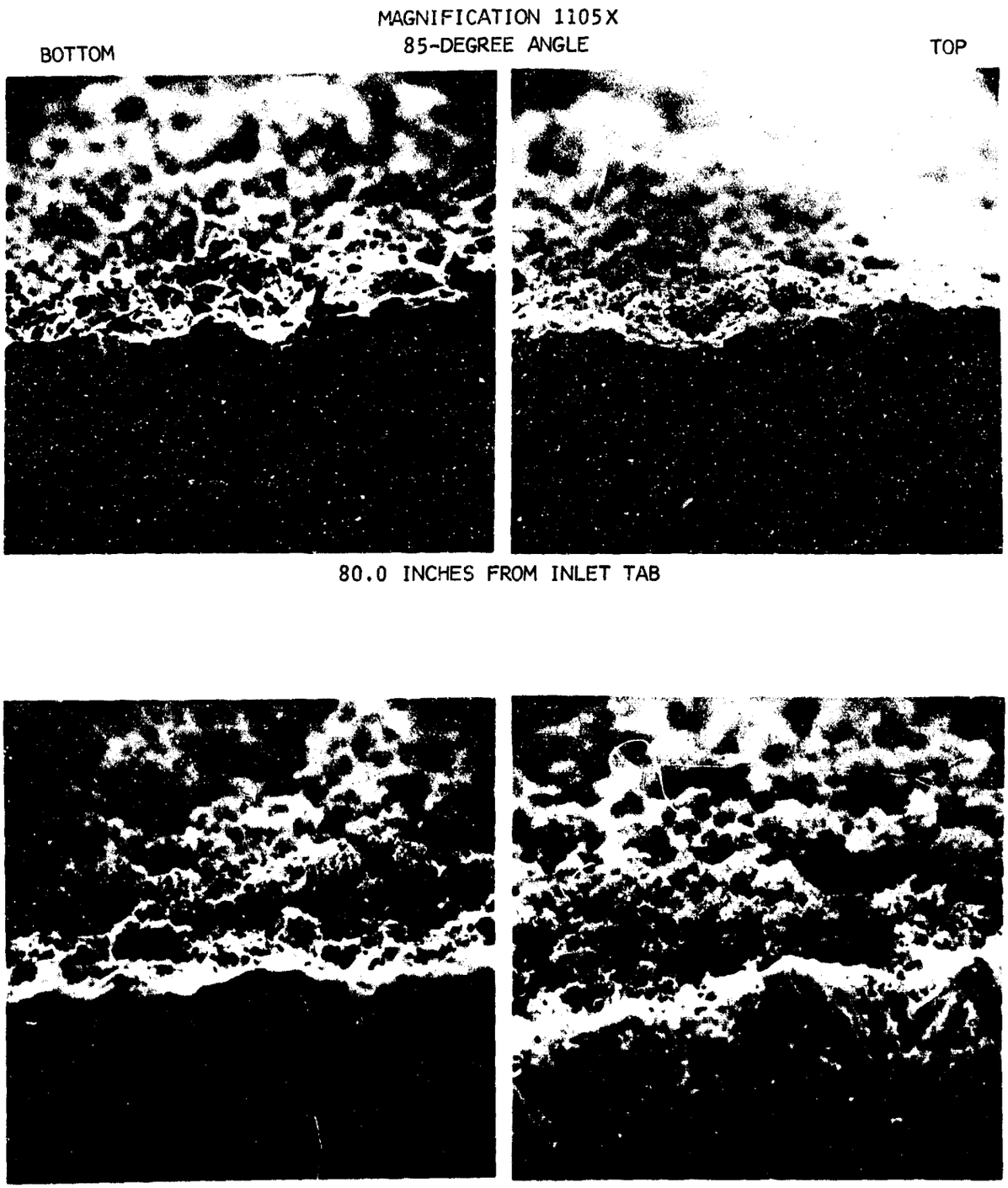

Figure 20. Edge View of Eighth Test Series Manifold

Visual Color Ratings

The AAS scale and Tuberator ratings of the manifold are shown in figure 18. The color of the manifold varied from tan to dark brown with no sharp transition range as was evident for fuel AFFB-11-68. No visual difference was observed between the top and bottom halves of the manifold.

Pressure Drop

The pressure drop of the manifold at a flow rate of 5.8 gpm was measured during the testing, and the measurements are shown in figure 21. An analysis using the least squares technique shows an increased pressure drop of 0.5 psi. However, the low correlation coefficient (0.1) indicates that it is doubtful a measurable change actually occurred.

NOZZLE SUBSYSTEM

The nozzle subsystem contained the same nozzle element for the duration of the 175 test cycles conducted. The results of measurements of the nozzle pressure drop are shown in figure 22. A decrease of approximately 2.6 psi (0.3 percent) is indicated by an analysis using the least squares technique on all the data including the pretest and posttest series calibration data. This change is less than the sensitivity of the instrumentation. However, considering the pretest and posttest data alone indicates that the pressure drop decreased 6.0 psi (0.8 percent). Additional analysis indicates that if the pretest data is omitted, the decrease in pressure drop is 1.3 psi (0.17 percent), which is well below the sensitivity of the instrumentation. A similar analysis of the pressure drop data for previous nozzles indicates that a significant decrease in pressure drop occurs during the first ten test cycles. It is considered that a physical change in the nozzle occurs during the first ten test cycles, probably due to heating. It is recommended that in future testing the data from the pretest calibration be omitted in determining the change in pressure drop.

A photograph of the nozzle is shown in figure 23 with a new nozzle. The nozzle screen rated D (AAS Scale) and did not contain any flakes. The deposit on the screen appears as a slight stain and is not thought to be sufficient to affect the nozzle performance.

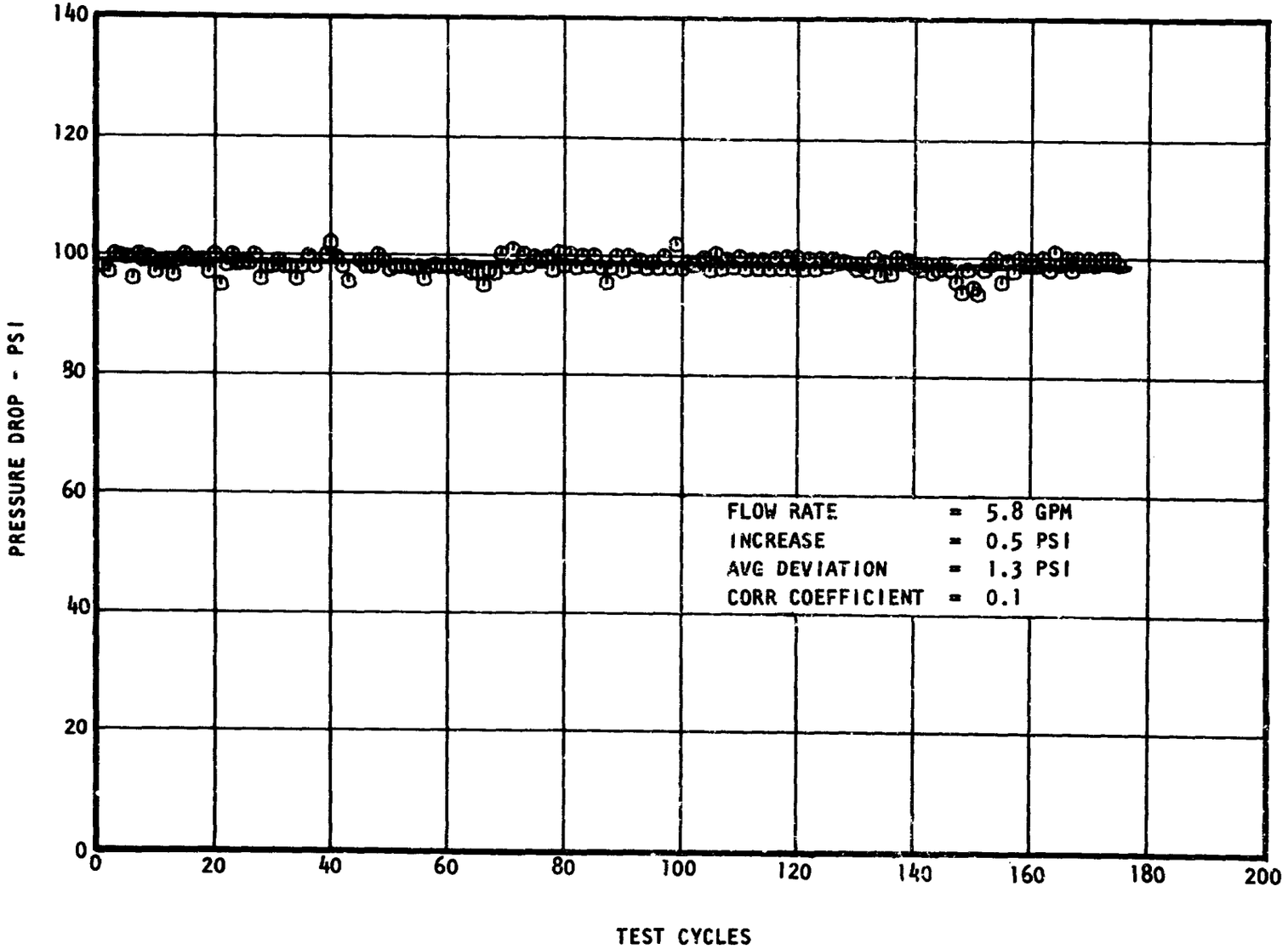

Figure 21. Pressure Drop Across Engine Manifold

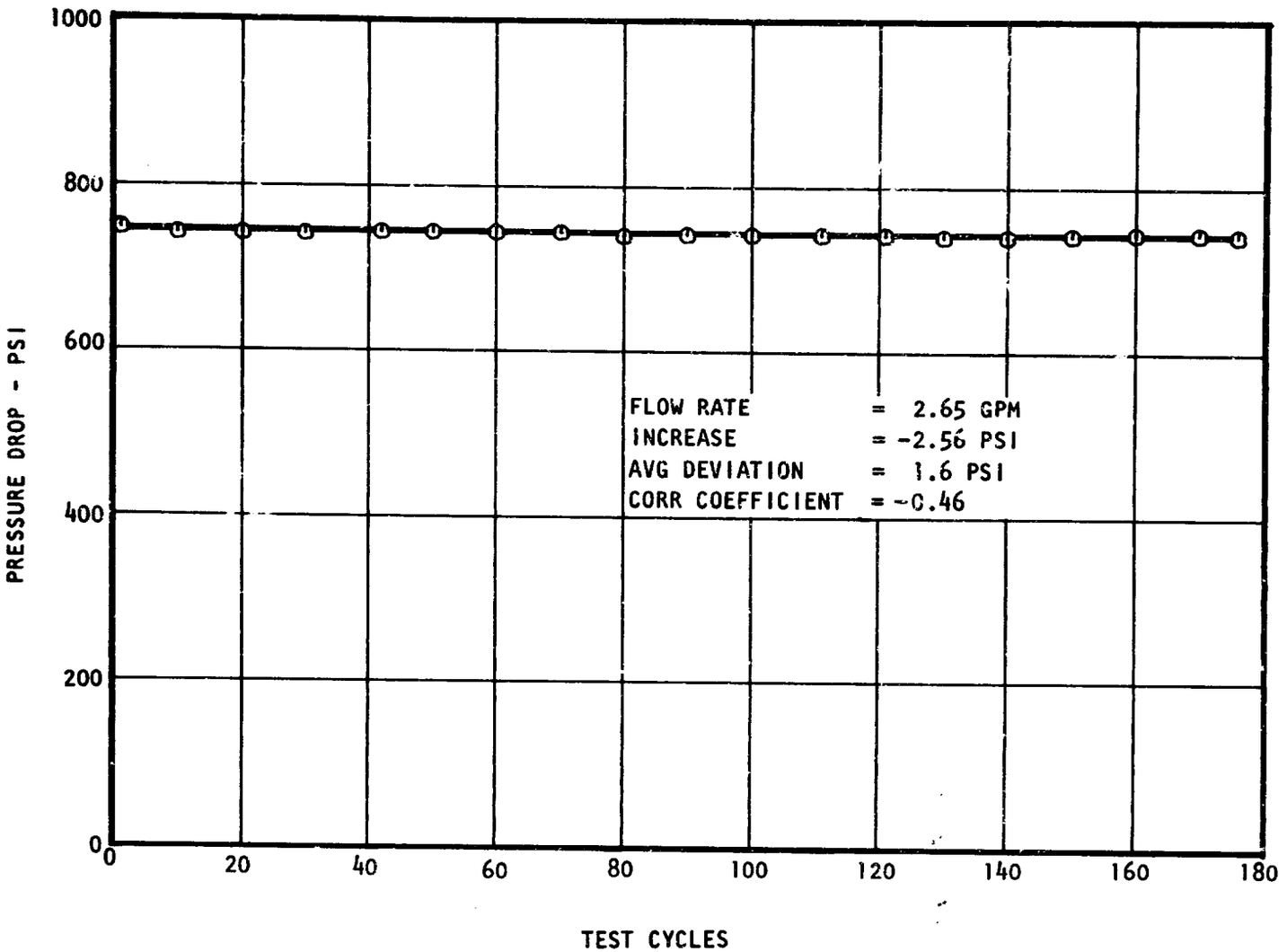

Figure 22. Pressure Drop Across Engine Nozzle

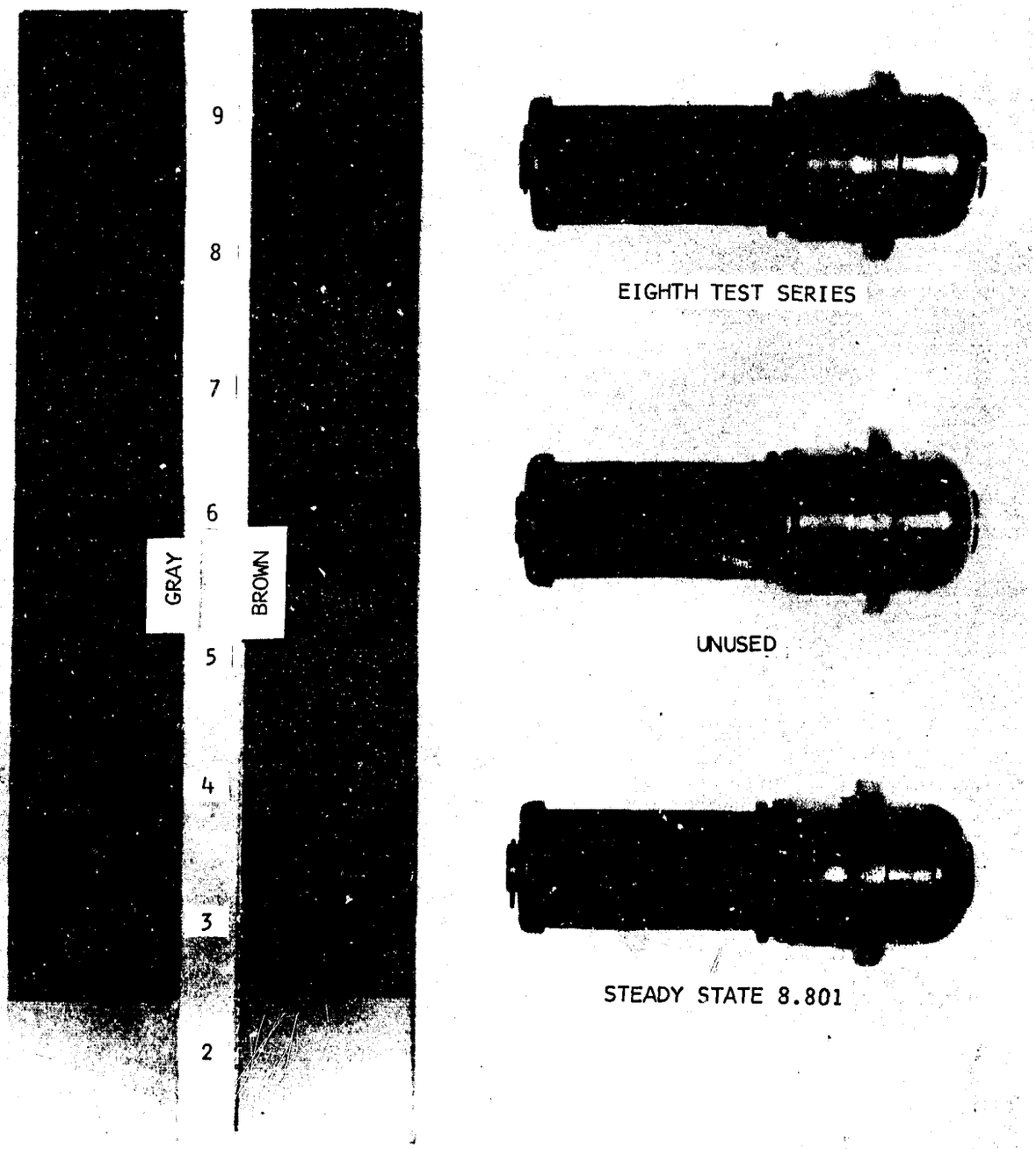

Figure 23. Engine Nozzles

ADDITIONAL LABORATORY ANALYSES

Millipore Filtration

During test cycles 8.056 and 8.115, fuel samples, each 500 milliliters in volume, were taken at the outlet of the manifold and filtered through 0.45-micron Millipore filters. The samples were taken at average manifold outlet temperatures of 319°, 366°, 400°, 421° and 565° F. The filters were clean except for the filters from the 565° F samples. These two filters were very slightly discolored (ivory color) but are darker than the corresponding filter from fuel AFFB-11-68.

Oxygen Content

The dissolved oxygen in the fuel was measured during the eighth test series by Southwest Research Institute for the Air Force Aero Propulsion Laboratory. The method used for oxygen analysis was developed by Phillips Petroleum Company (reference 8) and modified as reported in references 4 and 6. The results from previous fuel series indicate a greater variation in the oxygen analysis results than desired. The following modifications were made in an attempt to minimize the variations:

1. Duplicate injections of air-saturated hexane were made with each set of samples

2. Larger fuel samples were injected (40 µl versus 20 to 26 µl)

3. Duplicate injections of each sample were made

The larger fuel samples were considered necessary in order to obtain adequate response for fuel samples of low oxygen content. The use of air-saturated hexane as a standard was investigated since it was believed that day-to-day variations in the chromatographic response to oxygen might be better compensated for by using a liquid hydrocarbon as a calibration standard rather than using air.

The results of the oxygen analysis are shown in table II. All results are calculated using air injection peaks for calibration. The table also includes the values for the oxygen content of air-saturated hexane based on air injection peaks.

The determinations of the oxygen content of air-saturated hexane show considerable variations. However, these variations do not parallel those of oxygen in the incoming fuel, i.e., low results for hexane are not necessarily encountered when results are low for incoming fuel samples. Therefore, calculation of the oxygen contents for fuel based on the response to air-saturated hexane would not compensate for the variation encountered with liquid fuel samples, whose calculated oxygen content was based on the response to air injections.

TABLE II. SIMULATOR OXYGEN ANALYSIS MEASUREMENTS - FUEL AFFB-12-68 (PPM)

Condition	Before Test Startup	Beginning of Cruise				End of Cruise				Descent	Hexane	
Test/Minutes	0	25				120				131	Sample No. 1(a)	Sample No. 2(b)
Sample Valve*	3	4	5	6	7	4	5	6	7	7		
8.093	67	14	15	13	13	10	8	10	8	4	118	114
8.095	67	14	11	11	12	9	9	8	7	<2	122	118
8.097	54	10	10	10	9	7	6	8	7	<2	99	111
8.099	80	14	13	13	13	6	6	8	10	<2	110	104
8.101	61	10	12	11	13	7	13	7	6	<2	116	122
8.104	72	15	13	15	18	6	7	12	16	3	115	129
8.108	54	12	11	14	11	8	9	7	7	<2	109	133
8.110	66	14	18	15	17	8	7	10	11	4	122	122
8.112	50	11	12	11	11	7	9	7	6	<2	116	132
8.114	48	15	13	13	17	13	7	9	10	<2	124	124
8.116	59	11	10	11	12	8	7	7	7	<2	127	127
8.118	62	14	13	12	11	7	7	9	8	<2	117	123
8.120	65	15	14	15	13	8	10	15	8	<2	115	127
8.124	54	9	9	10	10	6	8	9	7	<2	121	129
8.126	56	11	11	9	9	7	5	5	6	<2	114	126
Average	61	13	12	12	13	8	8	9	8	<2	116	123

(a) Run at same time as the before test startup and beginning of cruise samples.

(b) Run at same time as the end of cruise and descent samples

Source of data: Southwest Research Institute, Letter No. 12-2497-D, dated 9 July 1969

*Sample Valve No. — Location

3 — Simulator refueling lines
4 — Fuselage tank outlet
5 — Engine pump outlet
6 — Engine heat exchanger outlet
7 — Engine manifold outlet

Southwest Research Institute suggested the following improvements in the method used to determine the oxygen content of the fuel:

1. Change the type of sampling device to minimize the possibility of air contamination between sampling and analysis and during withdrawal of the sample from the device.

2. Reduce the electronic noise level of the chromatograph to allow greater sensitivity.

3. Redesign the sample port of the chromatograph to provide more efficient atomization of liquid samples.

The repeatibility of the oxygen measurements was evaluated by determining the standard deviation for each column of data for all the fuels tested and comparing the results for equivalent conditions. The standard deviations are shown in table III.

A comparison of the results at the cruise and descent conditions show no significant difference in the standard deviations between the methods used. Comparison of the "before test startup" data shows a two-to-one improvement in repeatibility between fuels AFFB-8-67 and AFFB-9-67. A small improvement seems to have occurred between fuels AFFB-9-67 and AFFB-10-67 with the repeatibility from fuels AFFB-10-67 and AFFB-11-68 approximately the same. A worse repeatibility appears to have occurred for fuel AFFB-12-68 when compared to the results from fuel AFFB-11-68.

TABLE III. STANDARD DEVIATION OF OXYGEN MEASUREMENTS (PPM)

Condition	Before Test Startup	Beginning of Cruise				End of Cruise				Descent
Test/Minutes	0	25				120				131
Sample Valve	3	4	5	6	7	4	5	6	7	7
AFFB-8-67	15.0	4.5	3.5	3.6	2.5	2.4	2.1	2.4	1.0	0.0
AFFB-9-67	7.1	1.4	2.1	1.7	1.8	2.3	1.6	1.7	1.2	1.4
AFFB-10-67	5.9	3.5	3.7	2.5	2.8	1.6	1.6	2.0	2.0	1.6
AFFB-11-68	6.5	2.3	2.0	2.0	2.2	1.9	2.8	3.0	2.4	0.9
AFFB-12-68	8.7	2.1	2.3	2.0	2.8	1.8	2.0	2.4	2.6	-

SECTION IV

SIMULATOR STEADY-STATE MANIFOLD TESTS

The purpose of the steady-state and steady-state-flush manifold tests is to determine the rate of deposit formation of fuel AFFB-12-68 under constant temperature conditions. These data are compared to the data obtained during the cyclic tests and will be used to provide a basis of correlation to the small-scale tests which are operated in a steady-state manner. The steady-state-flush portion of the tests include periods of simulated acceleration flow conditions.

STEADY-STATE OPERATIONAL PROCEDURE

Two steady-state tests were performed on fuel AFFB-12-68 and were designated as 8.801 and 8.802. These tests were performed prior to the cyclic tests and at the same environmental conditions as steady-state tests 7.802 and 7.803 on fuel AFFB-11-68.

The tests were conducted for the following time durations and temperature conditions:

Test Designation	Fuel Temperature (° F) In	Out	Steady-State Time (Hr.)	Conditions
8.801	265	565	82	Steady-state
	265	565	24	Steady-state-flush
	265	565	11	Steady-state
8.802	265	565	67	Steady-state
	265	565	20.5	Steady-state-flush

The procedure used in the steady-state and steady-state-flush tests can be found in reference 5.

The temperature and flow rate data obtained during these tests were used in two computerized programs. One program provided for calculation of the heating rate, theoretical and actual heat transfer coefficients, inner tube wall temperature or maximum fuel film temperature, and deposit thermal resistance. The second program provided for plotting deposit thermal resistance as a function of steady-state elapsed time. The method of calculation for deposit thermal resistance is shown on page 63 of reference 3.

RESULTS

TEST 8.801

Deposition Rate

The computerized graphical output of the calculated deposit thermal resistance (x_d/k_d) for test 8.801 is shown in appendix II. It was noted that x_d/k_d was initially decreasing at the outlet tube wall thermocouple location. This indicated loss in deposit thickness prior to deposit buildup was also evident during the testing of fuels AFFB-10A-67 and AFFB-10B-67 (reference 5). The results of various investigations of the possible causes of this phenomenon are reported therein and it is concluded that the cause is an induced turbulence of the laminar sublayer by rough deposits. The induced turbulence causes the fuel side heat transfer coefficient to rise thus negating the effect of the initial deposit buildup on overall heat transfer efficiency. The initially decreasing x_d/k_d has only been evident with some fuels (i.e., fuels AFFB-10A-67, AFFB-10B-67 and AFFB-12-68) and, with these fuels, only at the outlet thermocouples under steady-state conditions.

The steady-state deposition rates, obtained from appendix II, are shown in figure 24. Only the linear deposition rates are shown since the duration of the initial deposition rates was relatively short.

The transition from steady-state to steady-state-flush conditions at 82 hours did not produce a loss in deposit as would be evidenced by a distinct drop in x_d/k_d nor was there a consistent change in the rates of deposit formation. The steady-state-flush deposition rates for thermocouples TC-7 and TC-8 were higher than the steady-state rates, and for thermocouples TC-9 and TC-10 the steady-state-flush rates were lower than the steady-state rates. As found with fuel AFFB-11-68, the rate of deposit formation for the deposit level attained is not dependent upon the flushing action, thus it appears that fuels of high thermal stability produce deposits which are more tenacious than deposits of lower quality fuels. Fuels AFFB-9-67 and AFFB-10-67 produced deposits that were eroded from the tube by application of the acceleration condition flow rate (5.8 gpm).

Deposit Thickness

The manifold was bisected and sectioned and is shown in figure 25. As in fuel AFFB-11-68 manifolds, there was a sharp transition from stain to heavy deposit with the transition occurring closer to the inlet on the top half than on the bottom half by 2.3 inches. The transition was sharper for the 8.801 manifold than for any of the manifolds from previously tested fuels. The transition started at approximately the same location, 63 inches from the inlet, as in manifold 7.803 (fuel AFFB-11-68). The portion of the manifold prior to the transition was grey with some slight differences in shading in the first 12 inches. The visual ratings of the manifold tube (AAS scale and Tuberator) are shown in figure 26.

The transition region was closer to the inlet on the top half of manifold 7.803 (reference 6) and it was concluded, based on micrometer measurements, that the deposits were thicker on the top half of the manifold. Since the transition region for manifold 8.801 was also closer to the inlet on the top half it was decided to investigate the deposit thickness of each half of the manifold.

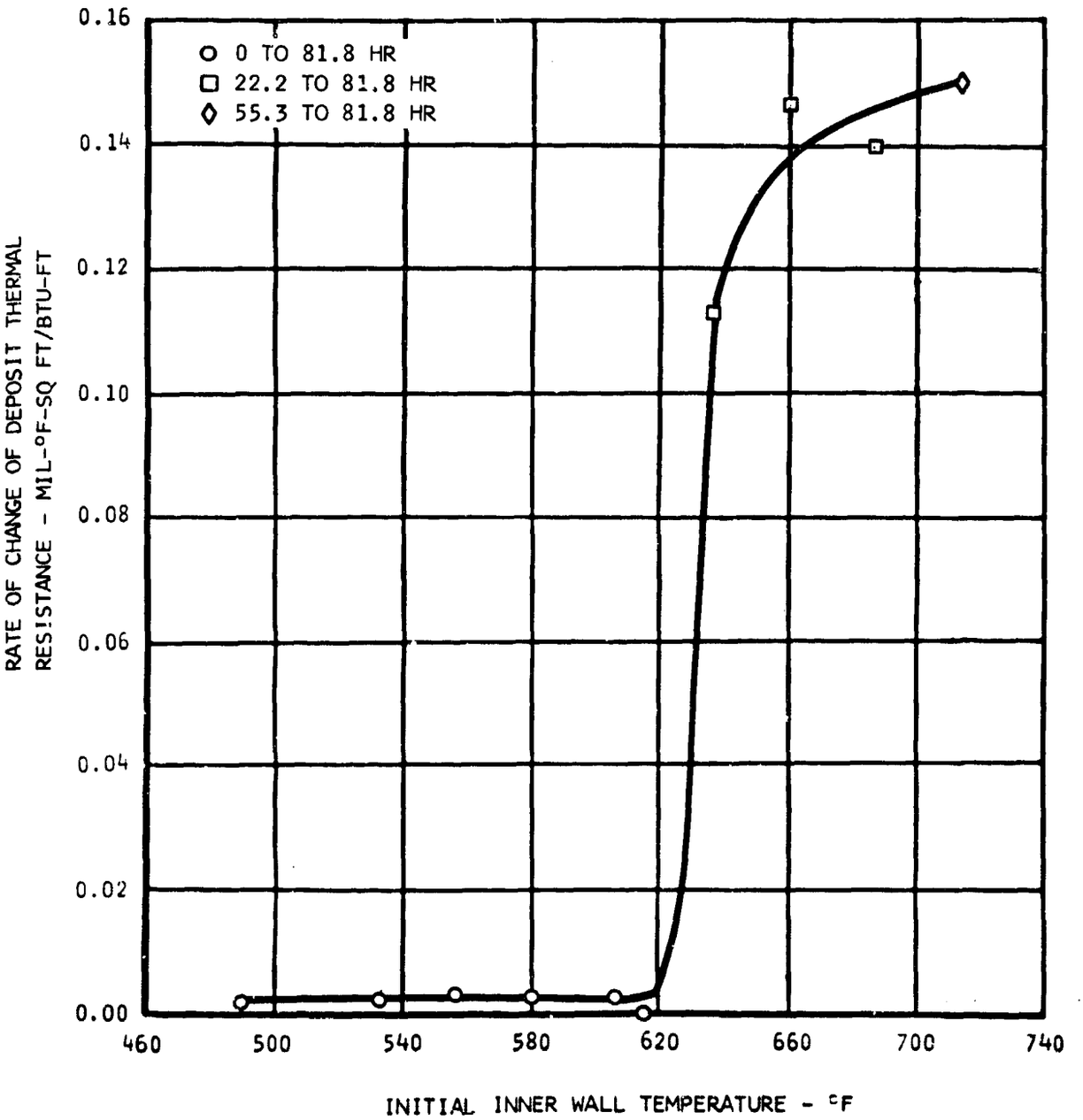

Figure 24. Linear Steady-State Deposition Rates - Test 8.801

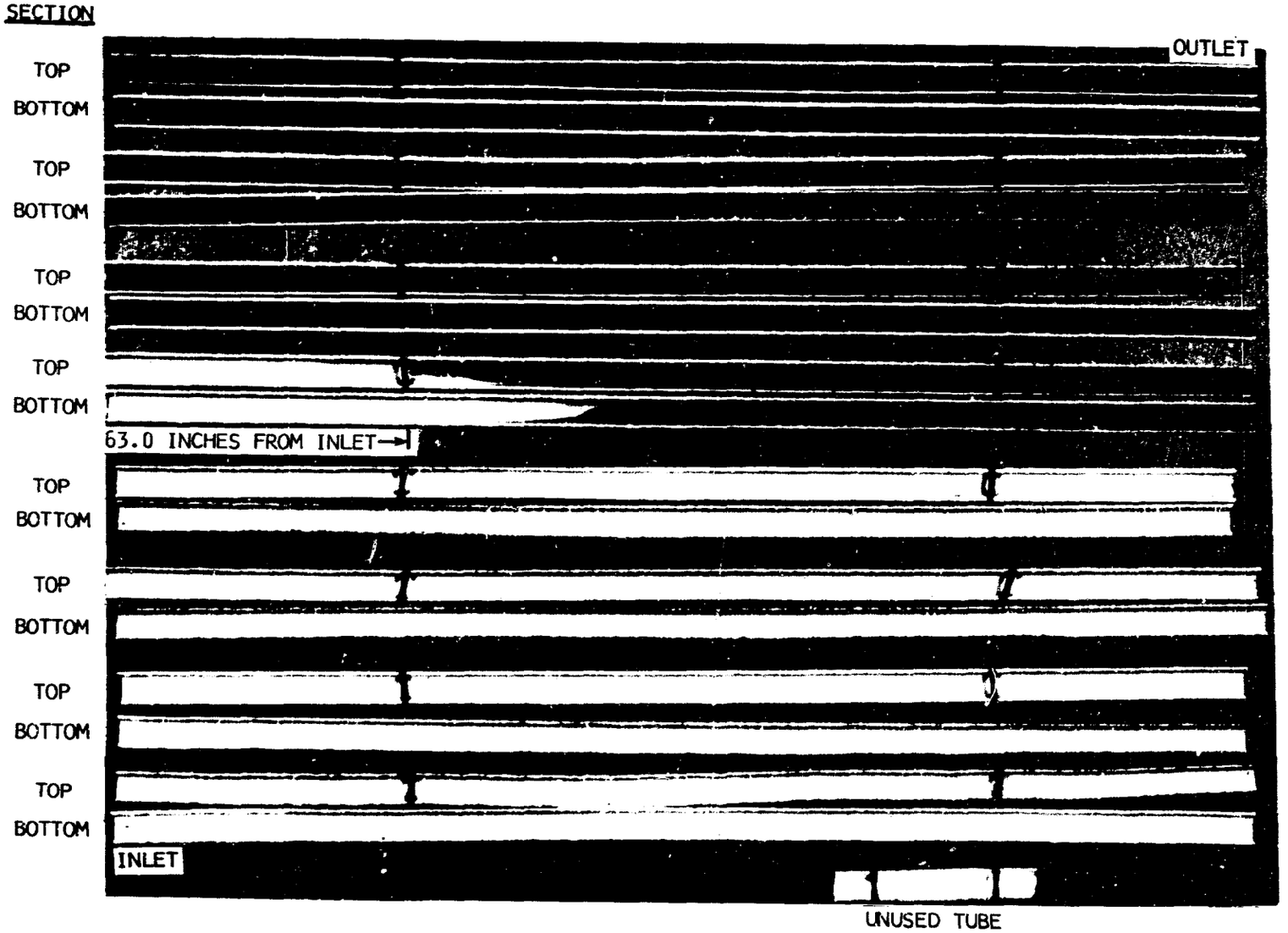

Figure 25. Manifold Used in Test 8.801

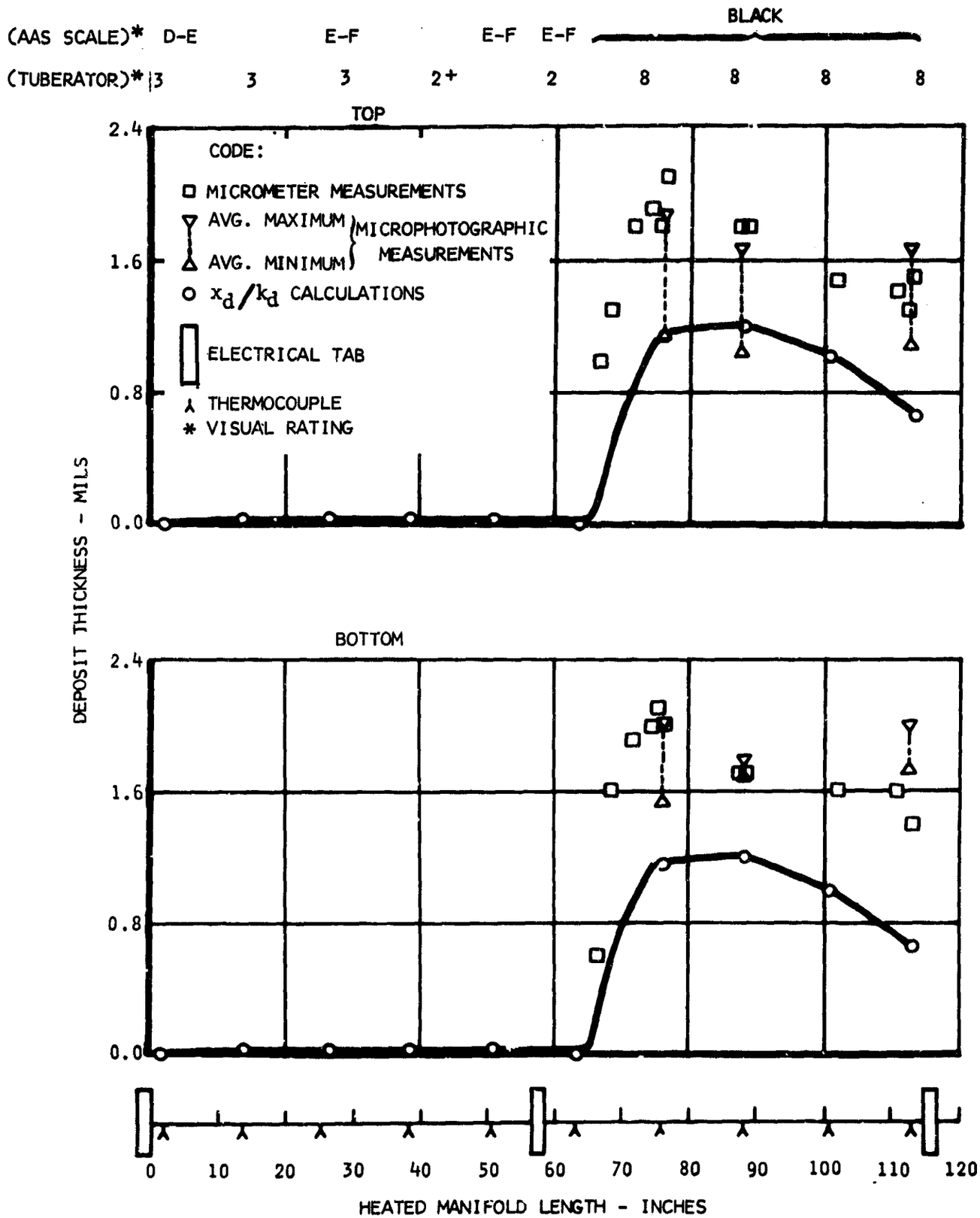

Figure 26. Manifold Deposit Thickness - Test 8.801

Deposit thickness measurements were made for each half of the manifold using an indicating micrometer. These measurements are shown in figure 26. It is considered that the measurements do not indicate any significant difference between the top and bottom of the manifold.

Microphotographs were taken of the deposit at several locations along the manifold tube. Representative microphotographs are shown in figure 27. These microphotographs show that the deposit is very porous at all locations. While preparing the specimens for microphotographs it was determined that the deposit near the outlet was very fragile. This condition is the probable reason why the deposit is thinner at the outlet than at 75 inches.

Deposit thicknesses determined from the microphotographs are shown in figure 26. The microphotographs indicate the deposit is thicker on the bottom of the manifold. The differences in thicknesses generally exceed the accuracy of the measurements (0.1 to 0.2 mil accuracy), therefore, there is a good confidence level that the deposits are actually thicker on the bottom half of the manifold. This result is not in agreement with the results from manifold 7.803 and seems to be inconsistent with the transition region being closer to the inlet on the top half of the manifold. The inconsistency with manifold 7.803 could have been caused by the manifold tube bowing in the opposite direction to manifold 7.803 (see discussion on effect of bowing in reference 6).

The deposit thickness based on the change in x_d/k_d was obtained for each thermocouple using the assumed thermal conductivity (k_d) of 0.07 BTU/hr-ft-° F. These thicknesses are shown in figure 26 for both halves of the manifold since the thermocouples are wrapped circumferentially around the manifold and produce average measurements of x_d/k_d.

Very good agreement is evident between the average thicknesses determined from micrometer and microphotographs. These values are higher than the thickness measurements determined from x_d/k_d and probably indicate that the correct value for k_d of this deposit is close to 0.11 BTU/hr-ft-° F.

Nozzle

The pressure drop across the nozzle was measured before and after test 8.801. Based on the results obtained there was a pressure drop increase of 0.8 percent at 2.65 gpm. The nozzle was then dried and inspected. The nozzle screen was slightly stained, rating from a G (AAS Scale) to black, with approximately 75 percent of the screen being black. The support tube was still visible through the screen. A photograph of the nozzle is shown in figure 23 with a new nozzle.

TEST 8.802

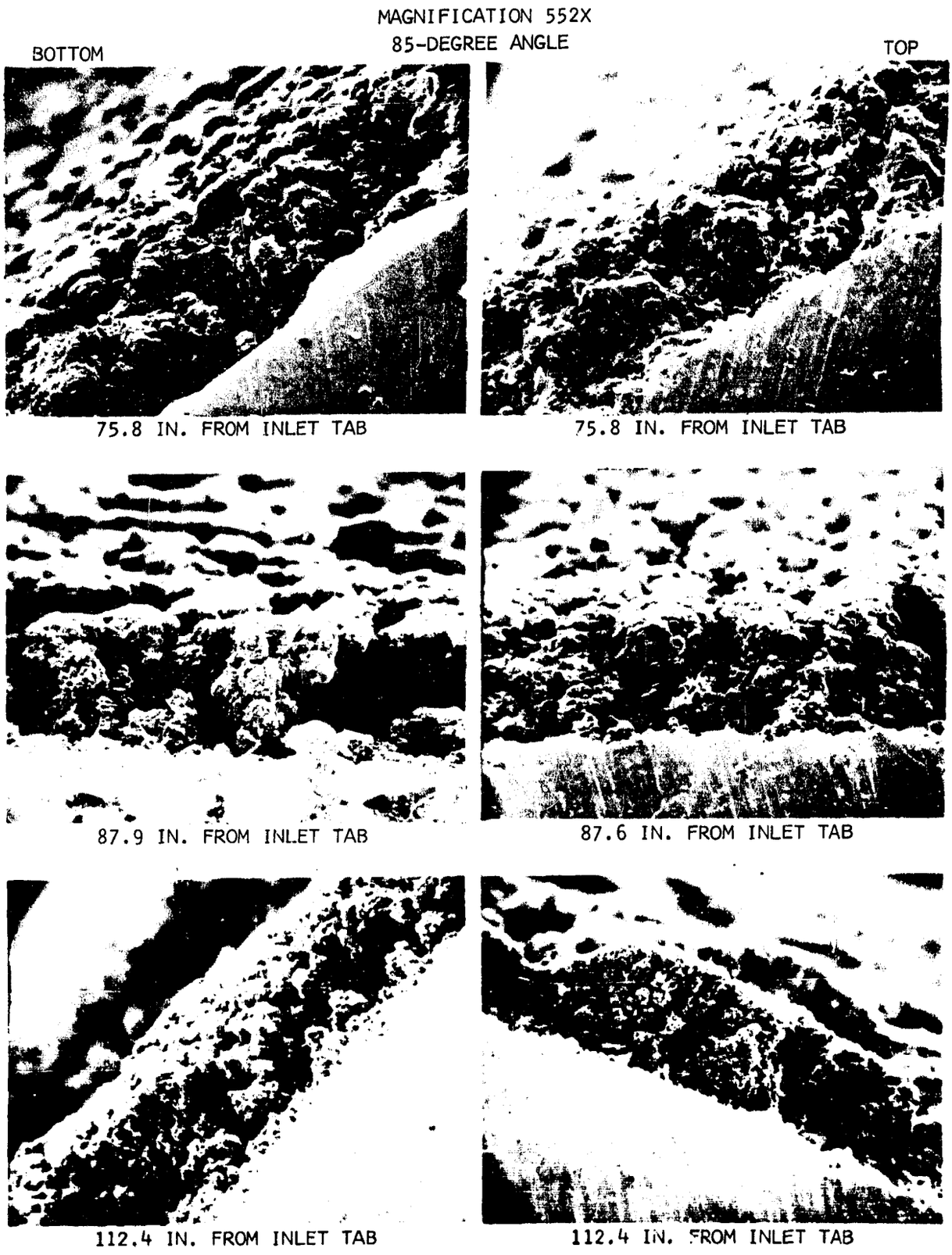

Figure 27. Edge View of Steady-State Manifold 8.801

Instrumentation

The stainless steel sheathed thermocouples used on all manifolds since the second steady-state test of fuel AFFB-8-57 are attached by circumferentially tack-welding the sheath 240 degrees (2/3 turn) around the manifold tube. Based on a suspected circumferential variation in manifold tube wall temperatures reported in reference 6, other methods of thermocouple attachments were additionally made in order to minimize or eliminate the temperature averaging effect that occurs with a circumferential thermocouple. Four thermocouples, two on the top of the tube, one on the bottom of the tube and one on the side of the tube, were longitudinally tack-welded for 0.75 inch to the manifold tube. Two thermocouples, one on the top of the tube and one on the bottom of the tube, were attached 45 degrees circumferentially around the tube and one thermocouple was attached 600 degrees (1-2/3 turns) around the tube.

With the exception of the 1-2/3 turns wrapped thermocouple, the new types of thermocouple attachment gave results which were not consistent with the normally attached circumferential thermocouple results. It was determined that these thermocouples were giving erroneous results and other attachment methods were not pursued because it would have interfered with the steady-state test.

It is considered that the error in the 45 degree circumferentially wrapped thermocouples (10° to 20° F) was caused by a lack of contact area between the tube and the thermocouple sheath. It is regarded that the error in the longitudinal thermocouples (10° to 40° F) was due to the longitudinally varying d-c voltage used to heat the manifold tube (see page 45 of reference 3).

The significant results obtained from the eight normally attached thermocouples and seven thermocouples attached as described above are as follows:

1. Two normally attached (2/3 turn circumferential) adjacent thermocouples produced the same results.

2. The thermocouple wrapped 1-2/3 turns around the tube produced the same results as an adjacent normally attached thermocouple.

3. Thermocouples attached 45 degrees circumferentially produce lower readings (10° to 20° F) than normally attached thermocouples.

4. Thermocuples attached longitudinally produce higher readings (10° to 40° F) than normally attached thermocouples. Also, the readings obtained could be changed by movement of the unattached portion of the sheathed thermocouples.

5. The specially attached thermocouples, though producing erroneous values, increased in temperature at a rate consistent with nearby normally attached thermocouples.

6. The specially attached thermocouples, both 45 degree circumferential and longitudinal produced results showing the bottom of the manifold tube was hotter than top of the manifold tube. This is in agreement with that predicted on page 73 of reference 6 for a tube which has a downward bow. The manifold was also purposely bowed downward during the test and it was observed that the readout of the normally attached thermocouples and the top longitudinal thermocouple were unaffected. The readout of the side longitudinal thermocouple was slightly affected; no more than 2° F. The bottom longitudinal thermocouple increased by 10° F and remained at the increased level until the manifold was rebowed at which time the temperature decreased to its previous value. The 45 degree circumferential thermocouples had not been attached when this bowing test was made. The indicated temperature change caused by the bowing could be a false readout due to movement of the thermocouple assembly (see item 4) or an actual temperature change confirming the higher temperature of the bottom of a bowed tube.

Deposition Rate

The calculated x_d/k_d values for test 8.802 is shown in appendix III for the normally attached thermocouples and those specially attached thermocouples which were connected for most of the test.

The steady-state deposition rates are calculated in appendix III for the linear portion of the test only since the duration of the initial rate of deposit formation was relatively short. These rates are shown in figure 28 compared to the linear rates for test 8.801. With the exception of the rates obtained at approximately 720° F, very good agreement (within 10 percent) was obtained between the results of test 8.801 and 8.802.

As found in test 8.801, the transition from steady-state to steady-state-flush conditions at 67 hours did not produce a loss in deposit nor a significant or consistent change in deposition rate.

A comparison of fuel AFFB-12-68 steady-state linear deposition rates to those data obtained from the previous four fuels is shown in figure 29. It is evident that in this comparison that fuel AFFB-12-68 is not significantly different from fuel AFFB-11-68 under these conditions.

Deposit Thickness

The bisected 8.802 manifold is shown in figure 30. The transition from stain to heavy deposit occurred 4.5 inches closer to the inlet on the top half than on the bottom half compared to 2.3 inches for manifold 8.801. The transition started approximately 1.5 inches further downstream (64.5 inches from the inlet) than for manifold 8.801. The portion of the manifold

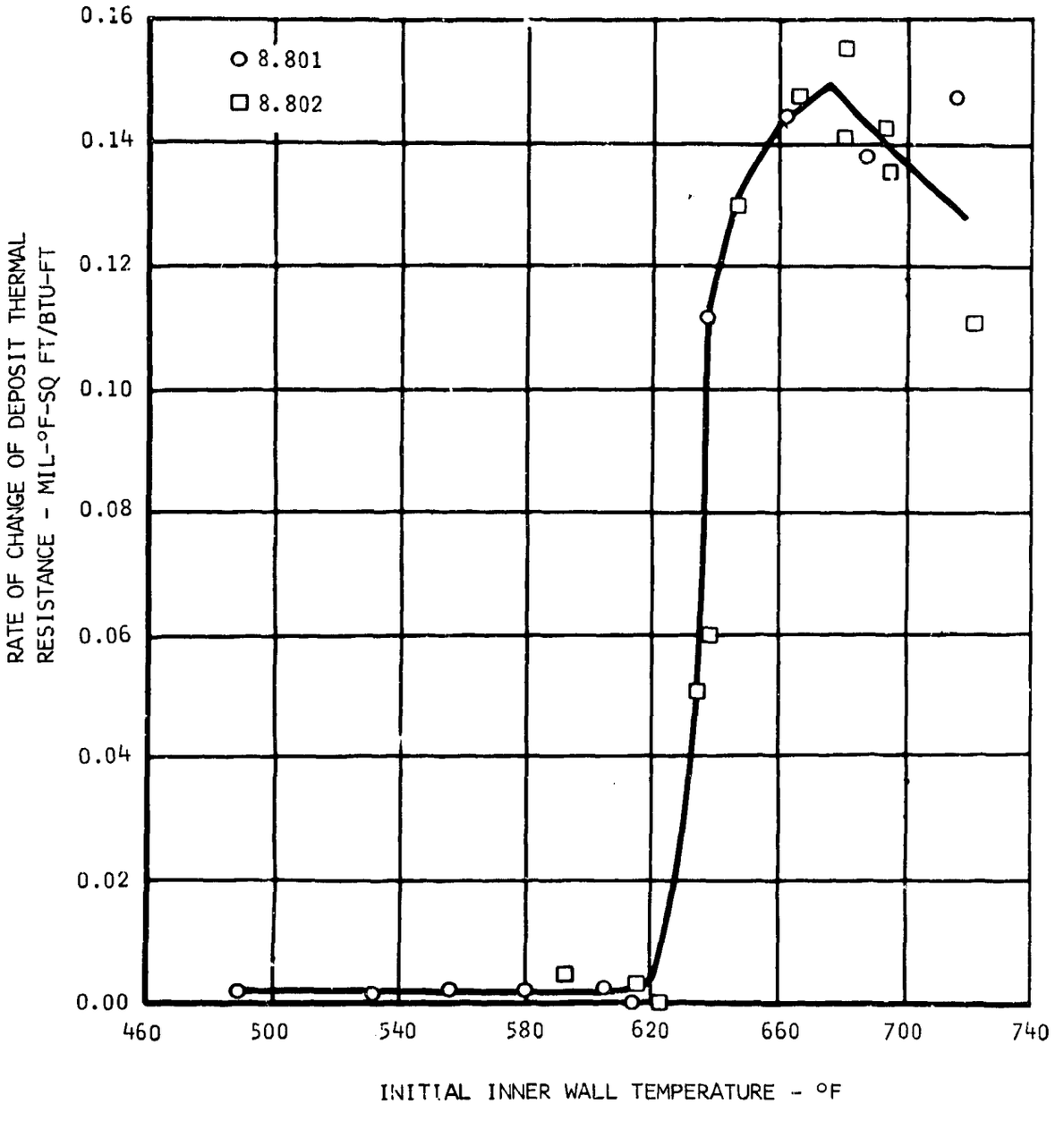

Figure 28. Linear Steady-State Deposition Rates - Tests 8.801 and 8.802

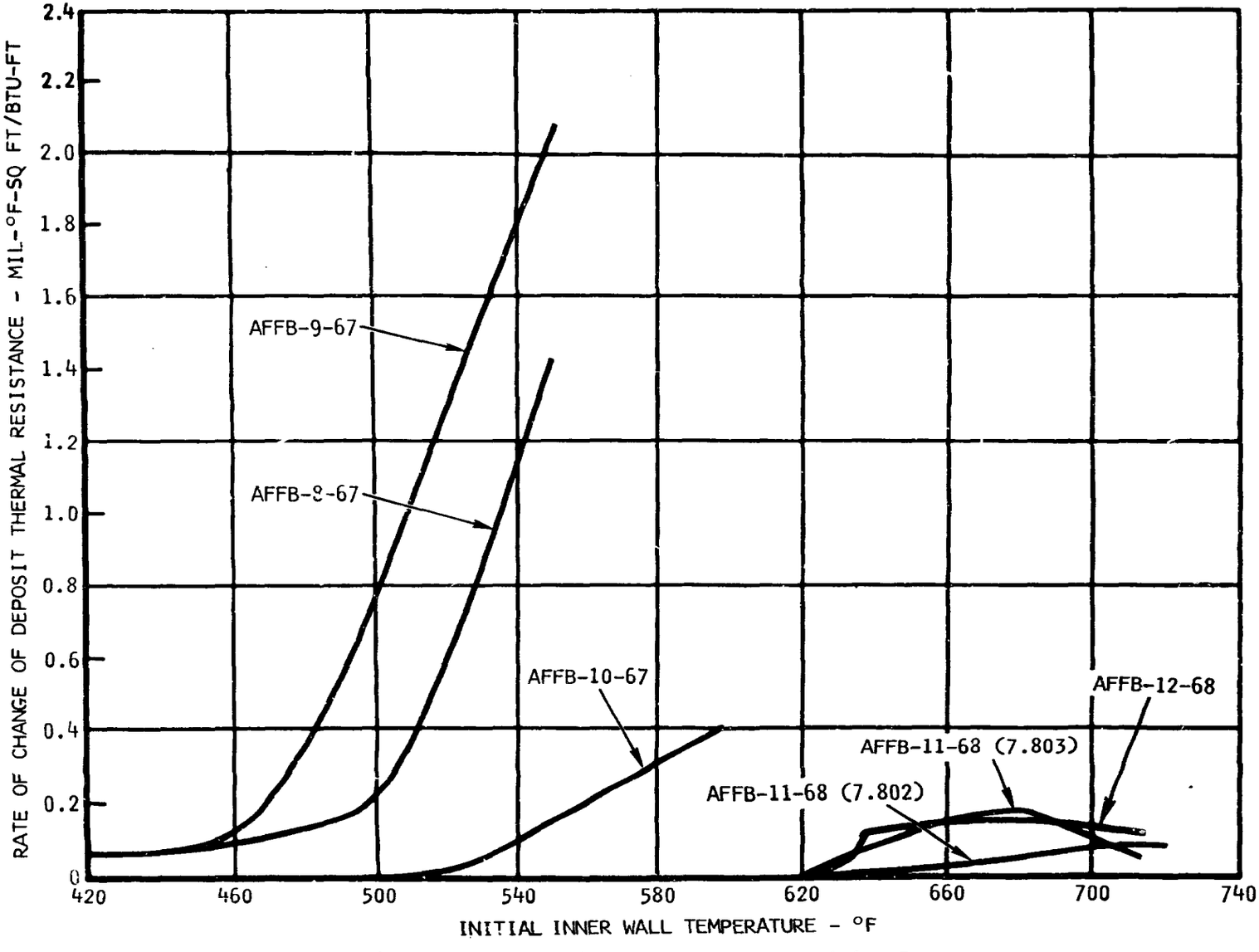

Figure 29. Steady-State Linear Deposition Rates

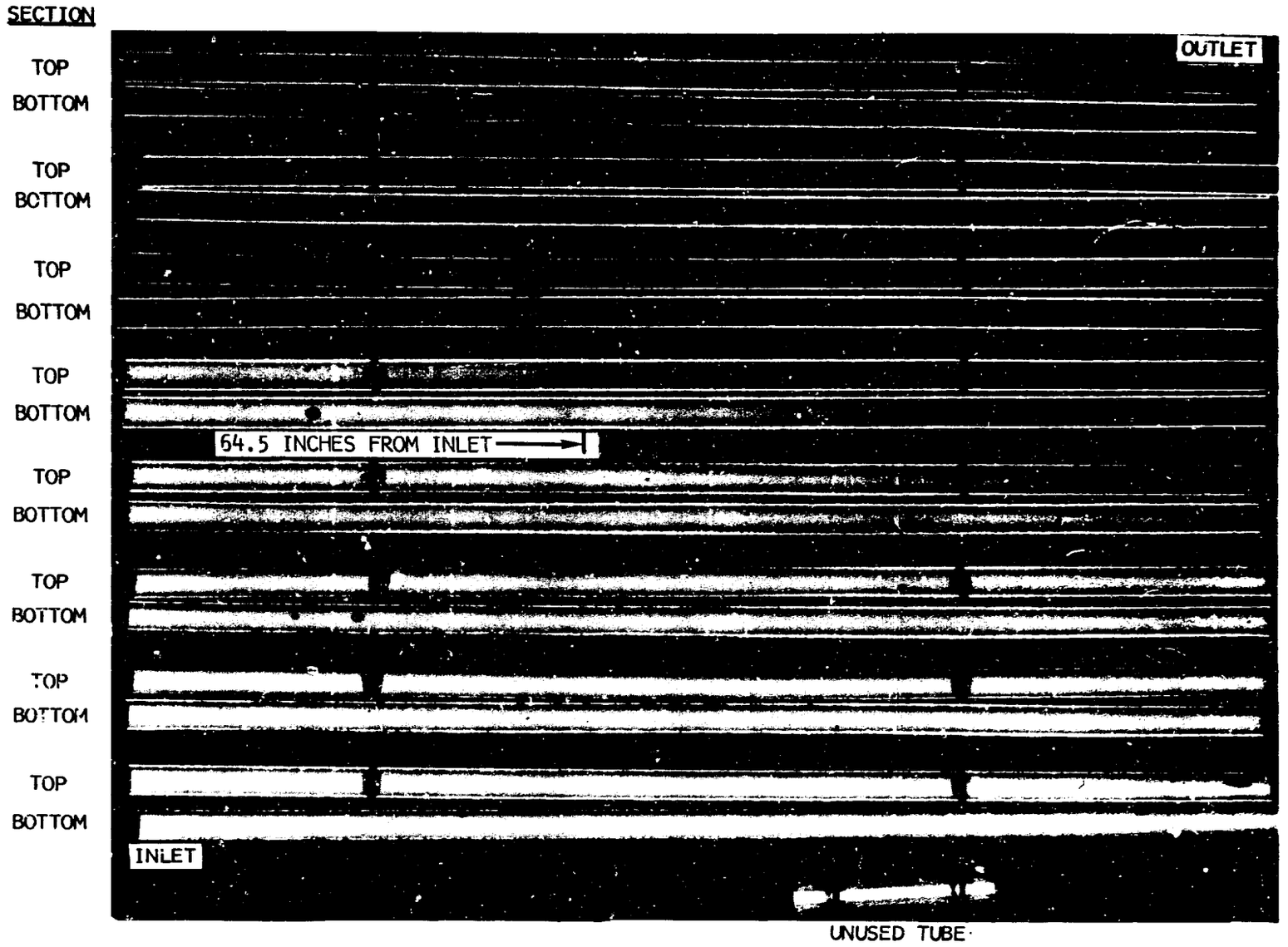

Figure 30. Manifold Used in Test 8.802

prior to the transition was a weak yellow color while that portion of the 8.801 manifold was much greyer. The visual ratings of the manifold tube are shown in figure 31.

As with manifold 8.801 it was considered appropriate to investigate the deposit thickness of each half of the manifold. Deposit thickness measurements were made for each half of the manifold using an indicating micrometer. The results of the measurements are shown in figure 31. It is considered that the measurements do not indicate any significant difference between the top and bottom of the manifold.

Microphotographs were taken of the deposit at selected locations along the manifold tube. Representative microphotographs are shown in figure 32. The microphotographs show that the deposits are porous, comparing closely in appearance to the manifold 8.801 deposits shown in figure 27. As observed for manifold 8.801, it was found that deposits near the outlet were the most fragile. It was also observed that the deposits on manifold 8.802 were more easily removed than the deposits on manifold 8.801.

Deposit thicknesses determined from the microphotographs are shown in figure 31. It is considered that the microphotographs, like the micrometer measurements, do not indicate any significant difference in deposit thickness between the two halves of the manifold.

The deposit thickness based on the change in x_d/k_d was obtained for each thermocouple using the assumed thermal conductivity (k_d) of 0.07 BTU/hr-ft-° F. These thicknesses are shown in figure 31 for both halves of the manifold since, as previously noted, the thermocouples produce average measurements of x_d/k_d.

Very good agreement is evident between the average thicknesses determined from micrometer and microphotographs. These values are higher than the thickness measurements determined from x_d/k_d and probably indicate the correct value for k_d of this deposit is close to 0.12 BTU/hr-ft-° F. This is in reasonable agreement with the value of 0.11 BTU/hr-ft-° F calculated for manifold 8.801.

Transition Region

The deposit formation in the transition region from stain to heavy deposit was investigated. Microphotographs were taken at 69.6 inches on the bottom half of the tube and are shown in figure 33. The direction of fuel flow through the manifold is from bottom to top in each picture.

Figure 33A shows the transition region magnified 55 times. In the right portion of the microphotograph spheriods are seen on essentially bare tube. The left portion shows the spheriods on a background of uniform deposit. These two areas are shown in figure 33B and 33C magnified 221 times. It can be seen that a "tail" of deposit exists downstream of many of the spheriods. The tails appear to have formed in groves in the tube.

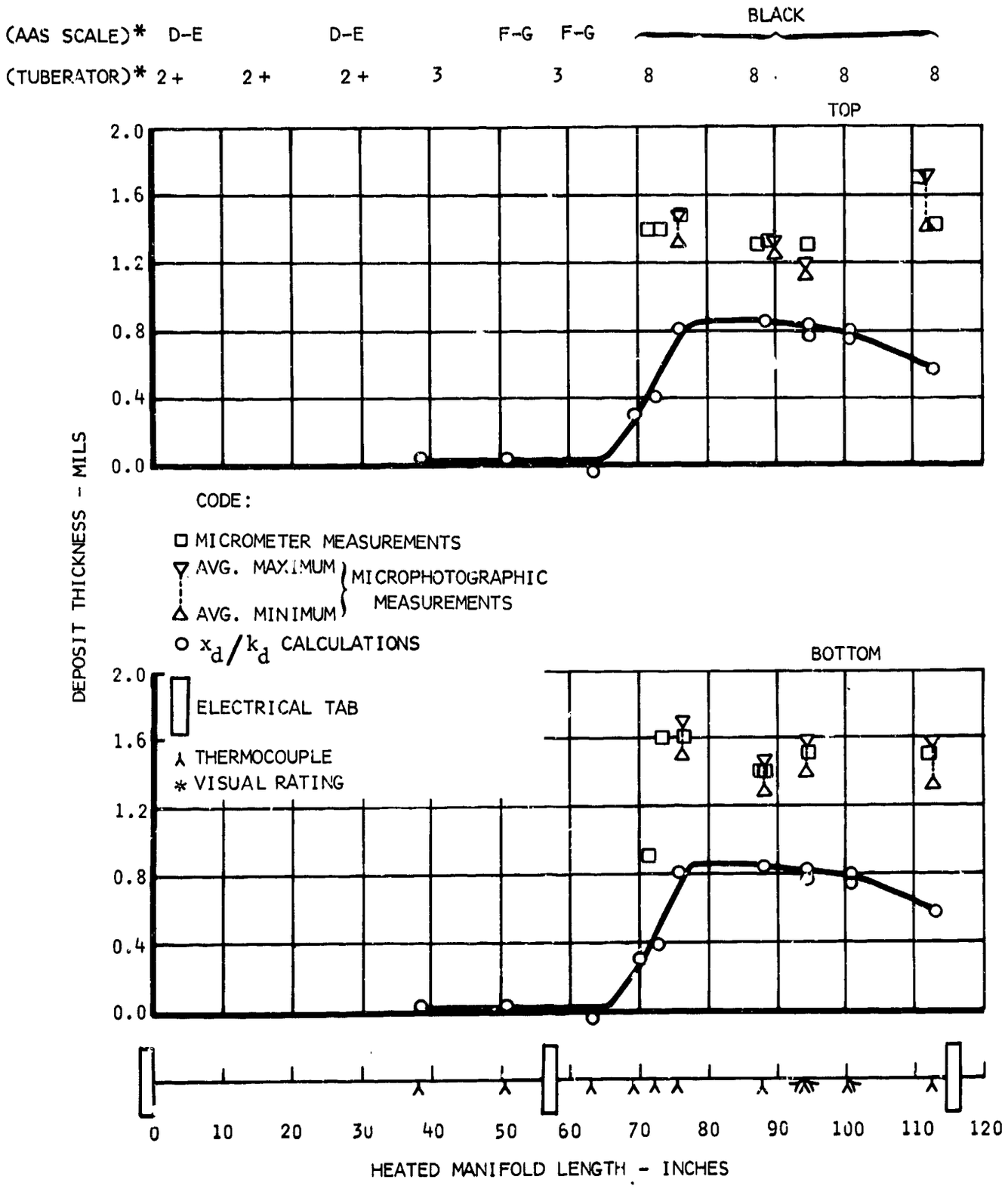

Figure 31. Manifold Deposit Thickness - Test 8.802

MAGNIFICATION 552X
85-DEGREE ANGLE

BOTTOM

TOP

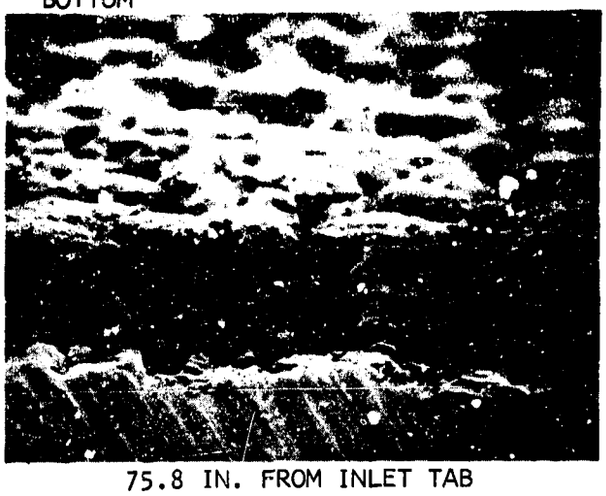

75.8 IN. FROM INLET TAB

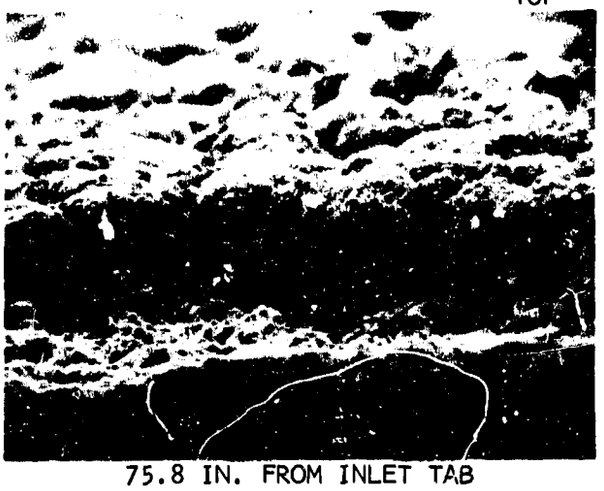

75.8 IN. FROM INLET TAB

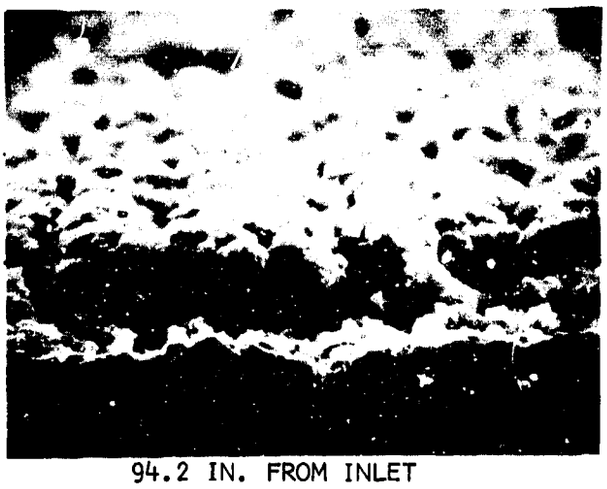

94.2 IN. FROM INLET

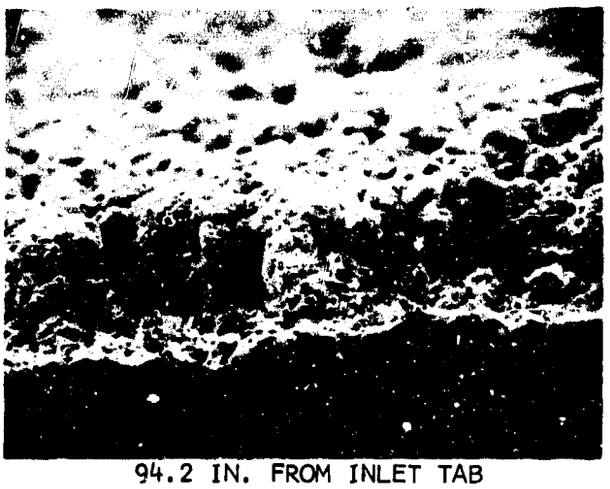

94.2 IN. FROM INLET TAB

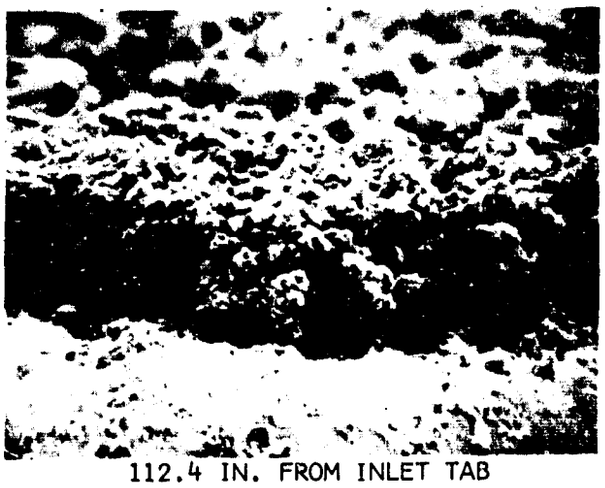

112.4 IN. FROM INLET TAB

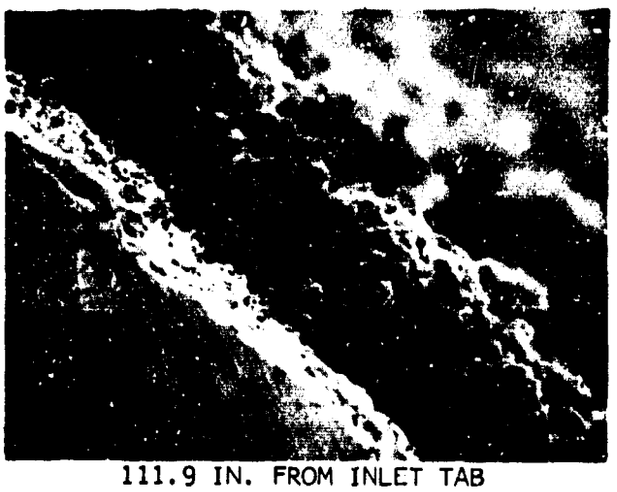

111.9 IN. FROM INLET TAB

Figure 32. Edge View of Steady-State Manifold 8.802

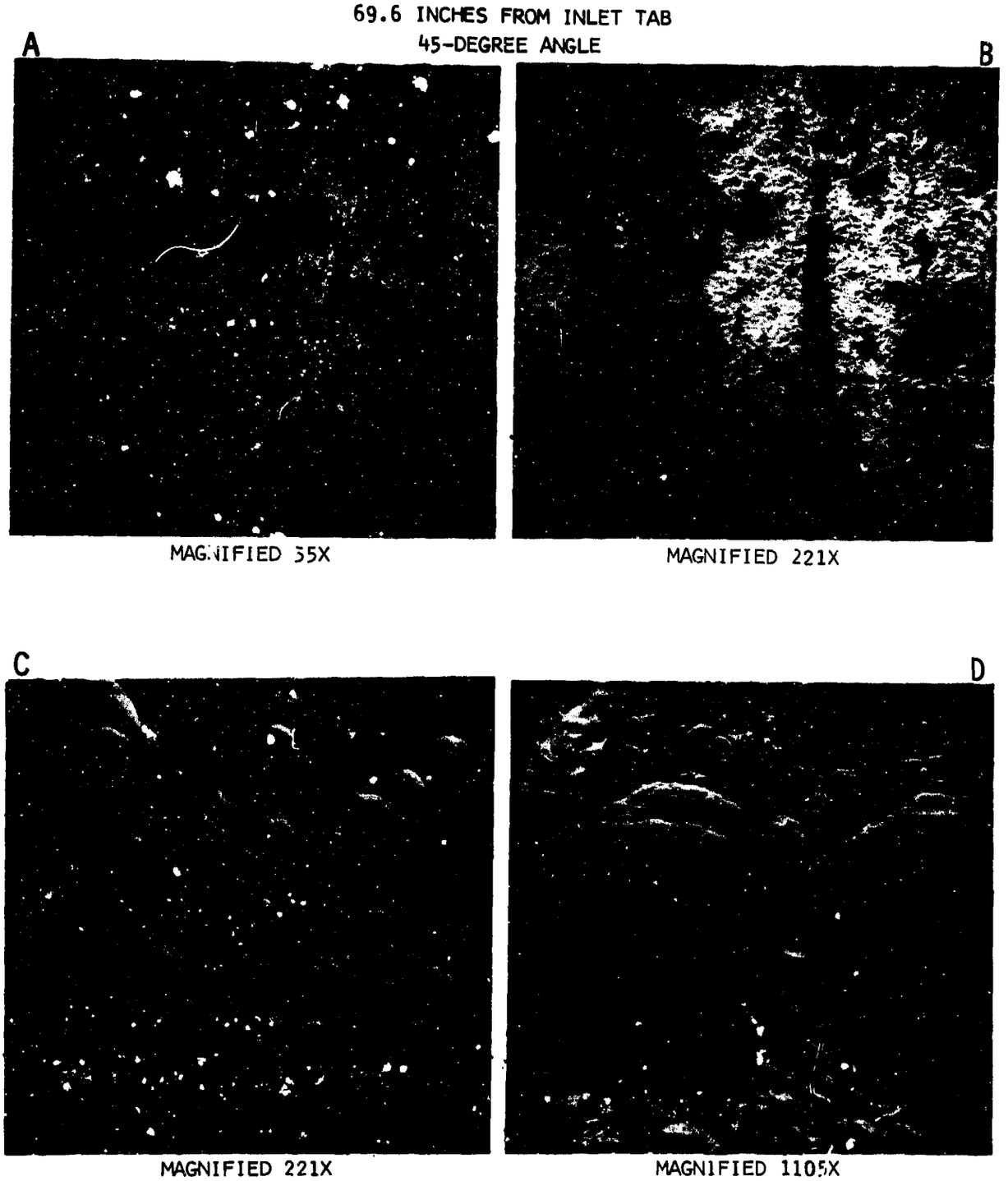

Figure 33. Top View of Bottom Half of Manifold 8.802

A close up of one of the spheriods (magnified 1105 times) is shown in figure 33D. This spheriod appears to have built up in segments.

CORRELATION OF STEADY-STATE TO TEST CYCLES

Steady-state data were used in the correlation to test cycle data since it was found that there are no significant differences in deposition rates between steady-state and steady-state-flush for fuel AFFB-12-68 at the deposit levels attained. The data were compared on the basis of the full radial spectrum of fuel temperature (maximum film to average stream). The rates predicted from linear steady-state data were in agreement with the rates obtained from test cycle data (appendix I).

PREDICTED RATES BASED ON STEADY-STATE DATA

The predicted rate of deposit formation under cyclic conditions was obtained on the basis of the complete radial spectrum of fuel temperature in the same manner as that for fuel AFFB-11-68. The radial temperature spectrum covers the temperatures from the maximum film temperature (which is the same as the calculated, initial, inner wall temperature) to the average stream temperature. Figure 28 was used to obtain the following relationships between the rate of change of deposit thermal resistance ($x_d/k_d\Theta$) and the calculated maximum film temperature (Tf):

$$x_d/k_d\Theta = 0.0 \qquad \text{for } T_f \leq 460^\circ \text{ F}$$

$$= 0.0000125(T_f-460) \qquad \text{for } 460^\circ \text{ F} \leq T_f \leq 620^\circ \text{ F}$$

$$= 0.002 + 0.0034(T_f-620) \qquad \text{for } 620^\circ \text{ F} \leq T_f \leq 634^\circ \text{ F}$$

$$= 0.05 + 0.01167(T_f-634) \qquad \text{for } 634^\circ \text{ F} \leq T_f \leq 640^\circ \text{ F}$$

$$= 0.12 + 0.00121(T_f-640) \qquad \text{for } 640^\circ \text{ F} \leq T_f \leq 659^\circ \text{ F}$$

$$= 0.143 + 0.00035(T_f-659) \qquad \text{for } 659^\circ \text{ F} \leq T_f \leq 676^\circ \text{ F}$$

$$= 0.149 - 0.000485(T_f-676) \qquad \text{for } 676^\circ \text{ F} \leq T_f \leq 740^\circ \text{ F}$$

These deposition equations were applied in a computer program containing the calculated maximum fuel film temperatures as a function of test cycle time thereby computing deposition rate profiles (i.e., $x_d/k_d\Theta$ versus test cycle time, Θ). The areas under these profiles are then calculated and are the predicted x_d/k_d per test cycle. These predicted values, based on maximum film temperature are shown in figure 34. Also shown in figure 34, are the predicted values based on average stream temperatures. These rates are calculated in the same manner described above, except average stream temperatures are used instead of maximum film temperatures. The average stream temperatures were calculated by a linear interpolation of the manifold inlet and outlet fuel temperatures.

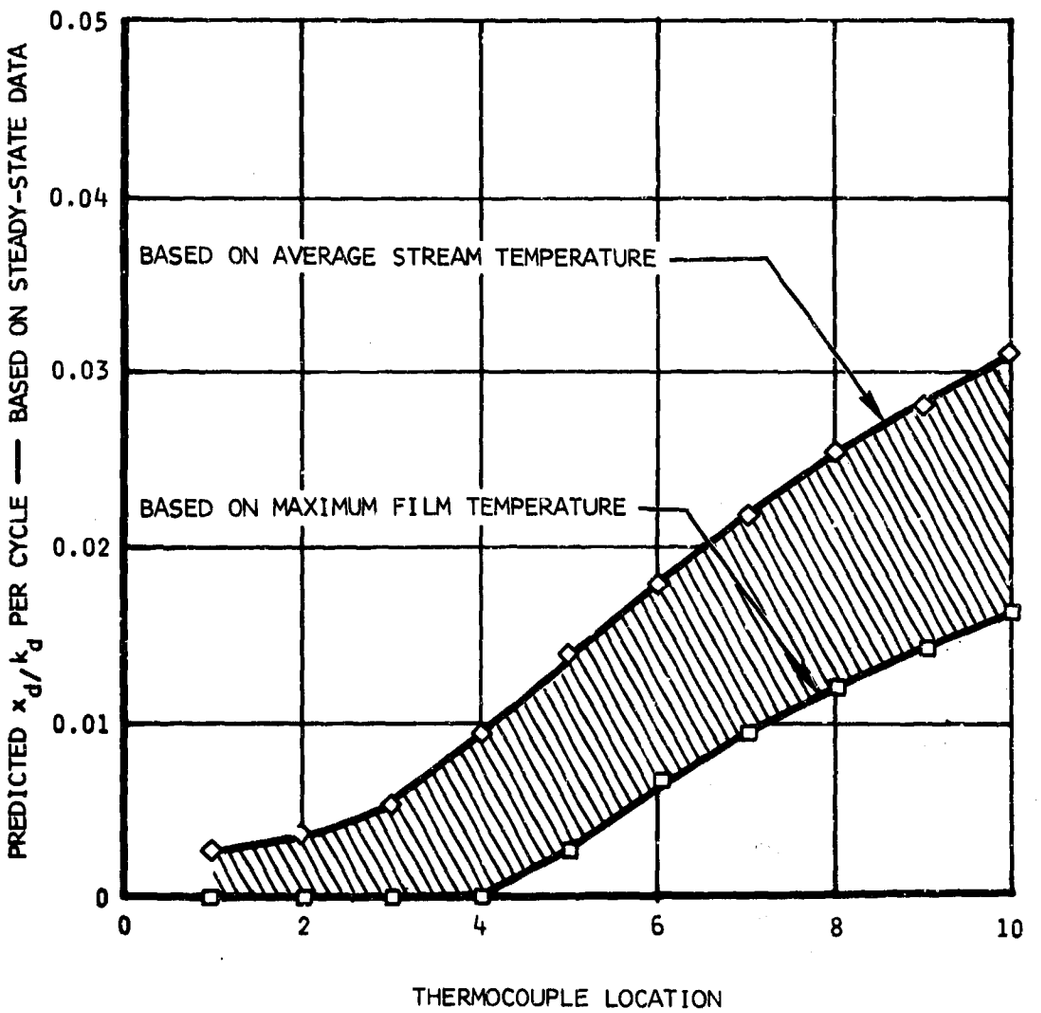

Figure 34. Predicted Test Cycle Deposition Rates

The shaded area shown in figure 34 represents the predicted x_d/k_d per test cycle values for the radial spectrum of fuel temperature. If the actual measured values of x_d/k_d per cycle are only a function of the radial spectrum of fuel temperatures, these measured values should lie in the band shown in figure 34.

COMPARISON TO RATES OBTAINED FROM TEST CYCLE DATA

The rates of change of x_d/k_d per test cycle were obtained from appendix I and are shown in figure 35 compared to the predicted rates based on steady-state data. All test cycle data were used for thermocouples 1 through 4 and higher rate data were used for thermocouples 5 through 10 in obtaining the rates from appendix I. This approach is taken because the predicted rates are based on the higher linear steady-state data rather than the lower initial steady-state data. The predicted rates based on the radial spectrum of fuel temperature are in agreement with the rates measured during cyclic conditions. It is indicated that the rate of deposit formation is not solely a function of fuel temperature at the outlet locations. It is considered that the rates at the outlet locations are controlled by such other factors as amount of remaining reactive constituents in the fuel and the deposit structural strength. These factors are not taken into consideration in obtaining the predicted rates by the above method.

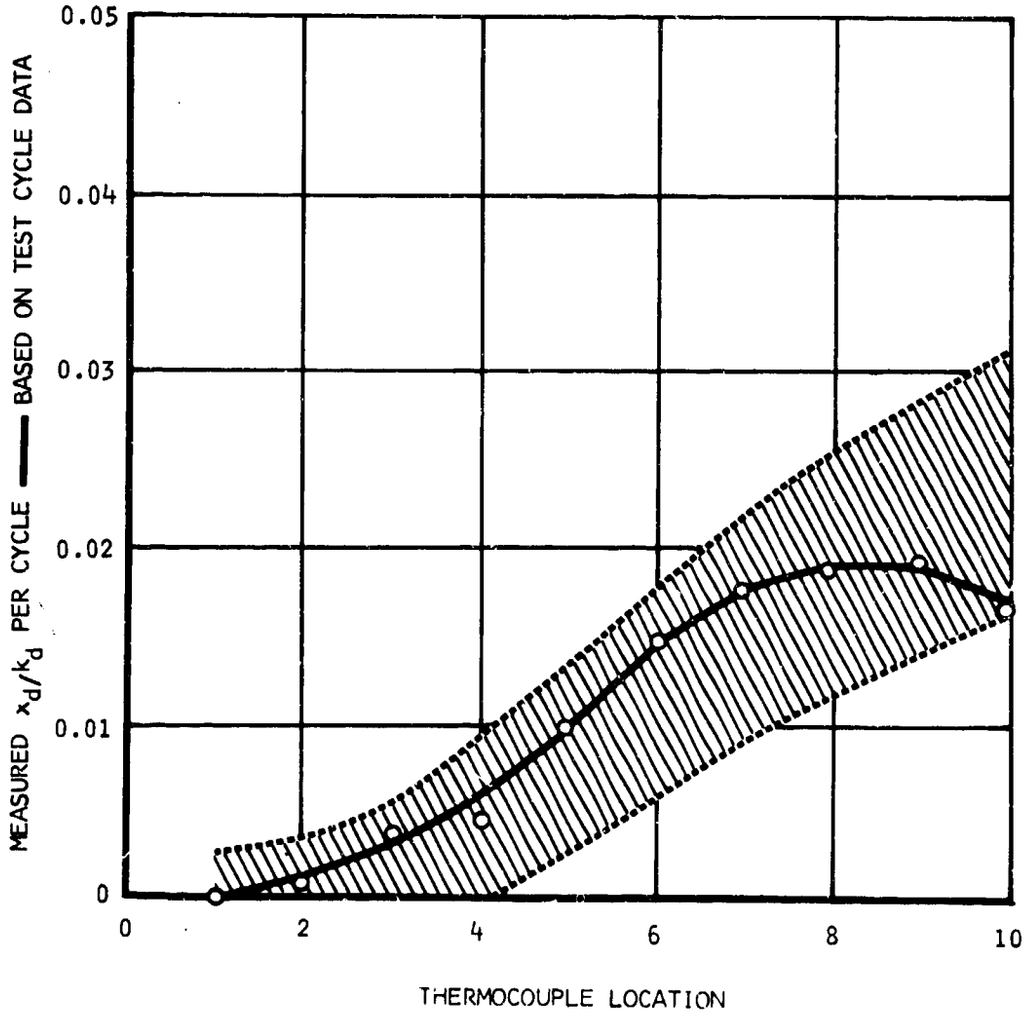

Figure 35. Comparison Between Steady-State Data and Test Cycle Data

REFERENCES

1. NR Report NA-66-1380, "Advanced Aircraft Fuel System Simulator Modification and Performance Report," 27 December 1966

2. NR Report NA-65-247, "Performance of Current Quality Commercial Jet Fuel in the Supersonic Transport Airframe and Aircraft Engine Fuel System Test Rig," Final Report, Federal Aviation Agency Contract FA-55-65-3, 14 May 1965

3. AFAPL-TR-67-116, "High Temperature Hydrocarbon Fuels Research in an Advanced Aircraft Fuel System Simulator on Fuel AFFB-8-67," September 1967

4. AFAPL-TR-68-25, "High Temperature Hydrocarbon Fuels Research in an Advanced Aircraft Fuel System Simulator on Fuel AFFB-9-67," February 1968

5. AFAPL-TR-69-5, "High Temperature Hydrocarbon Fuels Research in an Advanced Aircraft Fuel System Simulator on Fuel AFFB-10-67," February 1969

6. AFAPL-TR-69-88, "High Temperature Hydrocarbon Fuels Research in an Advanced Aircraft Fuel System Simulator on Fuel AFFB-11-68," September 1969

7. CRC Manual No. 5, "CRC Diesel Engine Rating Manual", page 36

8. Phillips Petroleum Company, Method RK-63R (Revision II), dated 16 March 1965

APPENDIX I

CALCULATED DEPOSIT THERMAL RESISTANCE OF THE EIGHTH TEST SERIES MANIFOLD

Contained herein are the computerized output (cathode-ray tube graphs) of the calculated values of deposit thermal resistance for the eighth test series manifold. Each of the pages shows the calculated x_d/k_d obtained from the data of one thermocouple location on the manifold. Also shown on each page are the slope or change in x_d/k_d per test cycle and the correlation coefficient based on the straight-line portions of the data points.

The peak metal temperature at the beginning of the test series and the total change in deposit thermal resistance (x_d/k_d) for each the thermocouple location are as follows:

Thermocouple Location	Outer Peak Metal Temperature (° F)	Change in x_d/k_d, Mil/BTU-ft/hr-sq ft-°F
TC-1	550	~0.0
TC-2	598	~0.2
TC-3	640	0.8
TC-4	640	0.9
TC-5	656	1.7
TC-6	680	2.4
TC-7	691	2.4
TC-8	708	2.3
TC-9	723	2.1
TC-10	736	1.8

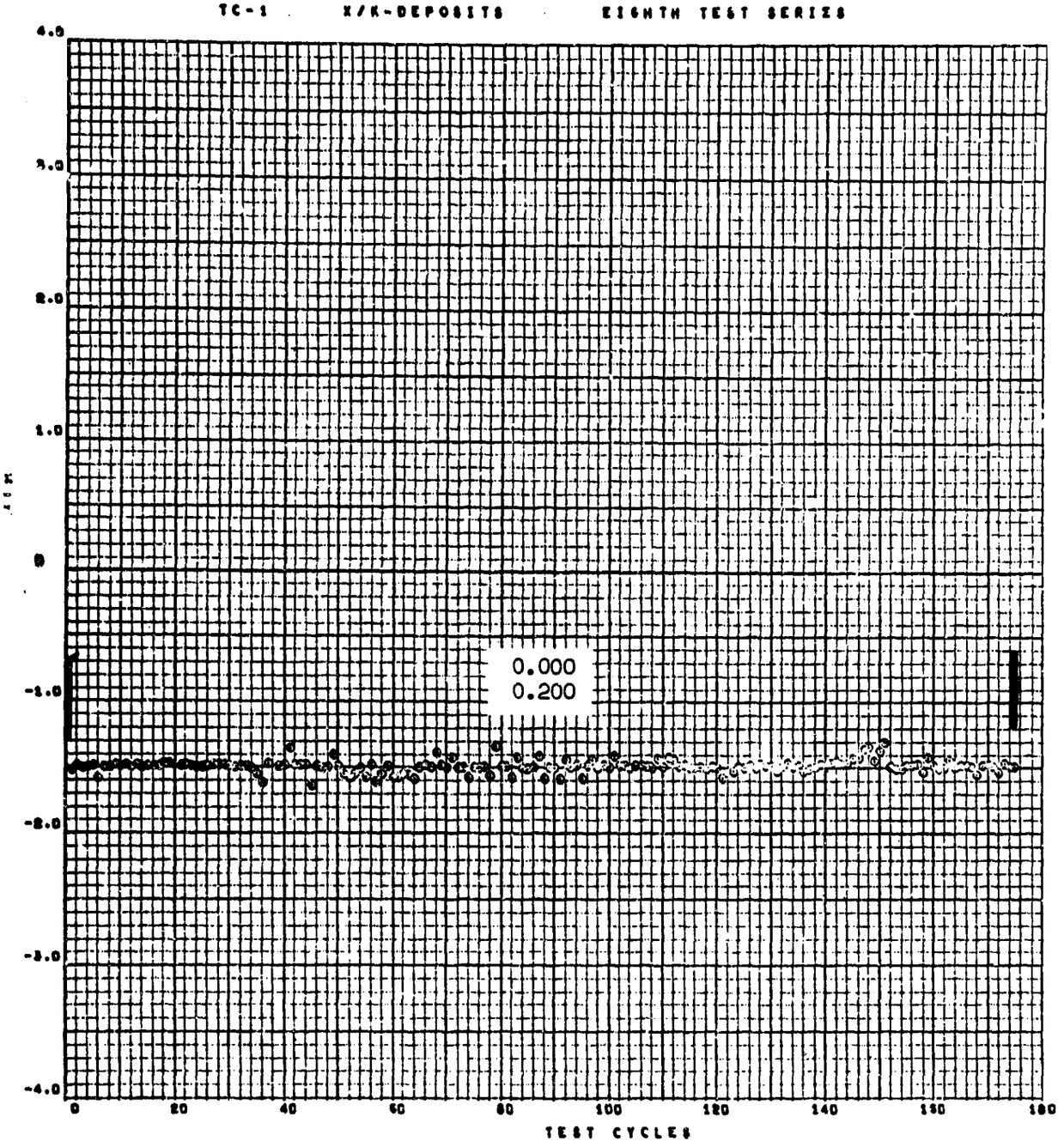
TC-1 X/K-DEPOSITS EIGHTH TEST SERIES
4.0
3.0
2.0
1.0
0
-1.0
-2.0
-3.0
-4.0
X/K
0.000
0.200
0
20
40
60
80
100
120
140
160
180
TEST CYCLES

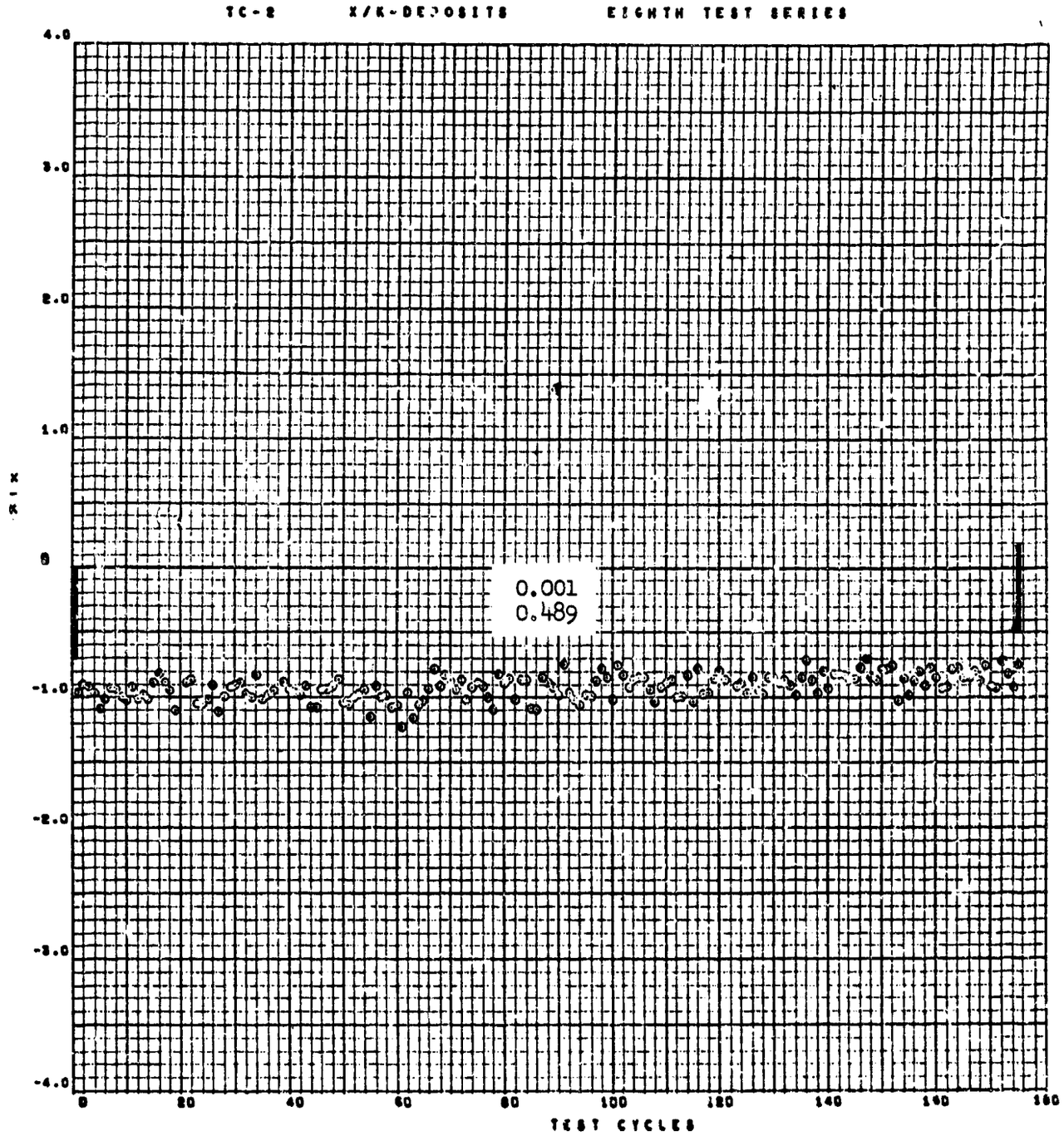
TC-2 X/K-DEPOSITS EIGHTH TEST SERIES
4.0
3.0
2.0
1.0
0
-1.0
-2.0
-3.0
-4.0
X - X
0.001
0.489
0
20
40
60
80
100
120
140
160
180
TEST CYCLES

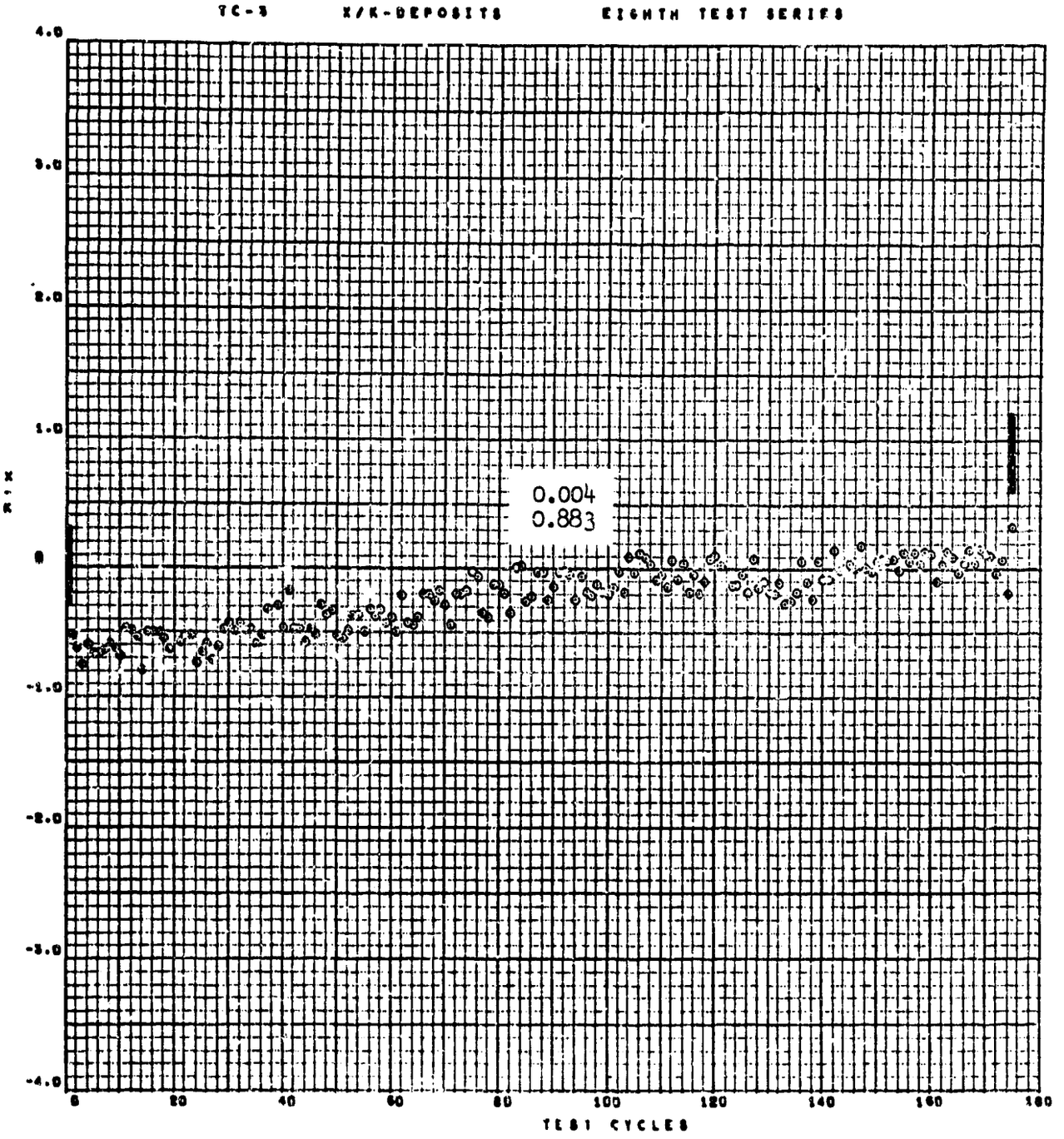
TC-3 X/K-DEPOSITS EIGHTH TEST SERIES
4.0
3.0
2.0
1.0
0
-1.0
-2.0
-3.0
-4.0
R : K
0.004
0.883
0
20
40
60
80
100
120
140
160
180
TEST CYCLES

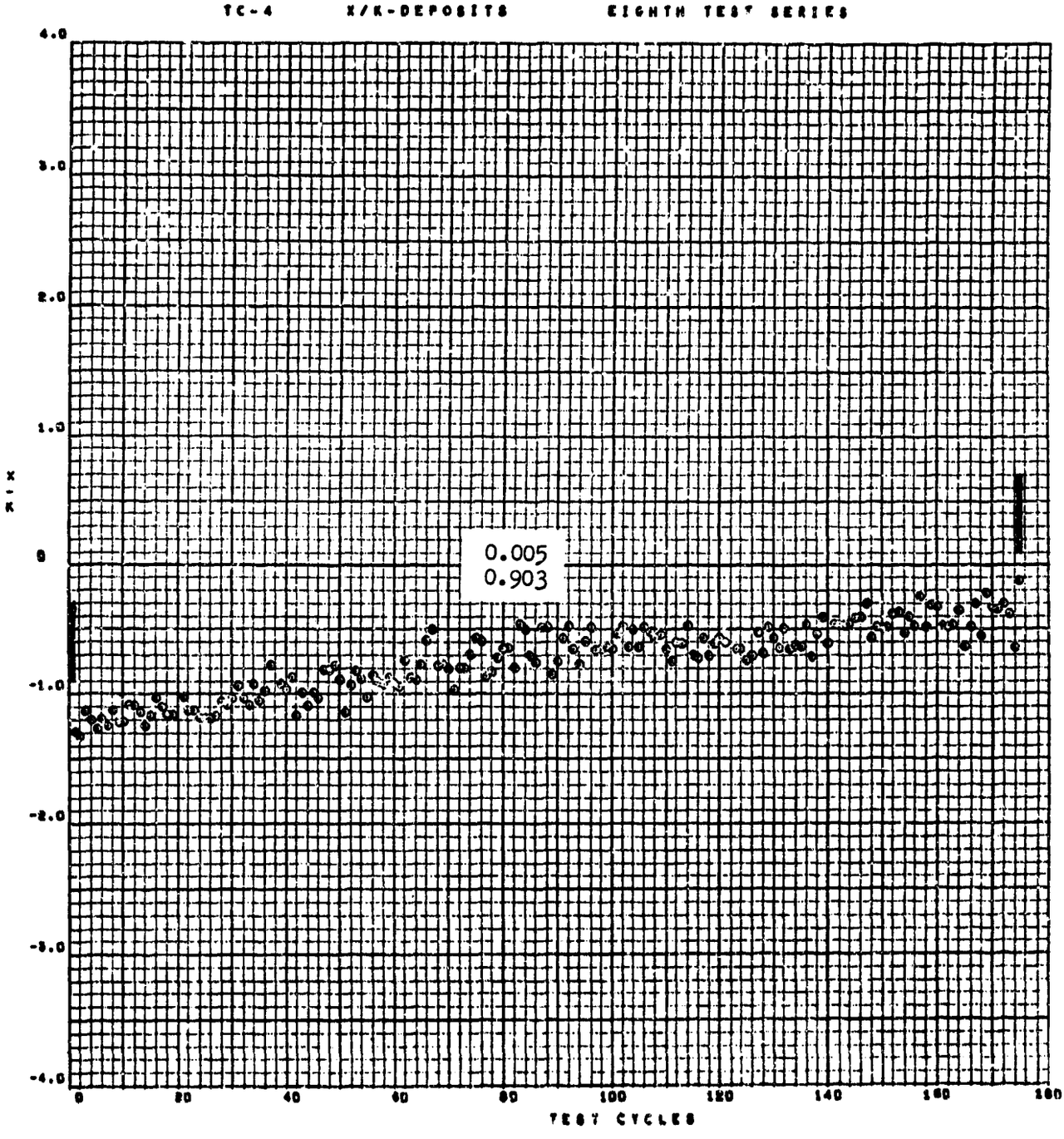
TC-4 X/K-DEPOSITS EIGHTH TEST SERIES
4.0
3.0
2.0
1.0
0
-1.0
-2.0
-3.0
-4.0
K - X
0.005
0.903
0
20
40
60
80
100
120
140
160
180
TEST CYCLES

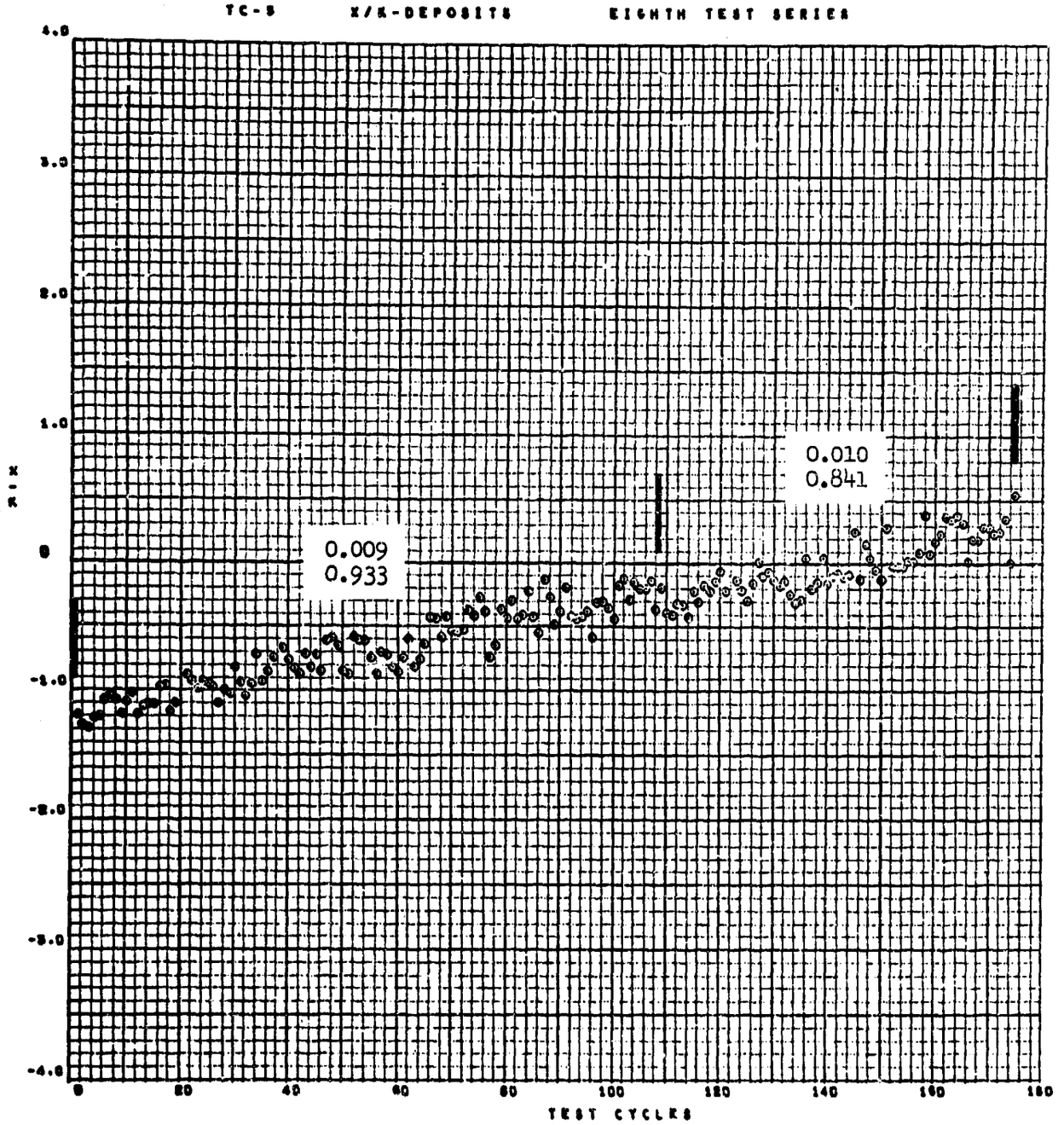
TC-8 X/K-DEPOSITS EIGHTH TEST SERIES
4.0
3.0
2.0
1.0
0
-1.0
-2.0
-3.0
-4.0
K - X
0.009
0.933
0.010
0.841
0
20
40
60
80
100
120
140
160
180
TEST CYCLES

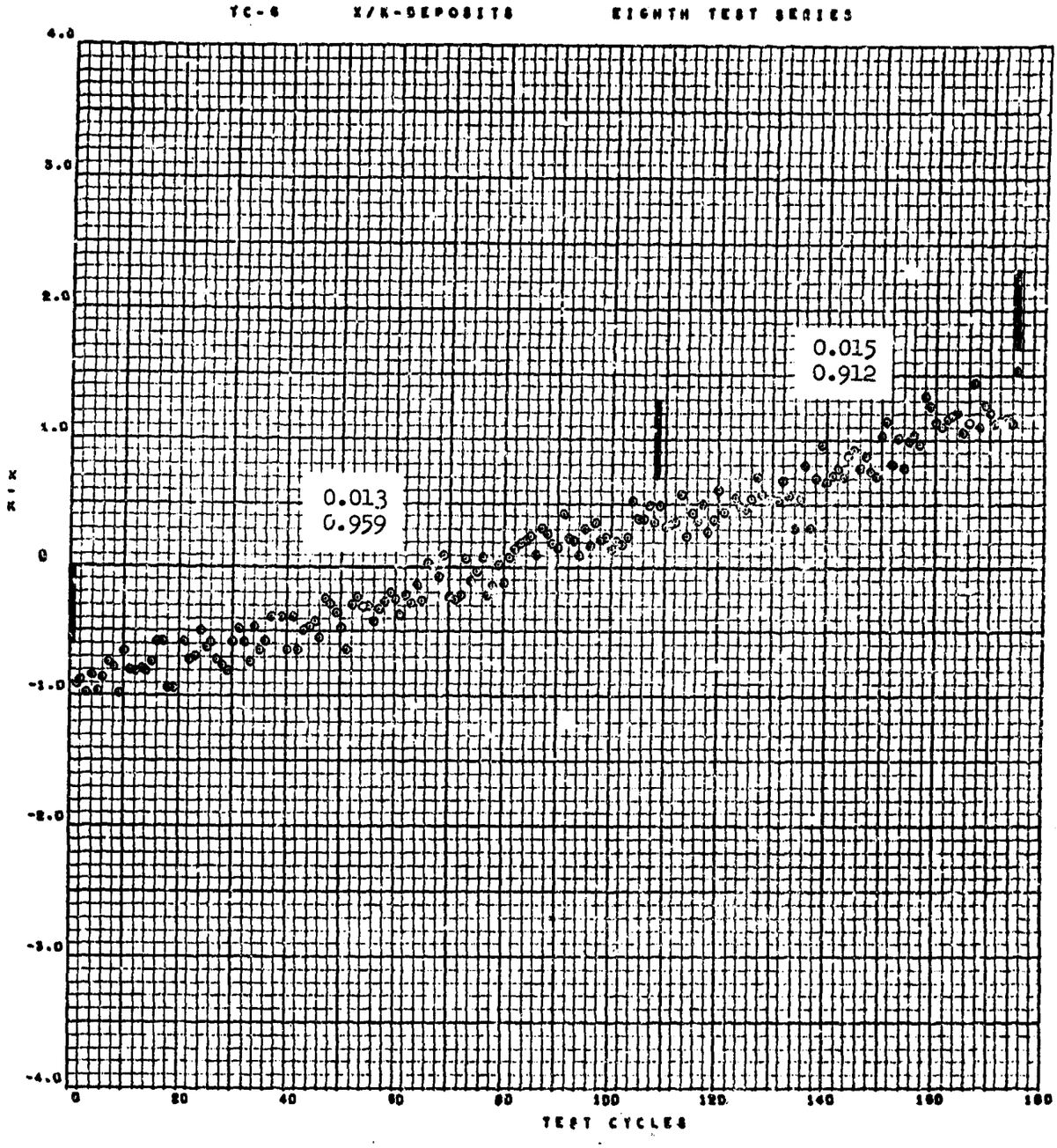
TC-6 X/K-DEPOSITS EIGHTH TEST SERIES
4.0
3.0
2.0
1.0
0
-1.0
-2.0
-3.0
-4.0
X - K
0.015
0.912
0.013
0.959
0
20
40
60
80
100
120
140
160
180
TEST CYCLES

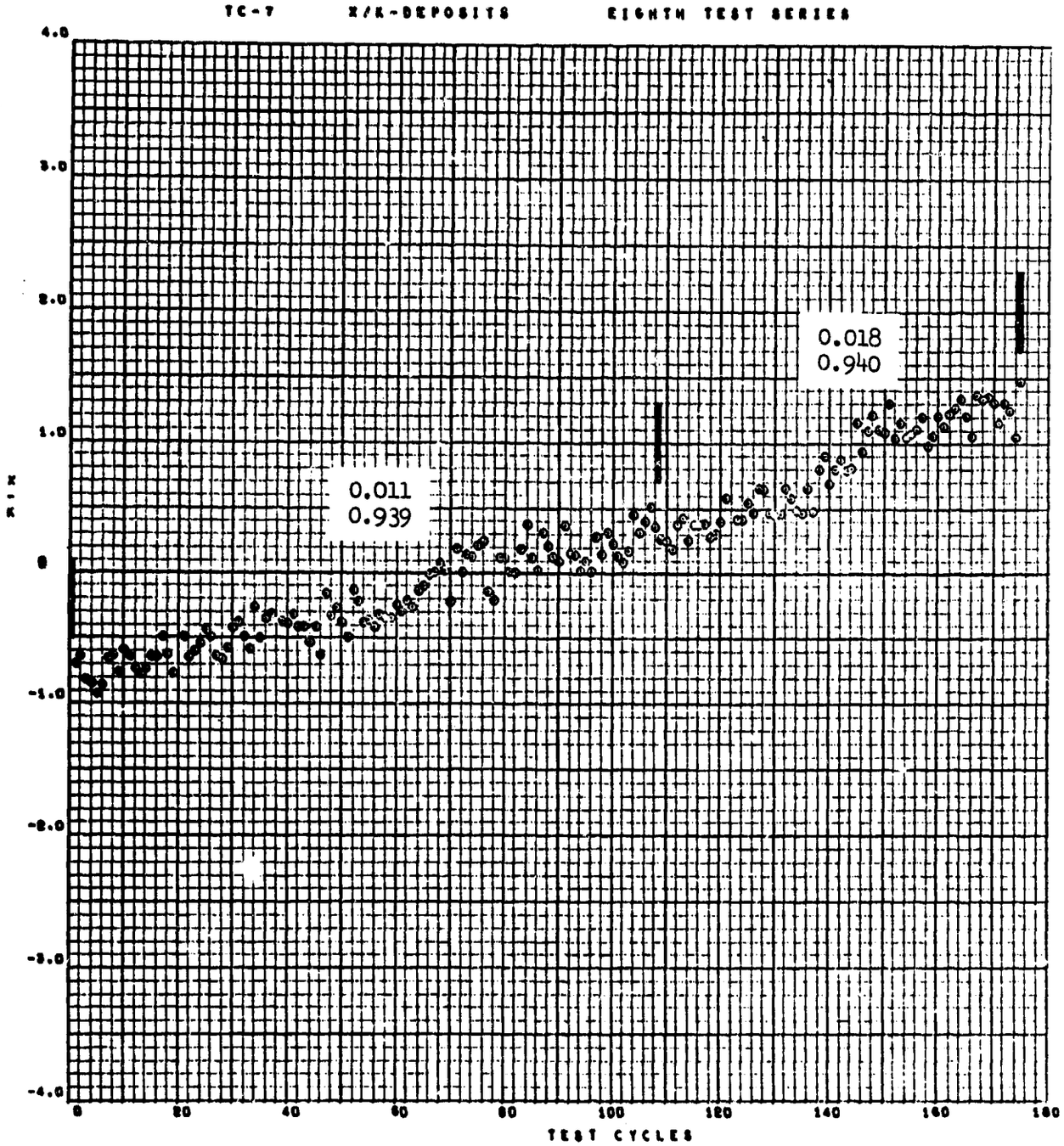
TC-7 X/K-DEPOSITS EIGHTH TEST SERIES
4.0
3.0
2.0
1.0
0
-1.0
-2.0
-3.0
-4.0
X - K
0.018
0.940
0.011
0.939
0
20
40
60
80
100
120
140
160
180
TEST CYCLES

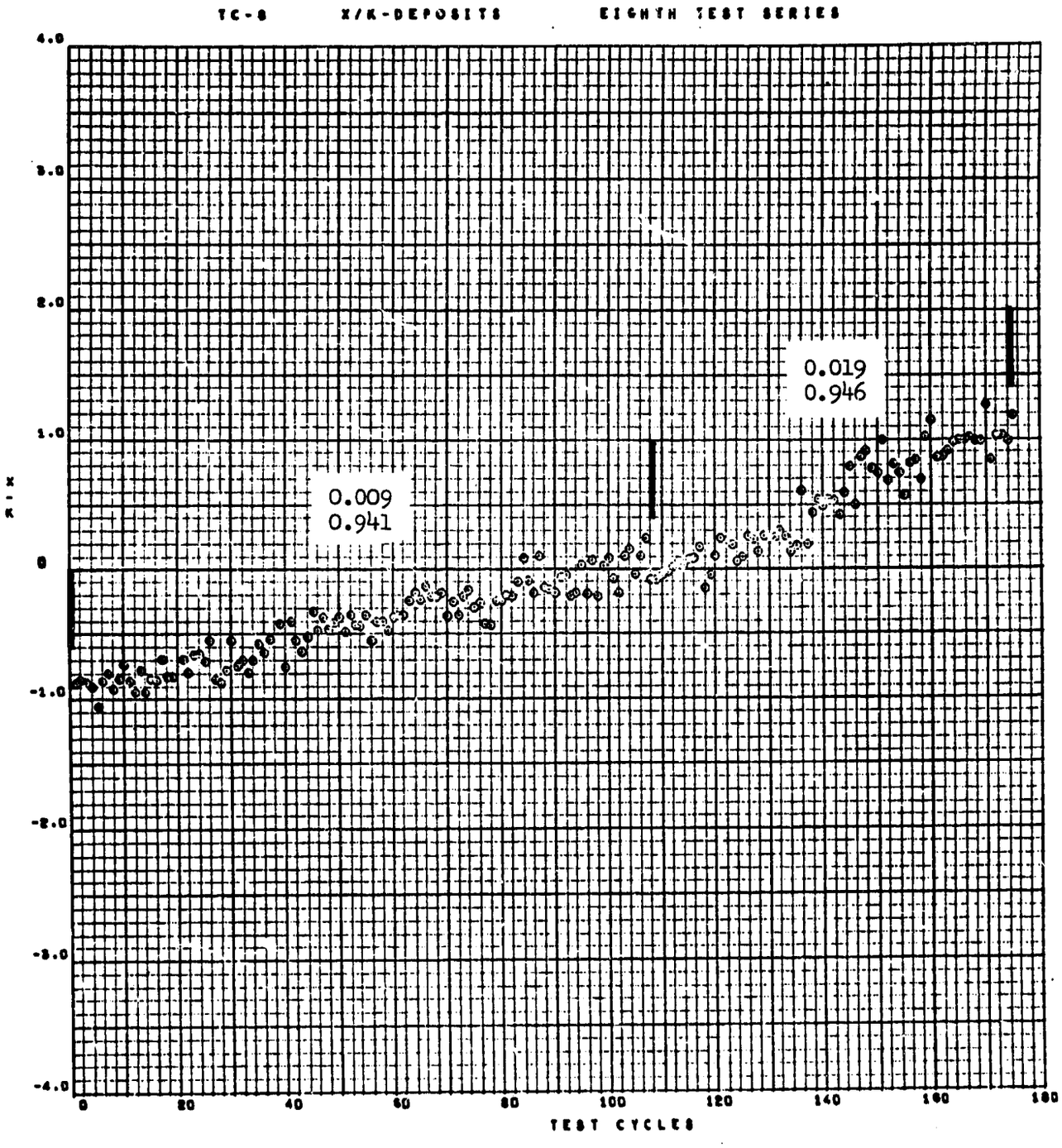
TC-8 X/K-DEPOSITS EIGHTH TEST SERIES
4.0
3.0
2.0
1.0
0
-1.0
-2.0
-3.0
-4.0
X - K
0.009
0.941
0.019
0.946
0
20
40
60
80
100
120
140
160
180
TEST CYCLES

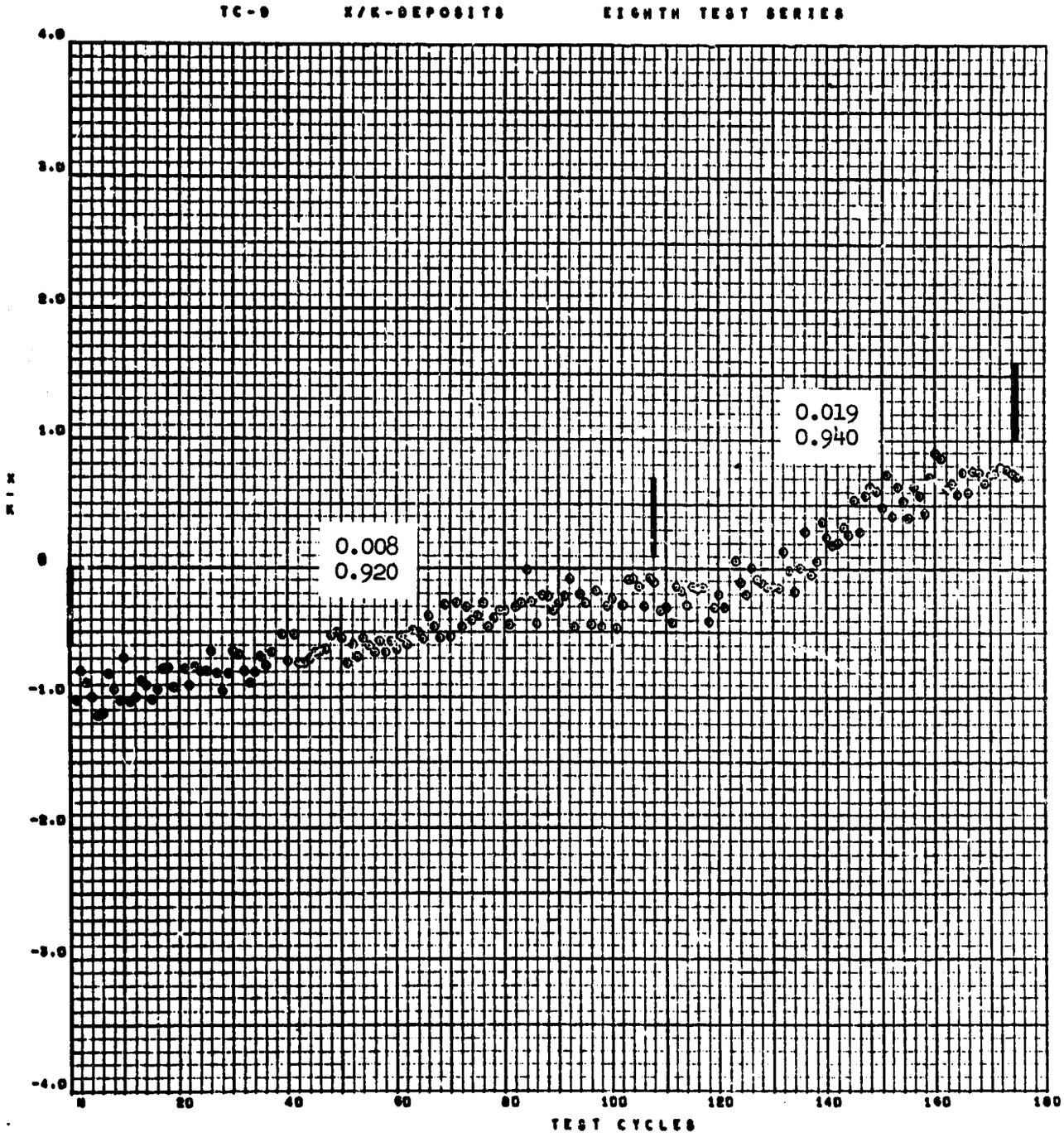
TC-9 X/K-DEPOSITS EIGHTH TEST SERIES
4.0
3.0
2.0
1.0
0
-1.0
-2.0
-3.0
-4.0
X - K
0.019
0.940
0.008
0.920
0
20
40
60
80
100
120
140
160
180
TEST CYCLES

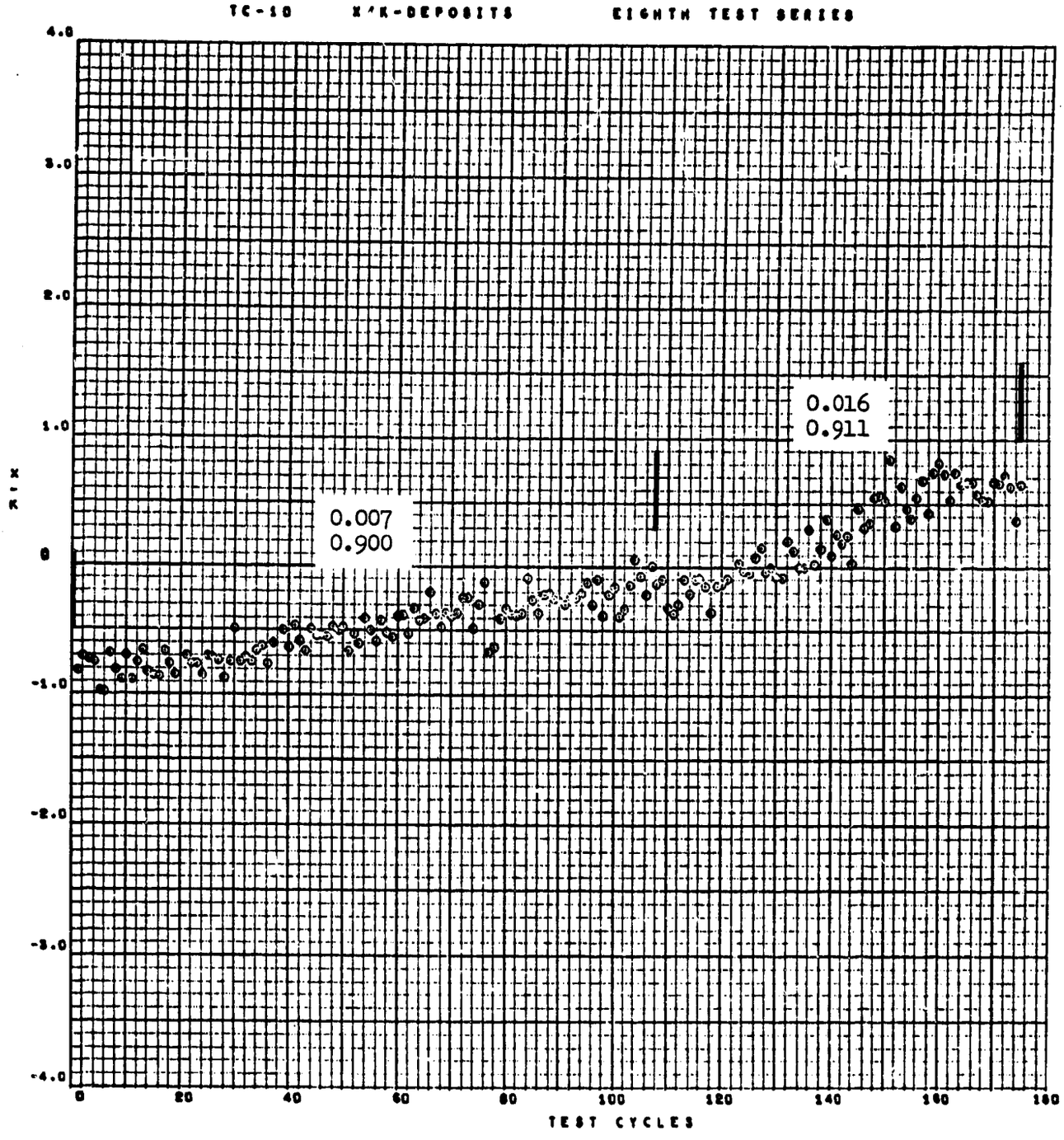
TC-10 K'K-DEPOSITS EIGHTH TEST SERIES
4.0
3.0
2.0
1.0
0
-1.0
-2.0
-3.0
-4.0
K - K
0.016
0.911
0.007
0.900
0
20
40
60
80
100
120
140
160
180
TEST CYCLES

APPENDIX II

CALCULATED DEPOSIT THERMAL RESISTANCE OF MANIFOLD 8.801

Contained herein is the computerized output of the calculated values of deposit thermal resistance for the steady-state and steady-state-flush manifold test 8.801 used in evaluating fuel AFFB-12-68. Each page contains the data obtained from one thermocouple location and the slope or deposition rate and correlation coefficient for the time periods of interest. The calculated inner, initial, wall temperature and the change in x_d/k_d, neglecting the decrease in x_d/k_d for TC-10, are as follows:

Thermocouple Location	Distance from Inlet Electrical Tab (Inches)	Calculated Inner Wall Temp. (° F)	Change in x_d/k_d
TC-1	1.9	489	~0.2
TC-2	13.8	532	~0.4
TC-3	26.3	556	~0.5
TC-4	38.5	580	~0.5
TC-5	50.8	606	~0.6
TC-6	63.2	615	~0.0
TC-7	75.8	637	16.7
TC-8	88.0	662	17.0
TC-9	100.4	687	14.4
TC-10	112.8	716	9.3

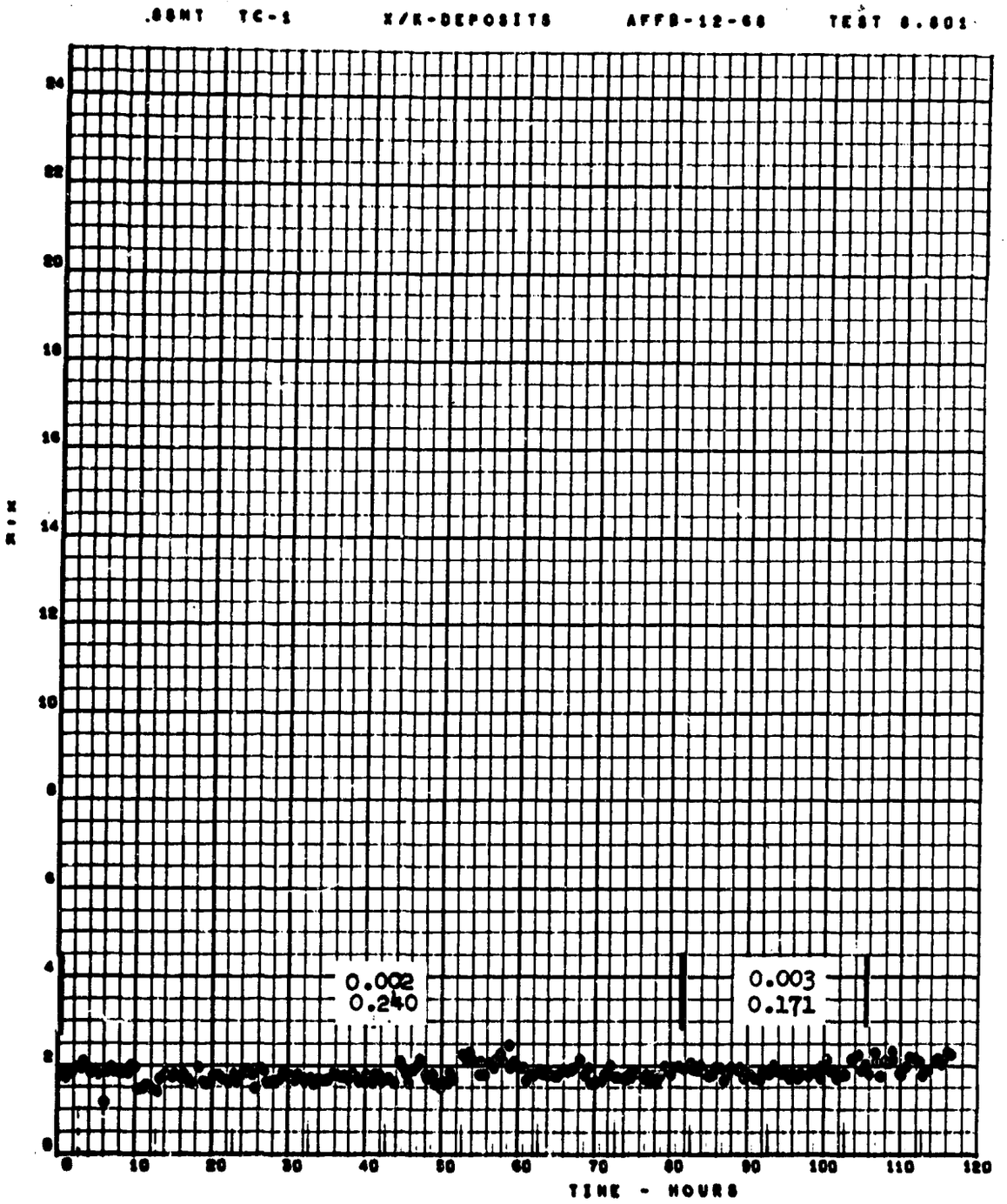
.88MT TC-1 X/R-DEPOSITS AFFB-12-68 TEST 8.801
R - X
0.002
0.240
0.003
0.171
0
10
20
30
40
50
60
70
80
90
100
110
120
TIME - HOURS

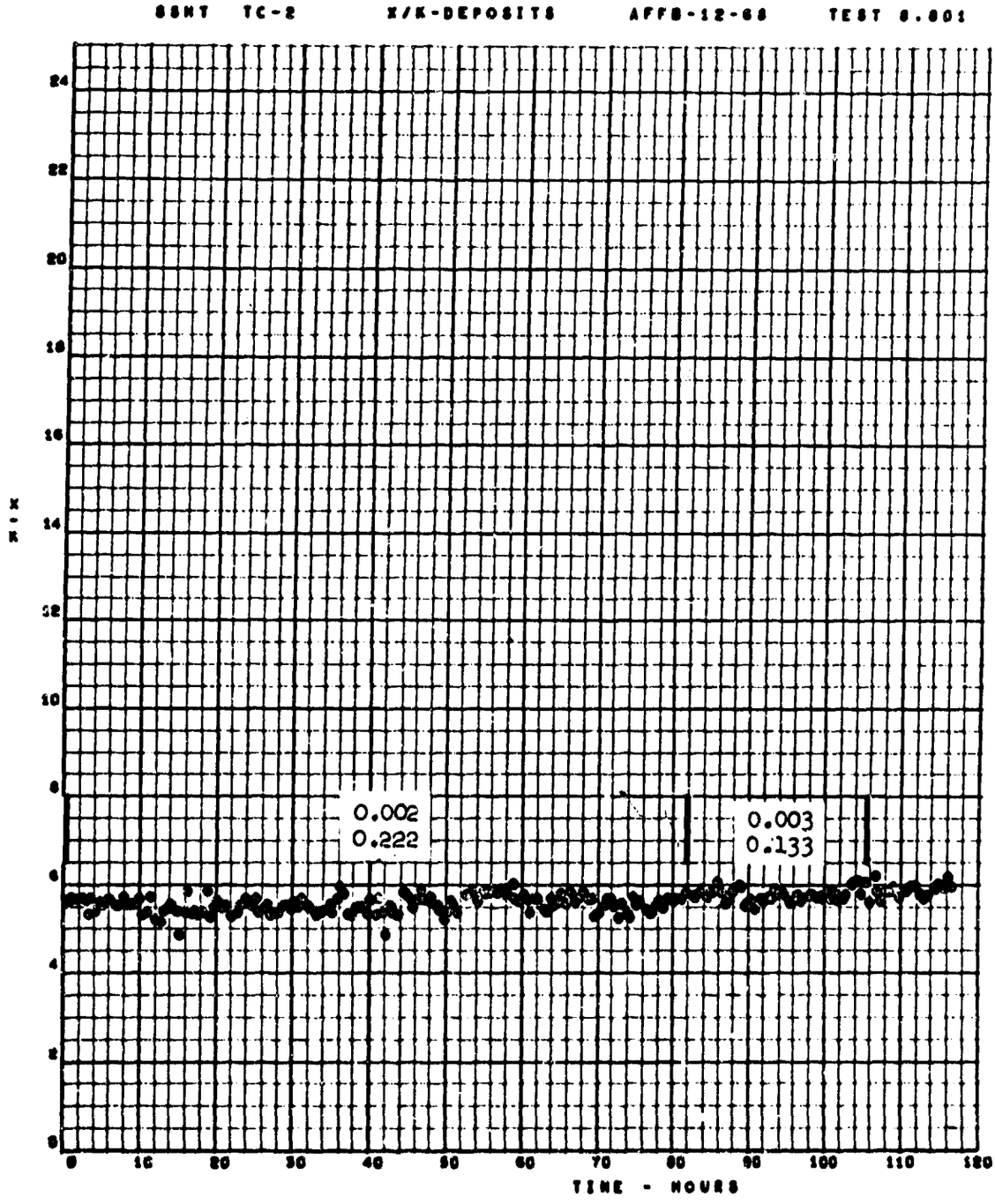
SSNT TC-2 X/K-DEPOSITS AFFB-12-68 TEST 8.001
X/K
0.002
0.222
0.003
0.133
TIME - HOURS

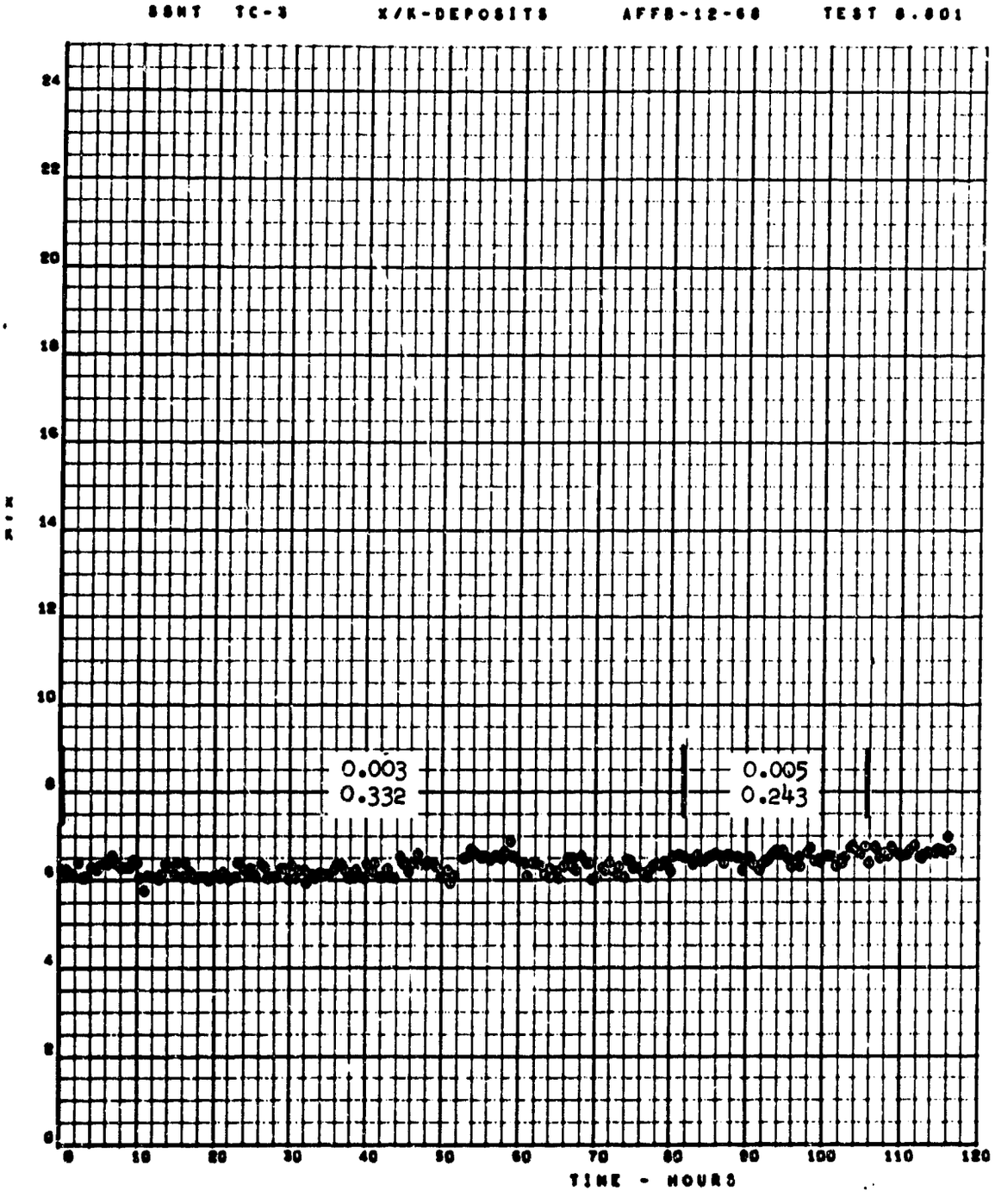
SSHT TC-3 X/K-DEPOSITS AFFB-12-68 TEST 8.801
X - K
24
22
20
18
16
14
12
10
8
6
4
2
0
0.003
0.332
0.005
0.243
0
10
20
30
40
50
60
70
80
90
100
110
120
TIME - HOURS

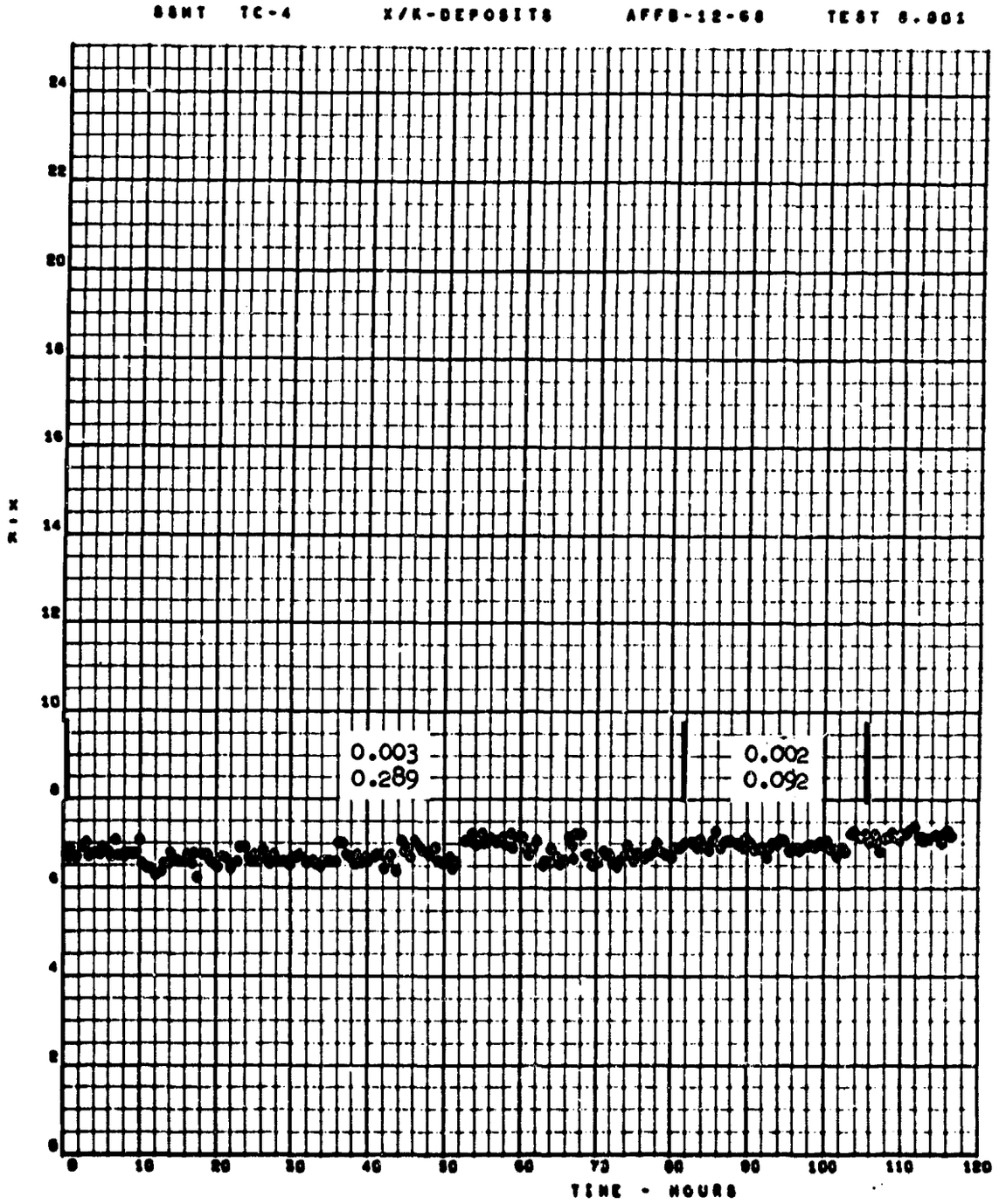
88MT TC-4 X/K-DEPOSITS AFFB-12-68 TEST 8.001
24
22
20
18
16
14
12
10
8
6
4
2
0
K - X
0.003
0.289
0.002
0.092
0
10
20
30
40
50
60
70
80
90
100
110
120
TIME - HOURS

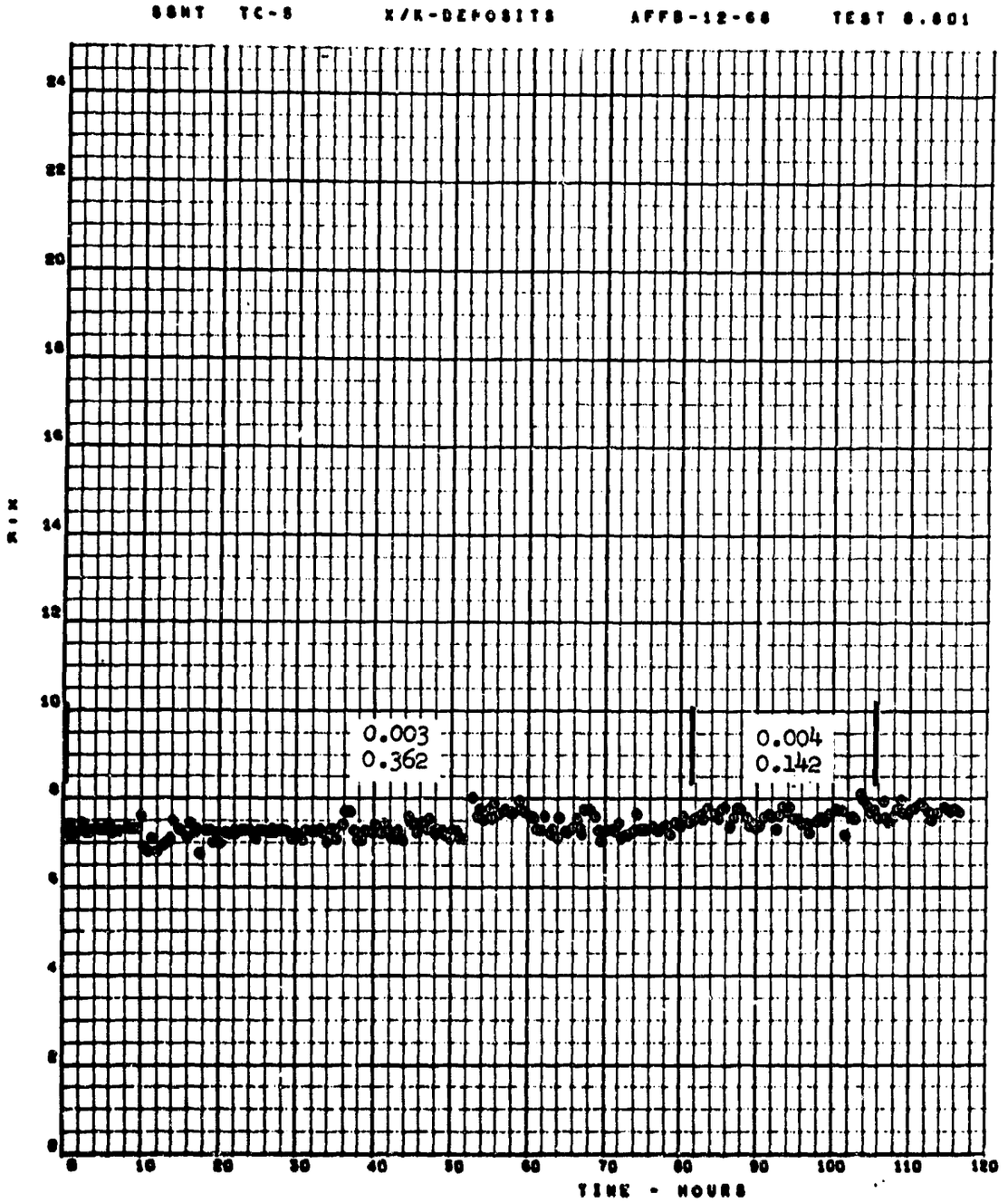
SSMT TC-8 X/K-DEPOSITS AFFB-12-68 TEST 8.801
K - X
TIME - HOURS
0.003
0.362
0.004
0.142

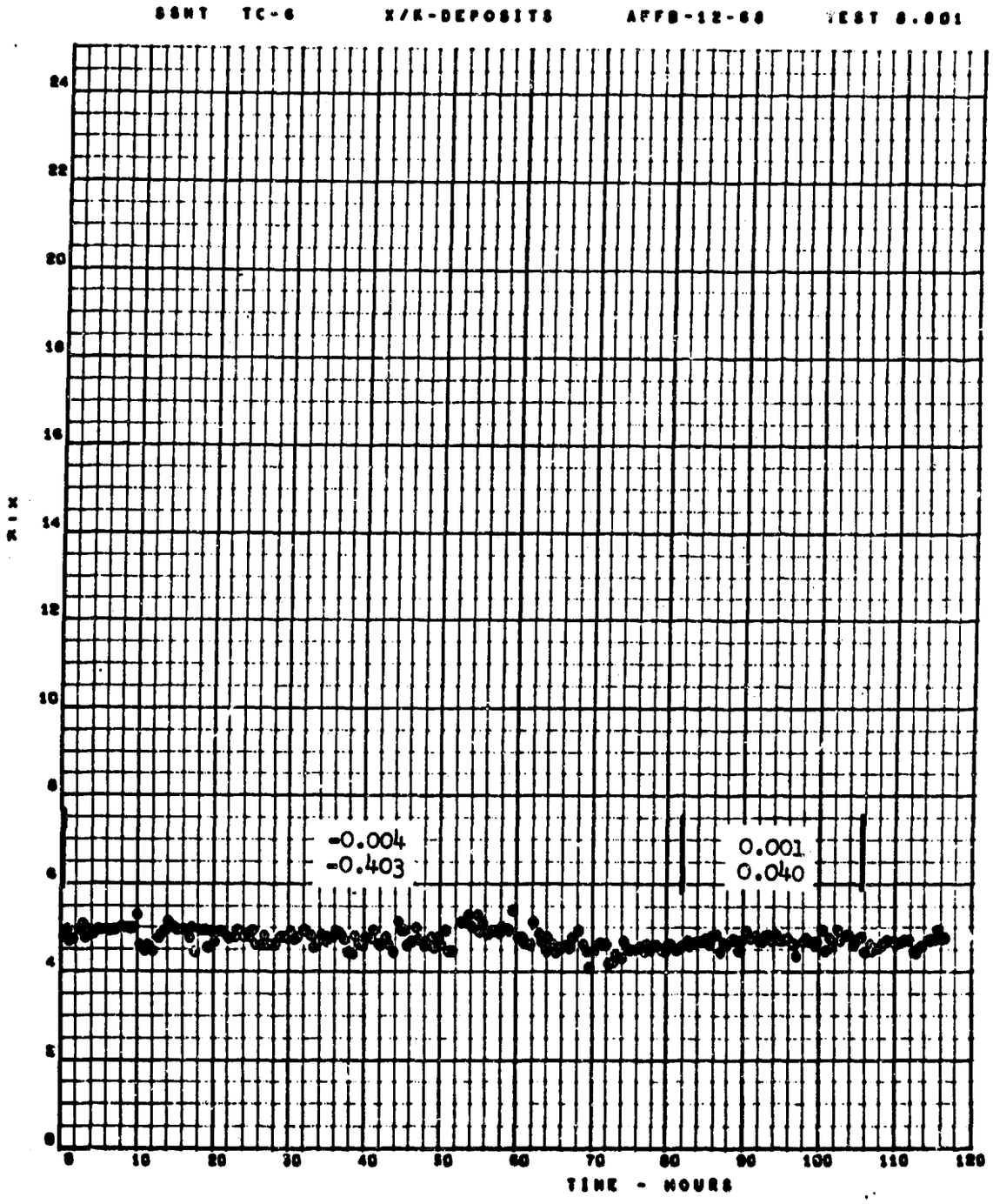
SSHT TC-6 X/K-DEPOSITS AFFB-12-68 TEST 8.001
24
22
20
18
16
14
12
10
8
6
4
2
0
X - X
-0.004
-0.403
0.001
0.040
0
10
20
30
40
50
60
70
80
90
100
110
120
TIME - HOURS

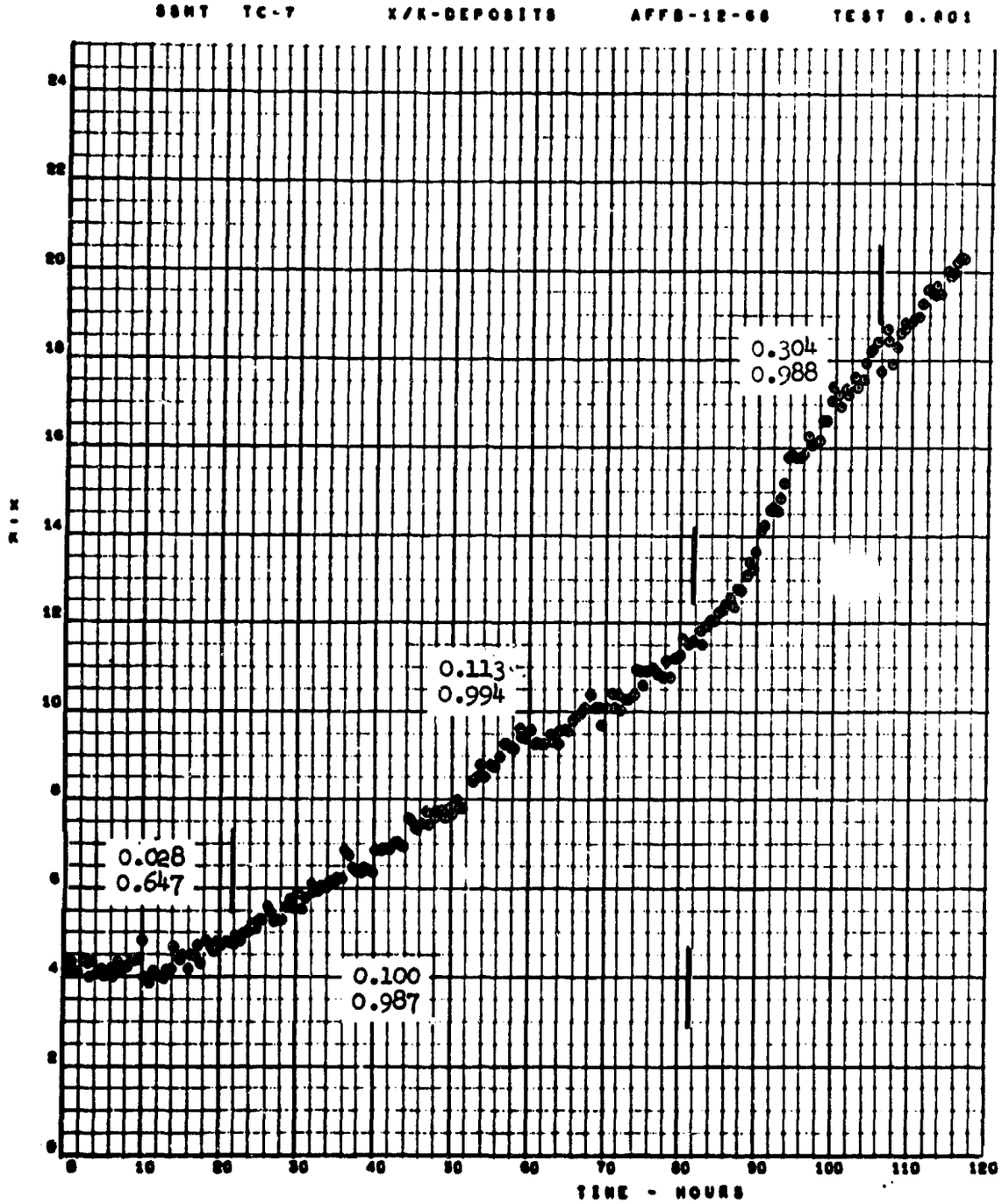
SSHT TC-7 X/K-DEPOSITS AFFB-12-68 TEST 8.801
X - K
TIME - HOURS
0.028
0.647
0.100
0.987
0.113
0.994
0.304
0.988

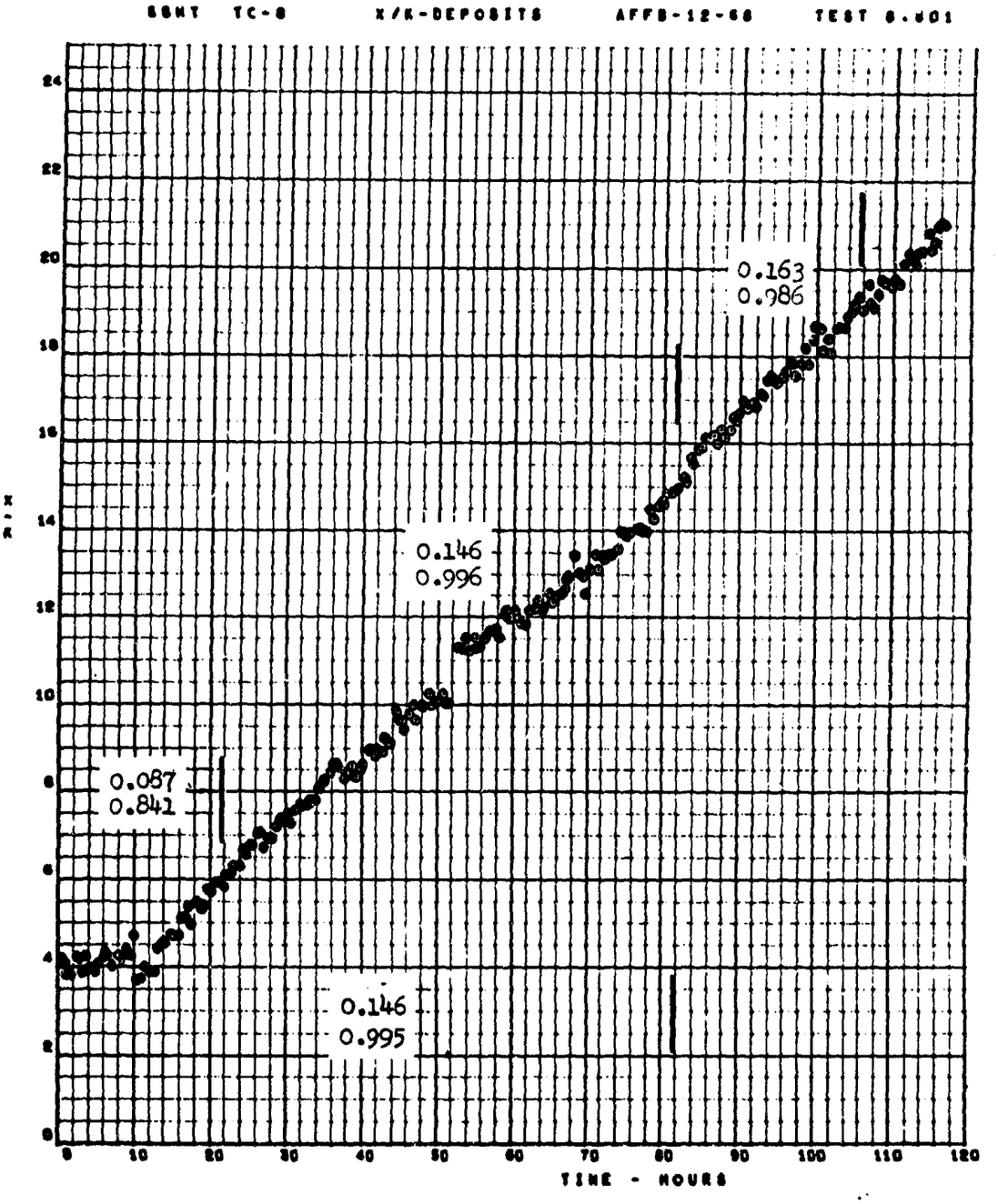
SSNT TC-8 X/K-DEPOSITS AFFB-12-68 TEST 8.401
X/K
TIME - HOURS
0.087
0.841
0.146
0.996
0.163
0.986
0.146
0.995

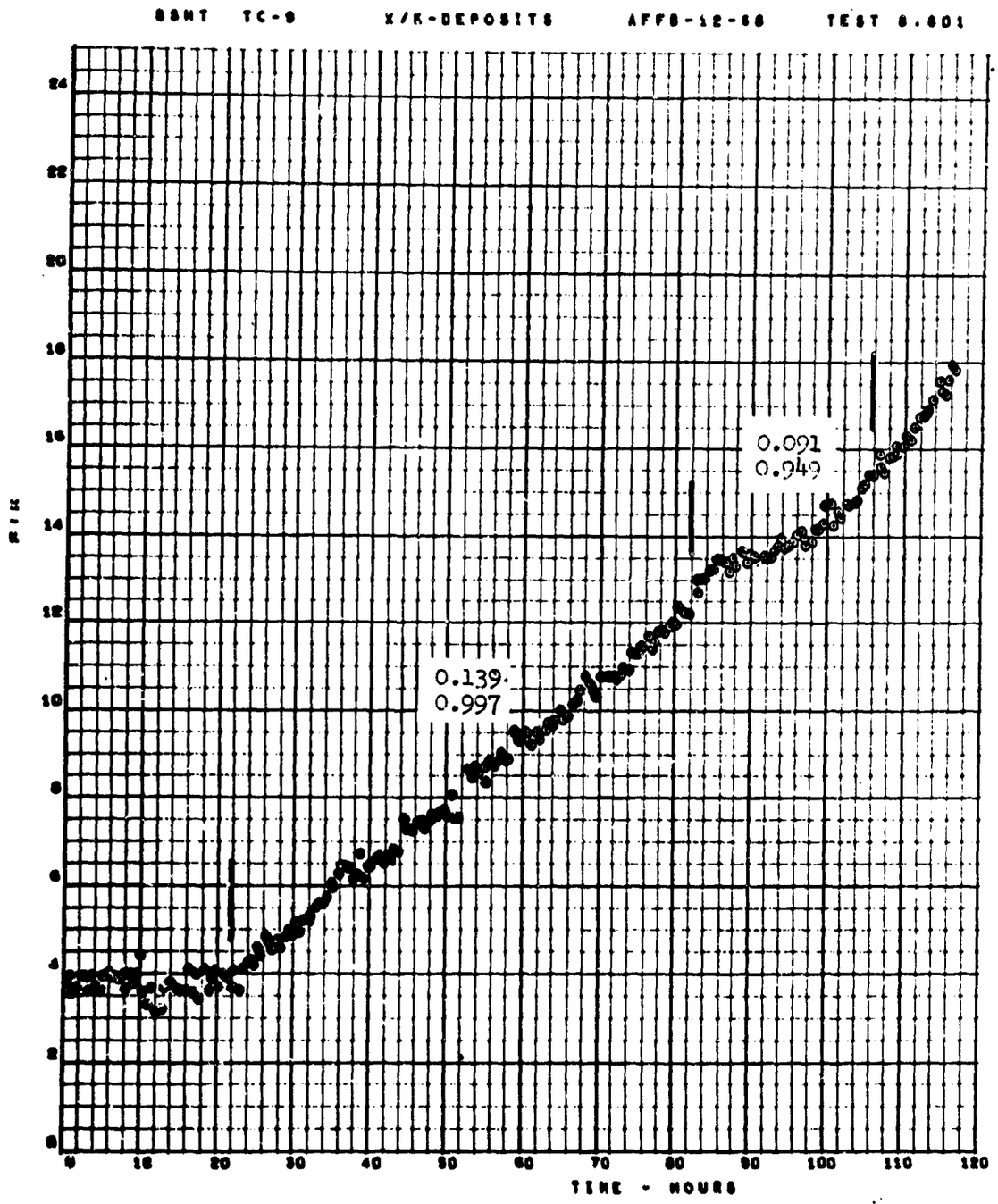
SSHT TC-9 X/K-DEPOSITS AFFS-12-68 TEST 8.801
0.091
0.949
0.139
0.997
X / K
TIME - HOURS

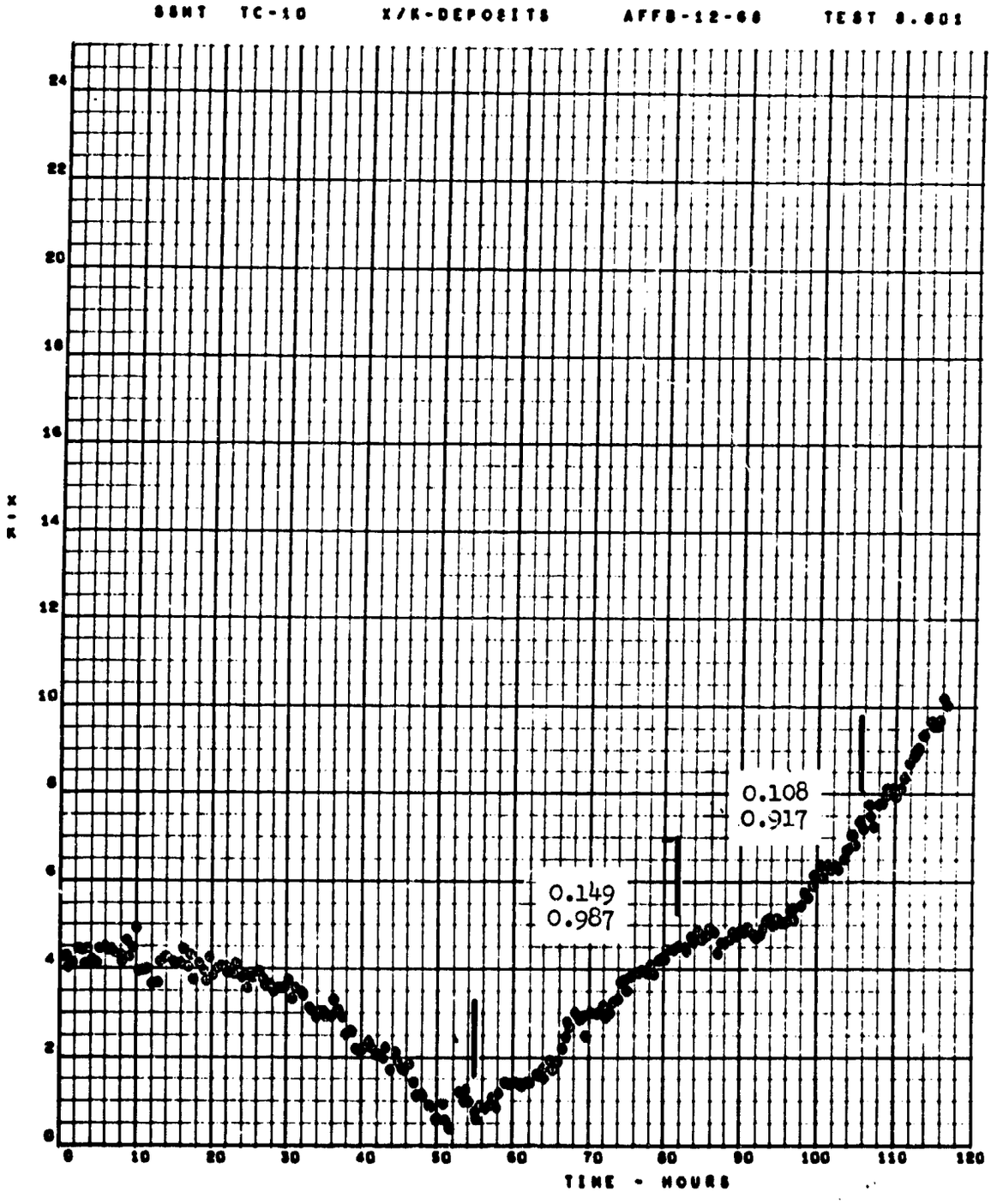
SSMT TC-10 X/K-DEPOSITS AFFB-12-68 TEST 8.801
K - X
TIME - HOURS
0.108
0.917
0.149
0.987

APPENDIX III

CALCULATED DEPOSIT THERMAL RESISTANCE OF MANIFOLD 8.802

Contained herein is the computerized output of the calculated values of deposit thermal resistance for the steady-state manifold test 8.802 used in evaluating fuel AFFB-12-68. Each page contains the data obtained from one thermocouple location and the slope or deposition rate and correlation coefficient for the time periods of interest. The calculated, initial, inner wall temperature and the change in x_d/k_d neglecting the decrease in x_d/k_d for TC-10, are as follows:

Thermocouple Location	Distance from Inlet Electrical Tab (Inches)	Type of Attachment	Calculated Inner Wall Temp. (° F)	Change in x_d/k_d
TC-4	38.5	Normal	593	~0.6
TC-5	50.8	Normal	616	~0.6
TC-6	63.2	Normal	622	~-0.5
TC-7	75.8	Normal	646	11.4
TC-8	88.1	Normal	666	12.3
TC-9	100.4	Normal	695	11.0
TC-10	112.8	Normal	721	7.8
TC-11	69.5	Normal	634	4.4
TC-12	94.2	Top-Longitudinal	680*	11.8
TC-13	94.2	Bottom-Longitudinal	680*	11.0
TC-14	72.7	Top-Longitudinal	637*	5.5
TC-15	100.4	1-2/3 Turns	692	11.2

* NOTE: These temperatures are based on interpolation of calculated temperatures obtained from normally attached thermocouples.

PRECEDING PAGE BLANK

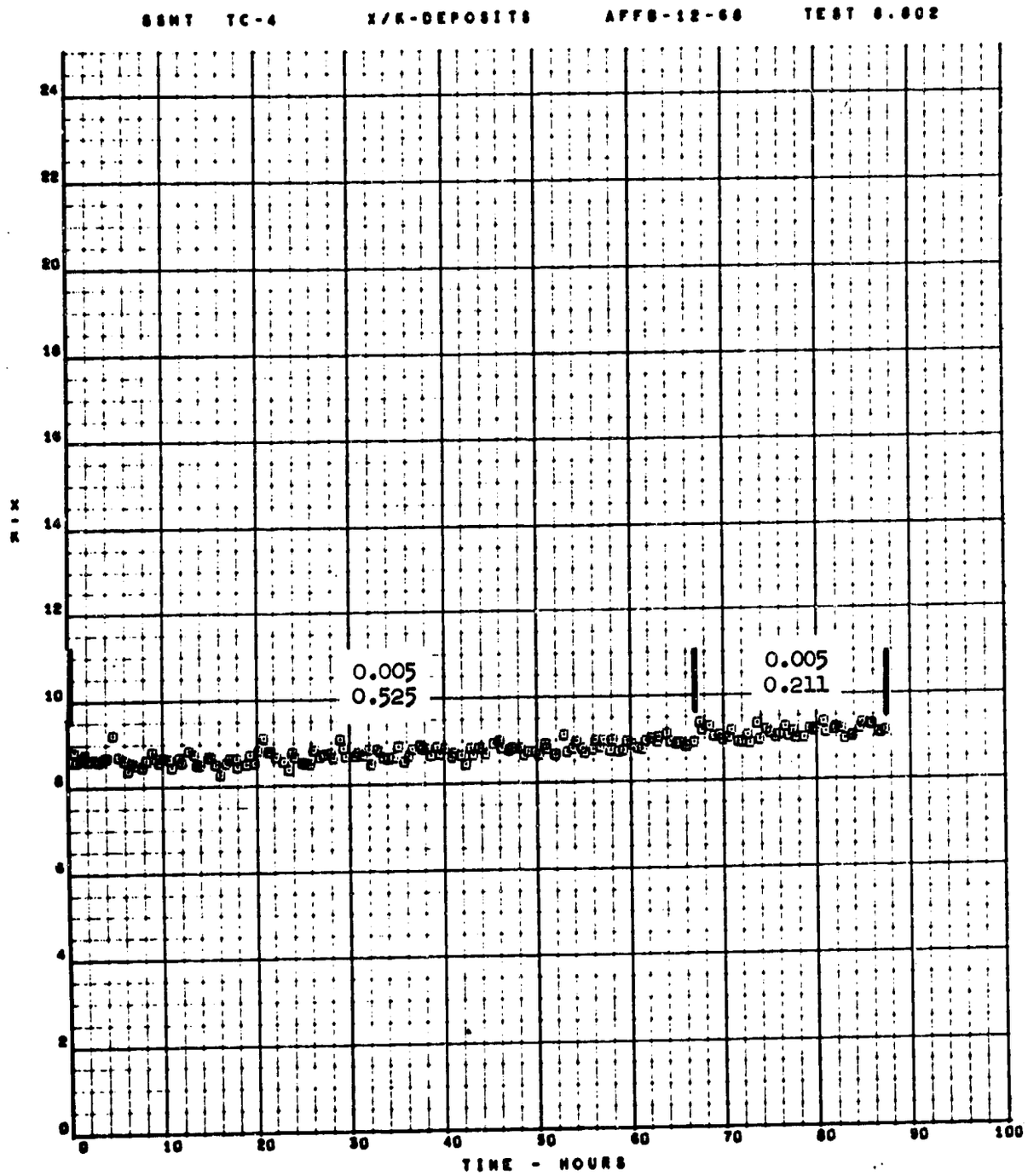
88MT TC-4 X/K-DEPOSITS AFFB-12-68 TEST 8.802
X - X
0.005
0.525
0.005
0.211
TIME - HOURS

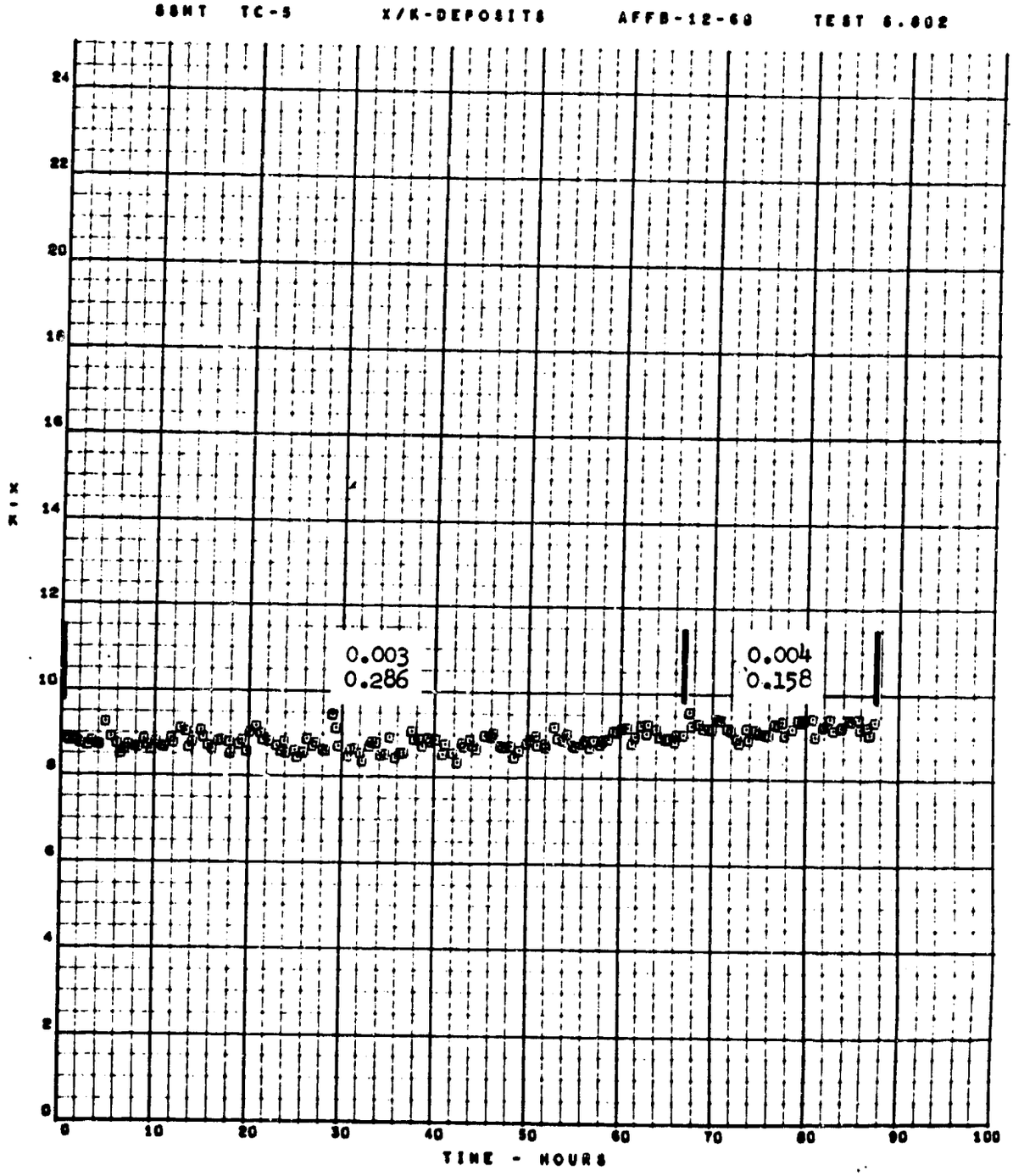
SSMT TC-5 X/K-DEPOSITS AFFB-12-68 TEST 6.802
X - K
0.003
0.286
0.004
0.158
TIME - HOURS
0
2
4
6
8
10
12
14
16
18
20
22
24
0
10
20
30
40
50
60
70
80
90
100

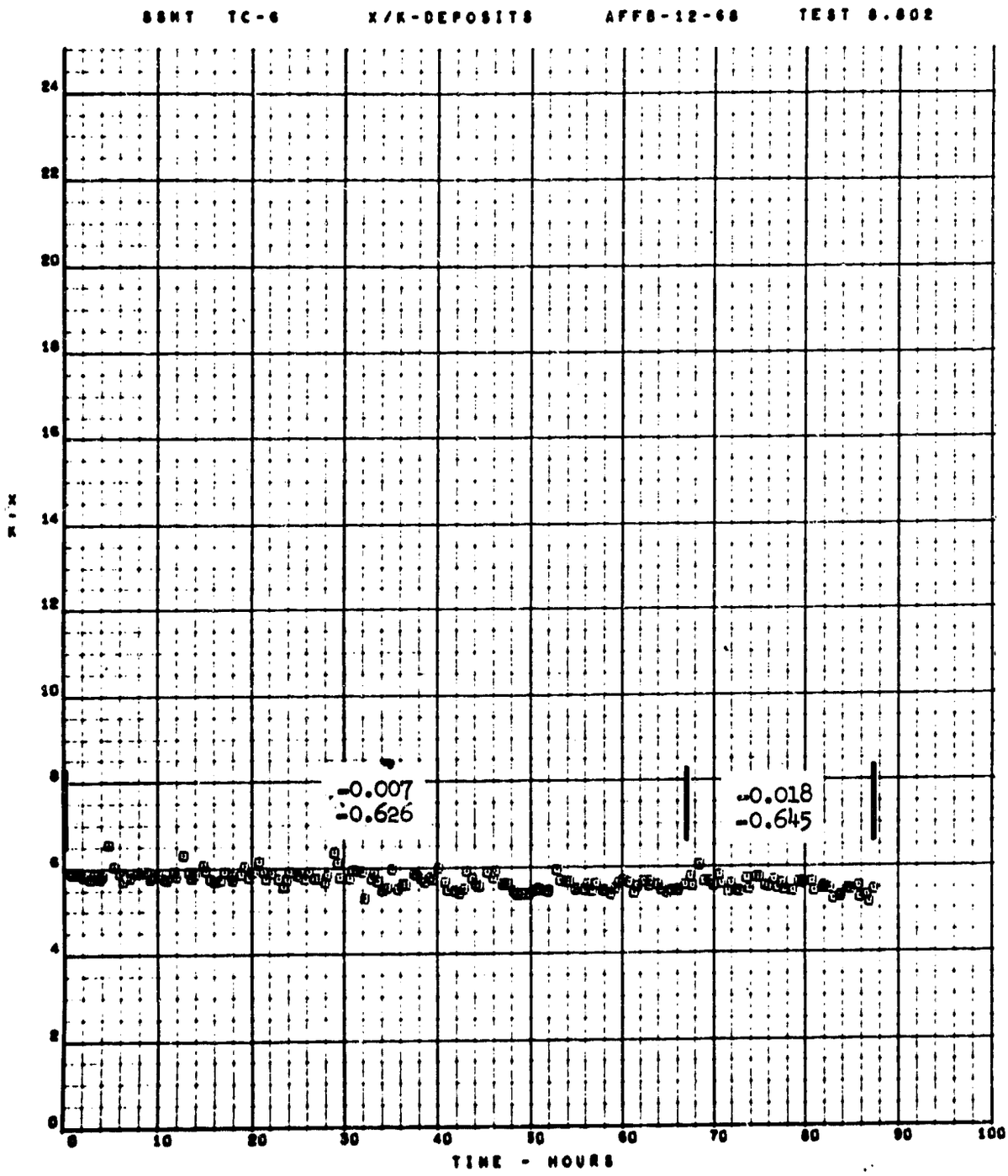
SSHT TC-6 X/K-DEPOSITS AFFB-12-68 TEST 8.802
X/K
24
22
20
18
16
14
12
10
8
6
4
2
0
-0.007
-0.626
-0.018
-0.645
0
10
20
30
40
50
60
70
80
90
100
TIME - HOURS

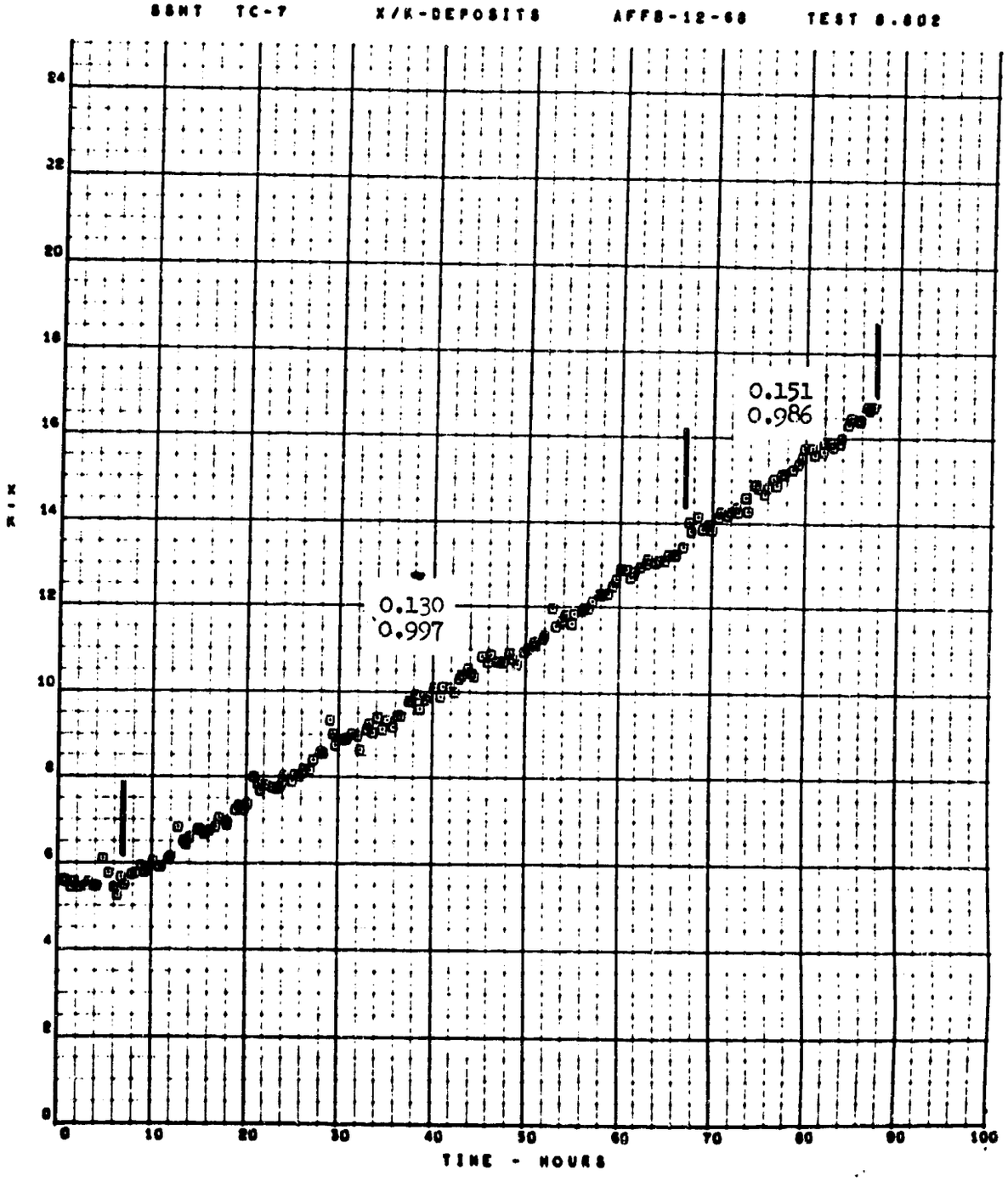
SSMT TC-7 X/K-DEPOSITS AFFB-12-68 TEST 8.802
0.130
0.997
0.151
0.986
K - X
TIME - HOURS
0
2
4
6
8
10
12
14
16
18
20
22
24
0
10
20
30
40
50
60
70
80
90
100

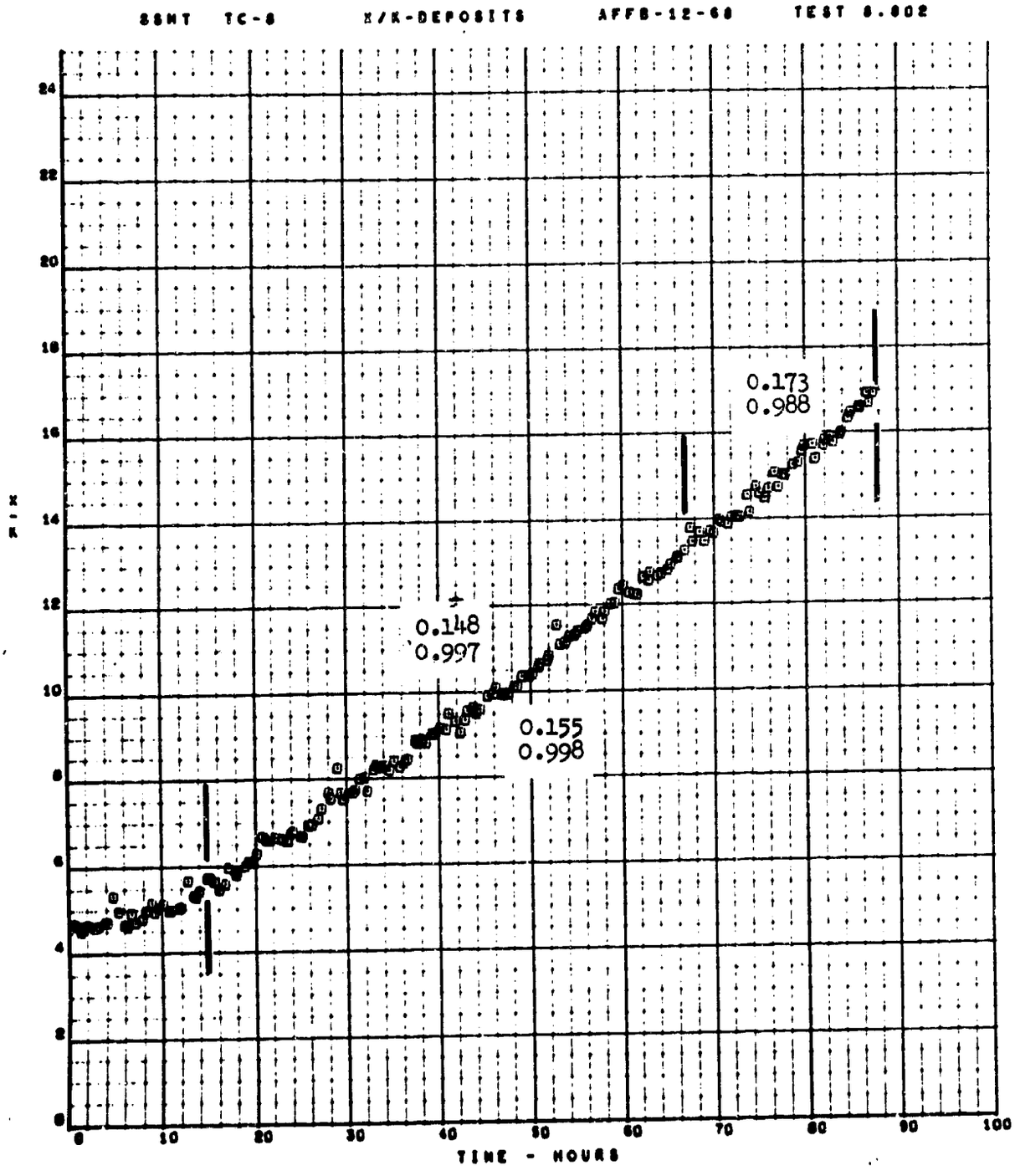
SSMT TC-8 X/K-DEPOSITS AFFB-12-68 TEST 8.802
X/K
TIME - HOURS
0.173
0.988
0.148
0.997
0.155
0.998

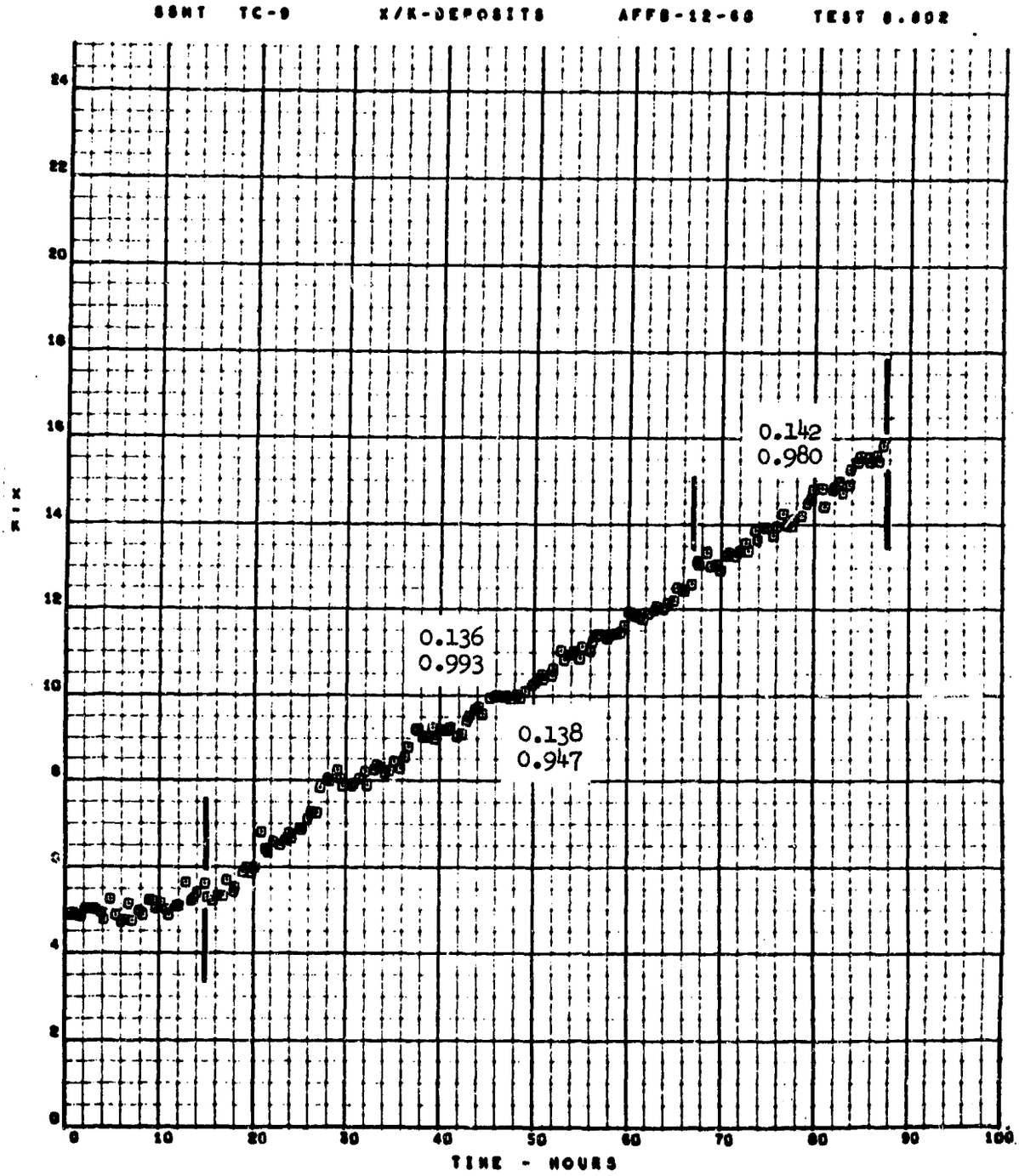
SSHT TC-9 X/K-DEPOSITS AFFS-12-68 TEST 8.802
0.142
0.980
0.136
0.993
0.138
0.947
K - X
TIME - HOURS

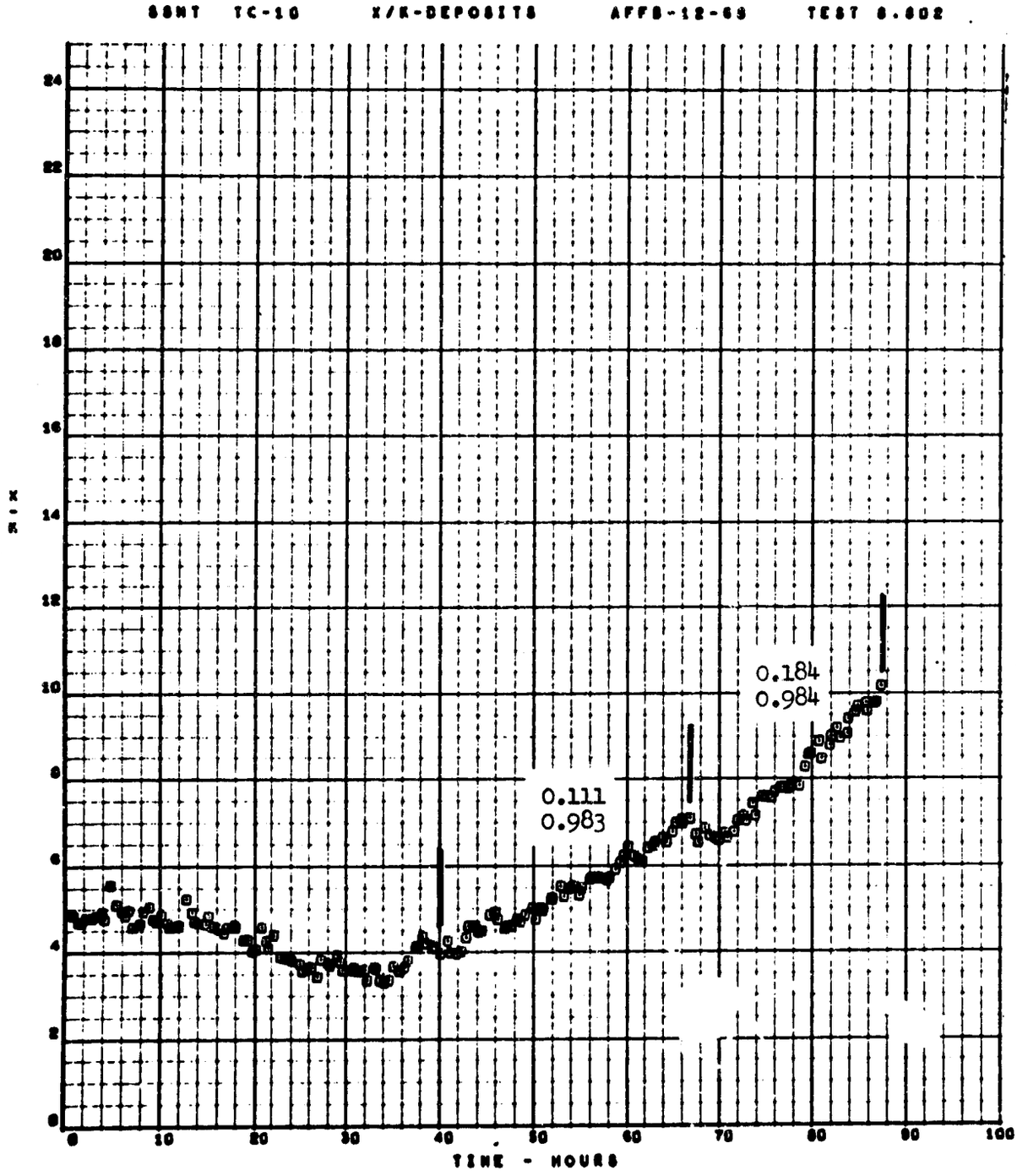
SSNT TC-10 X/K-DEPOSITS AFFS-12-69 TEST S.S02
R - X
TIME - HOURS
0.184
0.984
0.111
0.983

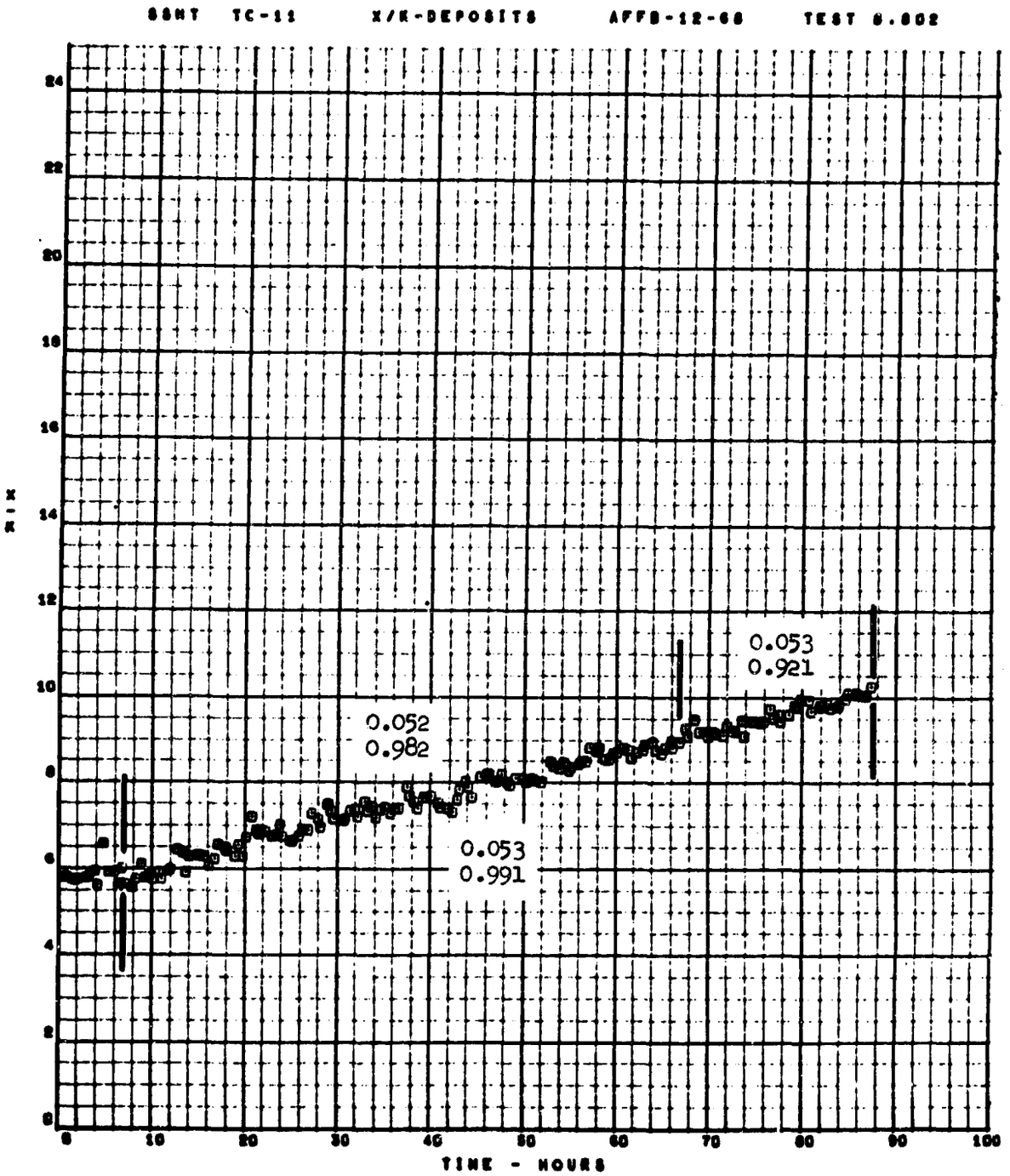
SSHT TC-11 X/K-DEPOSITS AFFB-12-68 TEST 8.802
X - X
TIME - HOURS
0.053
0.921
0.052
0.982
0.053
0.991

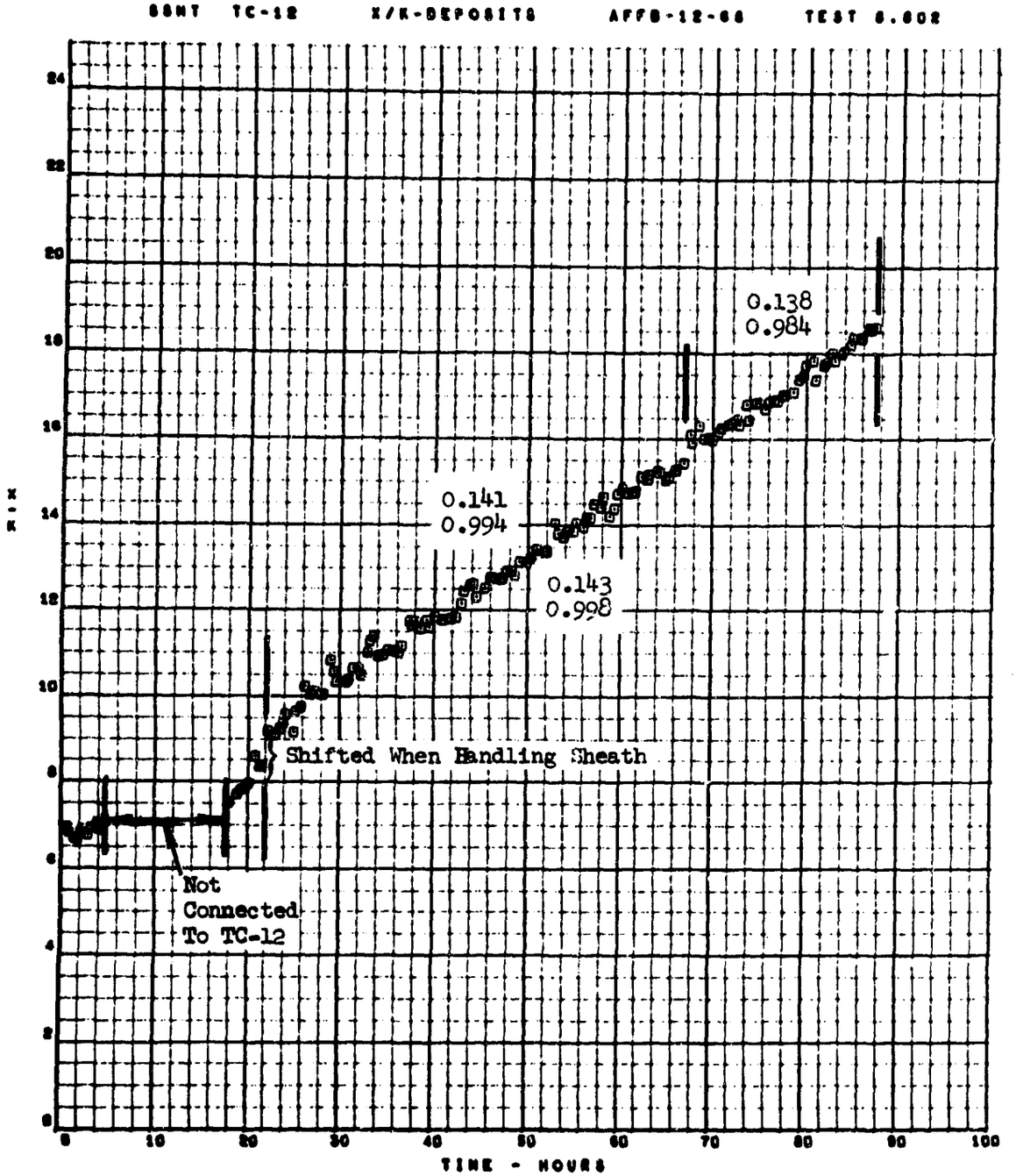
88MT TC-12 X/K-DEPOSITS AFFB-12-68 TEST 8.80R
0.138
0.984
0.141
0.994
0.143
0.998
Shifted When Handling Sheath
Not
Connected
To TC-12
X - K
TIME - HOURS

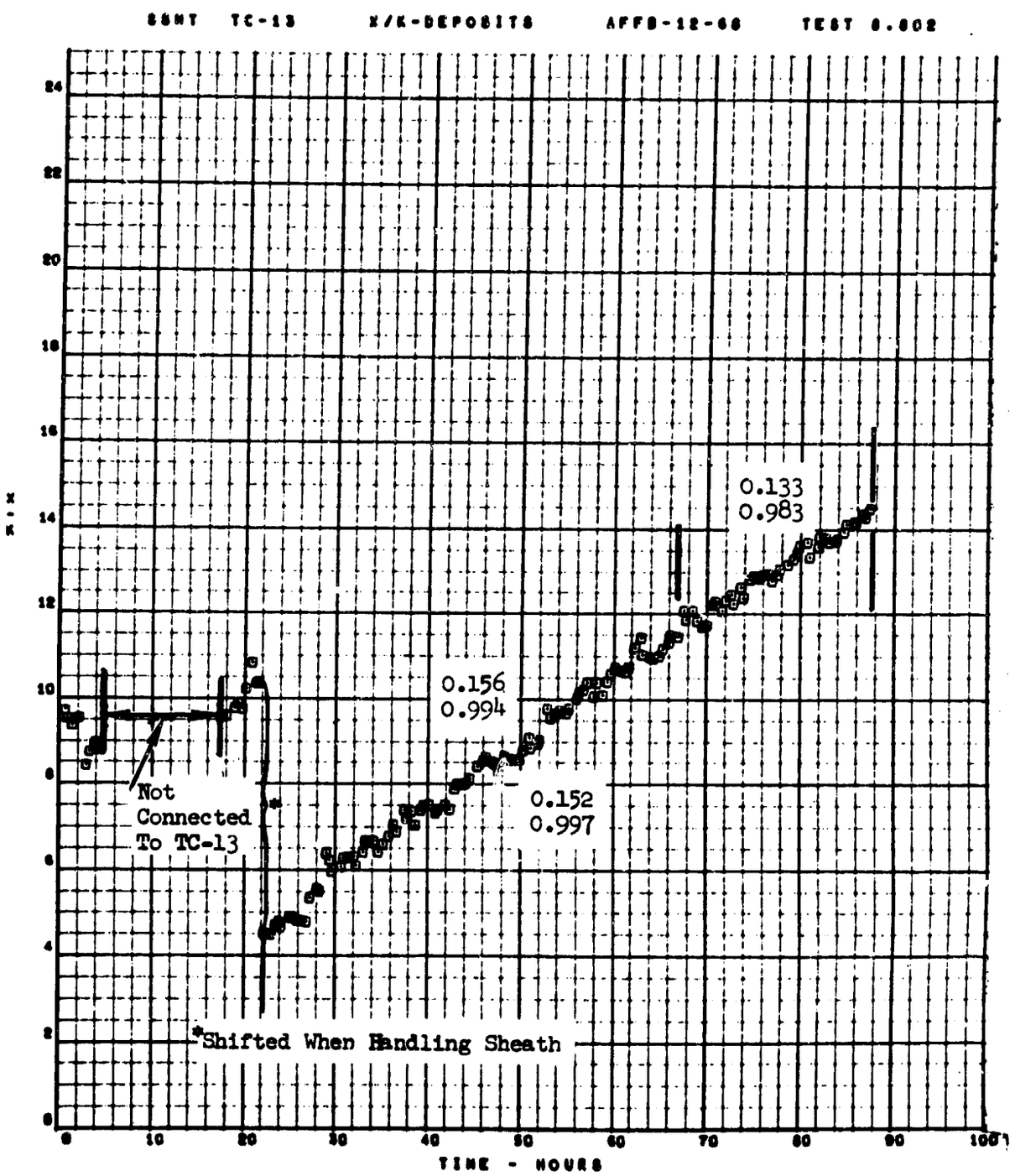
SSMT TC-13 X/K-DEPOSITS AFFB-12-66 TEST 8.802
X - K
TIME - HOURS
0.133
0.983
0.156
0.994
0.152
0.997
Not
Connected
To TC-13
*Shifted When Handling Sheath

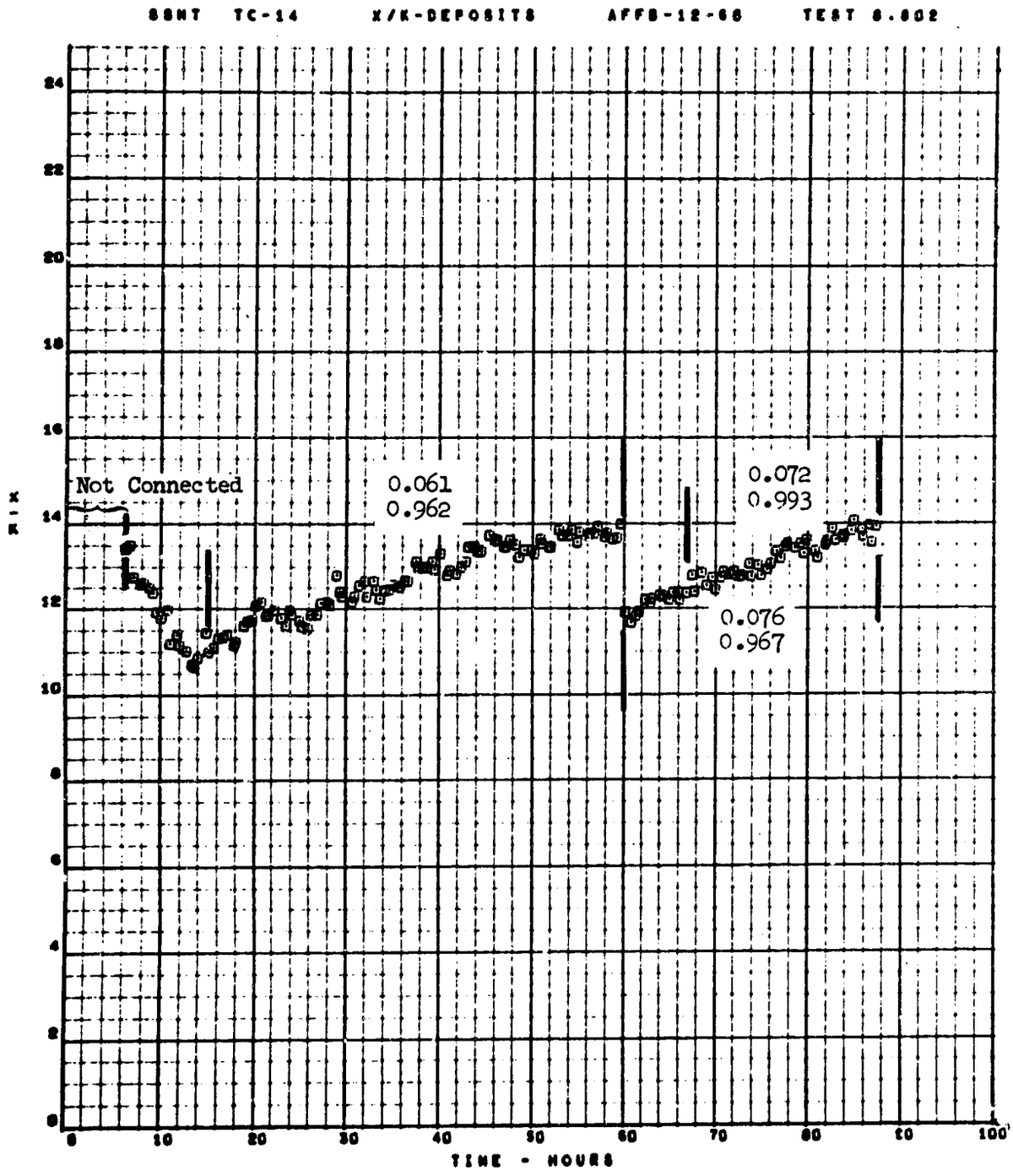
SSNT TC-14 X/K-DEPOSITS AFFB-12-68 TEST 8.802
Not Connected
0.061
0.962
0.072
0.993
0.076
0.967
X - K
TIME - HOURS

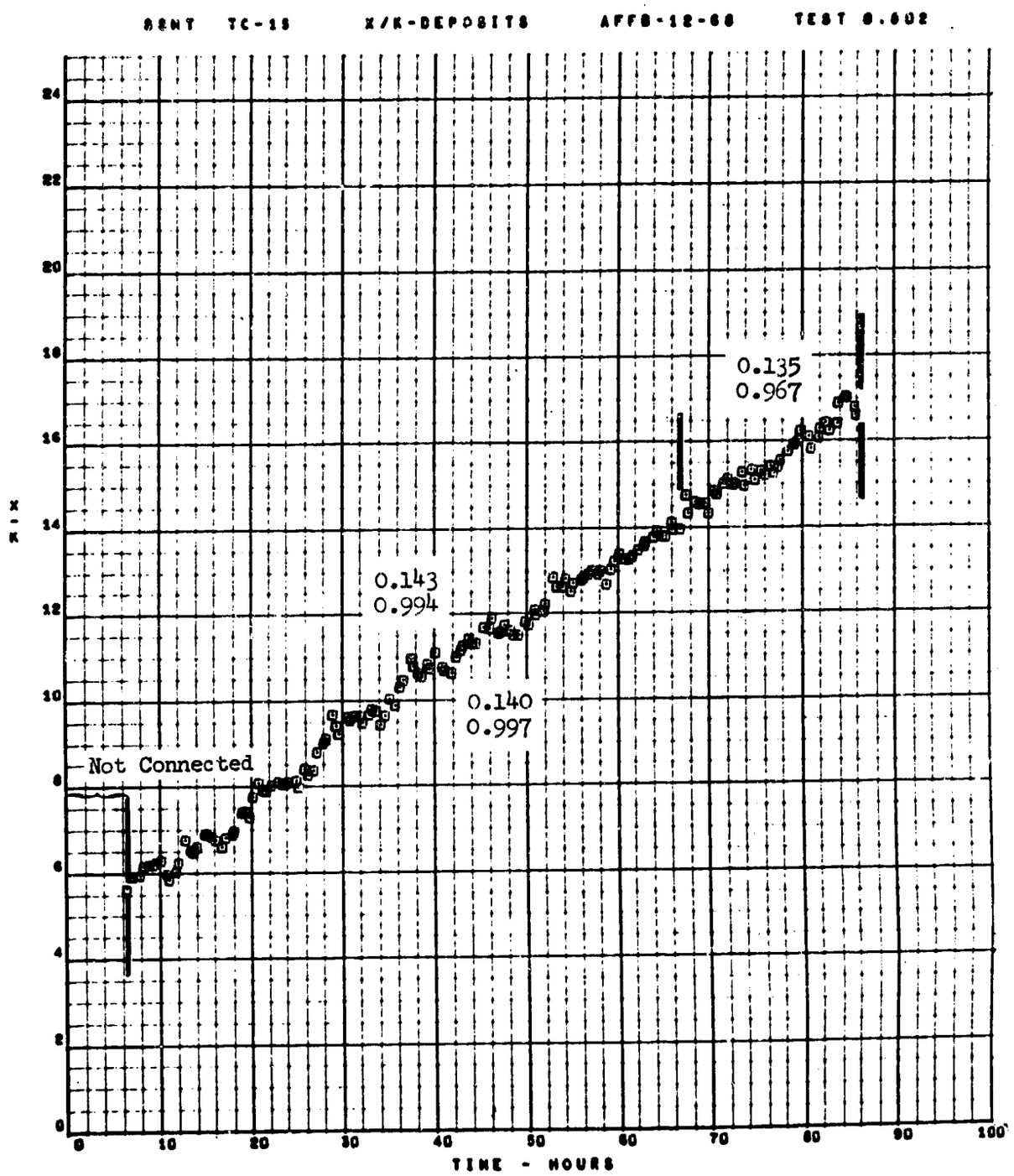
RENT TC-18 X/K-DEPOSITS AFFB-12-68 TEST 8.602
X - K
TIME - HOURS
0.135
0.967
0.143
0.994
0.140
0.997
Not Connected

UNCLASSIFIED

Security Classification

DOCUMENT CONTROL DATA - R & D

(Security classification of title, body of abstract and indexing annotation must be entered when the overall report is classified)

1. ORIGINATING ACTIVITY (Corporate author) North American Rockwell Corporation International Airport Los Angeles, California 90009	2a. REPORT SECURITY CLASSIFICATION UNCLASSIFIED 2b. GROUP N/A

3. REPORT TITLE

High Temperature Hydrocarbon Fuels Research in an Advanced Aircraft Fuel System Simulator on Fuel AFFB-12-68

4. DESCRIPTIVE NOTES (Type of report and inclusive dates)

Fifth Fuel Series Report, 6 December 1968 to 30 July 1969

5. AUTHOR(S) (First name, middle initial, last name)

Harold Goodman
Royce P. Bradley

6. REPORT DATE	7a. TOTAL NO. OF PAGES	7b. NO. OF REFS
26 November 1969	vi + 110	8

8a. CONTRACT OR GRANT NO. AF 33(615) - 3228 b. PROJECT NO. 3048, Task No. 304805 c. BPSN 6 (63 304801 62405214) d. BPSN 5 (68 0100 61430014)	9a. ORIGINATOR'S REPORT NUMBER(S) NA-69-838 9b. OTHER REPORT NO(S) (Any other numbers that may be assigned this report) AFAPL-TR-69-117

10. DISTRIBUTION STATEMENT This document is subject to special export controls and each transmittal to foreign governments or foreign nationals may be made only with prior approval of the Fuels Branch, Fuels, Lubrication, and Hazards Division, Air Force Aero Propulsion Laboratory, Wright-Patterson AFB, Ohio.

11. SUPPLEMENTARY NOTES	12. SPONSORING MILITARY ACTIVITY
	Air Force Aero Propulsion Laboratory Wright-Patterson AFB, Ohio 45433

13. ABSTRACT

Hydrocarbon jet fuels tend to form deposits at elevated temperatures that decrease heat exchanger efficiency and plug screens and filter elements. The Advanced Aircraft Fuel System Simulator provides generalized performance data, with respect to thermal stability, on various advanced fuels that will be used to correlate to small-scale test results and provide information on design criteria for future supersonic aircraft.

In this report, the thermal stability of the fifth fuel (AFFB-12-68) tested in the simulator is quantified in terms of the amount of deposit formed. The quantification of deposit formation is determined under cyclic conditions (mission profiles) and two types of steady-state test conditions (steady-state and steady-state-varied flow).

Deposits were evident in the wing tank after testing at either a maximum skin temperature of 425° or 500° F. The airframe and engine systems were clean except for the manifold and nozzle. There was no evidence of decreased performance of any of the components other than a loss in fuel side heat transfer efficiency of the manifold. The predicted rates of deposit formation under cyclic conditions, based on the radial spectrum of steady-state test fuel temperatures, are in agreement with the rates measured during cyclic conditions.

DD FORM 1 NOV 68 1473

UNCLASSIFIED

Security Classification

14. KEY WORDS	LINK A		LINK B		LINK C	
	ROLE	WT	ROLE	WT	ROLE	WT
Advanced Aircraft Fuel System Simulator						
Fuel Deposits						
Thermal Stability						
Fuel AFFB-12-68						
Hydrocarbon Jet Fuel						